

Role of MG491 protein in the motile machinery of
Mycoplasma genitalium

Luis García Morales

2015

Role of MG491 protein in the motile machinery of
Mycoplasma genitalium




Luis García Morales
2015

Tesi doctoral presentada per Luis García Morales, llicenciat en Biotecnologia, per optar al grau de Doctor en Bioquímica, Biologia Molecular i Biomedicina per la Universitat Autònoma de Barcelona.

Aquest treball ha estat realitzat a l'Institut de Biotecnologia i Biomedicina i al Departament de Bioquímica i Biologia Molecular, a la Facultat de Biociències de la Universitat Autònoma de Barcelona, sota la direcció dels Doctors Jaume Pinyol Ribas i Enrique Querol Murillo.



Dr. Jaume Pinyol Ribas



Dr. Enrique Querol Murillo

E pur si muove
- Galileo Galilei

To my family

Contents

Abbreviations	1
General introduction	3
1. The mycoplasmas	3
1.1. <i>Mycoplasma genitalium</i> as a sexually transmitted pathogen	4
1.2. Involvement in diseases	5
1.3. Infection and persistence	7
1.4. Immune evasion	8
1.5. Inflammation and toxins	9
1.6. Antibiotic treatment	10
2. Mycoplasmas as a subject of study for molecular biologists	10
2.1. Limited genetic tools	10
2.2. The minimal genome: a candy for synthetic biologists	11
3. A unique morphology and cell structure	12
3.1. Structure of the terminal organelle	14
3.2. Proteins involved in the terminal organelle structure	14
3.3. Motility of mycoplasmas	18
3.4. Implication of the terminal organelle in cell division	21
Objectives	23
Summary	25
Chapter 1: Gliding motility in electron-dense deficient mutants of <i>M. genitalium</i>	27
Introduction	28
Results	30
Part 1: Characterization of MG_491 null mutant strain	30
1.1. Isolation of Δ mg491 strain by homologous recombination	30
1.2. Additional mutations in the adhesins operon	30
1.3. Downstream destabilization of adhesion related proteins	31
1.4. Filamentous morphology and motility	33
1.5. Complementation of Δ mg491 null mutants	34
Part 2: Gliding motility in ΔMG491-P32Ch cells	35
2.1. Characterization of the motile machinery in the filaments	35
2.2. Ultrastructure of the cytoskeleton in Δ mg491-P32ch cells	37

Part 3: Characterization of Δmg218-P32Ch cells	38
3.1. Role of the cytoskeletal proteins in the motile machinery of <i>M. genitalium</i>	38
3.2. Rearrangements of the cytoskeleton in the Δ mg218-P32Ch strain	39
Discussion	41
Chapter 2: Mycoplasma genitalium strains with relevant mutations in the structure and function of MG491 protein	45
Introduction	46
Results	51
Part 1: Characterization of mg491-Δp1 strain	51
1.1. Isolation of mg491- Δ p1 strain	51
1.2. Complementation assay of mg491- Δ p1 strain	52
1.3. Gliding motility and cell morphology of mg491- Δ p1	52
Part 2: Characterization of mg491-C87S strain	54
Part 3: Characterization of mg491-F157A-F158A strain	56
Part 4: Characterization of mg491-ΔloopL2 strain	58
Part 5: Characterization of mg491-ΔNt strain	59
Summary of the phenotype of mutant strains used in this work	61
Discussion	62
Chapter 3: Quantitative Hemadsorption Assay for Mycoplasma Species using Flow Cytometry	65
Introduction	66
Results	68
Cell Titration and Biomass Estimation	68
FC Analysis of Mycoplasma HA	70
HA Properties of Different Mycoplasma Strains	75
Discussion	78
General discussion	81
Conclusions	85
Experimental procedures	87
1. Biologic material	87
1.1. Bacterial strains	87
1.2. Vectors	89
1.3. List of oligonucleotides used in this work	90

1.4. Culture conditions	91
1.4.1. Culture of <i>E. coli</i> strains	91
1.4.2. Culture of <i>M. genitalium</i> strains	92
1.4.3. Culture of <i>M. penetrans</i> strains	93
1.4.4. Culture of <i>M. hyopneumoniae</i> strains	93
2. DNA manipulations	93
2.1. Genomic DNA extraction from <i>M. genitalium</i> strains	93
2.2. DNA quantification	94
2.3. Agarose gel electrophoresis	94
2.4. DNA amplification	94
2.5. Two-step recombinant PCR or overlap extension	95
2.6. Exsite mutagenesis	95
2.7. Restriction of DNA	96
2.8. Dephosphorylation of plasmidic DNA	96
2.9. Ligation of DNA fragments	96
2.10. DNA transformation in <i>E. coli</i> XL1-Blue strain	97
2.11. Plasmidic DNA extraction	97
2.11.1. Minipreparations	97
2.11.2. Midipreparations	97
2.12. Transformation of <i>M. genitalium</i> strains	97
2.13. Southern blot	98
2.13.1. Non-radioactive probe labelling	99
2.13.2. Alkaline transference	99
2.13.3. Hybridization with the probe	99
2.13.4. Detection of the probe	99
2.14. DNA sequencing	100
2.15. Construction of plasmids	100
2.15.1. p Δ mg491	100
2.15.2. pMTnGmmg318:mcherry	101
2.15.3. pMTnecatmg491 and pMTnGmmg491	101
2.15.4. p Δ p1cat	102
2.15.5. pMTnecatC87S	102
2.15.6. pMTnecatF157A-F158A	103
2.15.7. pMTnecat Δ loopL2	103
2.15.8. pMTnecat Δ Nt	103
3. Protein analysis	104
3.1. Protein extraction from <i>M. genitalium</i>	104
3.2. SDS- polyacrylamide gel electrophoresis (SDS-PAGE)	104
3.3. Western blot	105

4. Quantification of the hemadsorption of mycoplasma strains	106
4.1. Purification of human erythrocytes	106
4.2. Qualitative hemadsorption assay	106
4.3. Quantitative hemadsorption assay	106
4.3.1. Preparation of the mycoplasma stock	106
4.3.2. Titration of the mycoplasma and RBCs stock	107
4.3.3. Hemadsorption reaction	107
5. Techniques in microscopy	108
5.1. Localization of P32:mCherry by epifluorescence microscopy	108
5.2. Time-lapse microcinematography	109
5.3. Scanning electron microscopy	109
5.4. Cryo-EM imaging	109
References	111

Abbreviations

AIDS	Acquired Immune Deficiency Syndrome
ATCC	American Type Culture Collection
BSA	Bovine Serum Albumine
CARDS	Community-Acquired Respiratory Distress Syndrome
Cryo-EM	Cryo-Electron Microscopy
CSP	Chemical Shift Perturbation
DNA	Deoxyribonucleic Acid
dNTP	Deoxynucleoside Triphosphate
EAGR	Enriched in Aromatic and Glycine Residues
ECT	Electron Cryotomography
FC	Flow Cytometry
FSC-H	Forward Scatter - Height
HA	Hemadsorption
HSQC	Heteronuclear Single Quantum Coherence
NBT/BCIP	Nitro-Blue Tetrazolium/ 5-bromo-4-chloro-3'-indolyphosphate
NGU	Non-Gonococcal Urethritis
NMR	Nuclear Magnetic Resonance
O/N	Overnight
ORF	Open Reading Frame
PAP	Primary Atypical Pneumonia
PCR	Polymerase Chain Reaction
PI	Propidium Iodide
PID	Pelvic Inflammatory Disease
PVDF	Polyvinylidene Difluoride
RBC	Red Blood Cell
RNA	Ribonucleic Acid
SARA	Sexually Acquired Reactive Arthritis
SDS-PAGE	Sodium Dodecyl Sulfate Polyacrylamide Gel Electrophoresis
SEM	Scanning Electron Microscopy
SPR	Surface Plasmon Resonance
SSC-H	Side Scatter - Height
TO	Terminal Organelle
WBC	White Blood Cell
WT	Wild Type

1. The mycoplasmas

The genus *Mycoplasma* belongs to the class Mollicutes. The cell wall-less bacteria from this class constitute a distinct phylogenetic lineage that have arisen from Gram-positive ancestors by genome reduction (Woese et al., 1980), with genome sizes ranging from 580 to 2,200 kb (Fraser et al., 1995, Tully et al., 1995b) and a G+C content usually as low as 23-31% (Barre et al., 2004, Razin et al., 1998a). Mollicutes only have one or two rRNA operons, fewer tRNA genes than other bacteria and their RNA polymerase is resistant to rifampin (Gaurivaud et al., 1996, Krieg et al., 2011). In some genus, the UGA codon encodes for tryptophan instead of a Stop (Inamine et al., 1990, Citti et al., 1992, Navas-Castillo et al., 1992). Mollicutes are among the smallest cells known, usually ranging from 200 to 500 nm in diameter and with a pleomorphic shape, varying from spherical, flask-shaped or branched or helical filaments (Krieg et al., 2011). The mollicutes membranes are rich in cholesterol and lipoproteins and the lack of a peptidoglycan layer confers them resistance to penicillins (Taylor-Robinson and Bebear, 1997). On solid media, colonies of mollicutes are also small and most of them have a fried-egg appearance (Meloni et al., 1980).

These small genome-containing cells possess limited metabolic pathways. They lack tricarboxylic acid cycle enzymes, quinones and cytochromes (Pollack et al., 1997); the synthesis of precursors of amino acids, purines and pyrimidines is limited as well and two-component and other common bacterial transcriptional regulators are missing (Manolukas et al., 1988, Himmelreich et al., 1996, Fraser et al., 1995). The members of this class have adopted a parasitic lifestyle to obtain essential nutrients from the host (Razin et al., 1998a). Namely, mycoplasmas and ureaplasmas are commensals or pathogens of vertebrate animals, while spiroplasmas or phytoplasmas are found in invertebrate animals and in plants (Krieg et al., 2011, Trachtenberg, 2005). The limited biosynthetic potential of mollicutes impairs their growth on cell-free media, and they often require complex media containing sterols and fatty acids. However, some species can grow on serum-free defined media (Yus et al., 2009). Many mollicutes are facultative aerobes, but some are strictly anaerobic. Main energy generation mechanisms among mollicutes include the fermentation of sugars to lactate, the oxidation of lactate or pyruvate to acetate and the metabolism of L-arginine to ornithine (Keceli and Miles, 2002, Miles, 1992). Individual species may possess one, two or the three routes of energy generation.

Human mycoplasma niches are usually the urogenital and respiratory tracts (Hartmann, 2009, Waites et al., 2012). The first mycoplasma isolated from humans was *Mycoplasma hominis*, the responsible agent of severe genital inflammation in women including pelvic inflammatory disease (PID) (Mardh, 1983), post-partum fevers (Taylor-Robinson and Lamont, 2011) and extragenital complications in new-borns (Hata et al., 2008, Embree,

1988). Later, *Mycoplasma pneumoniae* was described as the agent of the primary atypical pneumonia (PAP) and has been related with multiple respiratory and extrapulmonary diseases (Atkinson et al., 2008). *Mycoplasma genitalium* was isolated in the early 80s from two independent men with severe non-gonococcal urethritis (NGU) and has recently been related to chronic inflammation diseases (Tully et al., 1981, Manhart, 2013). To date, up to 16 mollicute species have been found as commensals and pathogens of humans (Waites et al., 2012).

Table I.1. Primary site of colonization, metabolism and pathogenesis of mycoplasmas isolated from humans. Adapted from Taylor-Robinson, 1997.

Species	Primary site of colonization		Metabolism of		Pathogenicity
	oropharynx	genitourinary	glucose	arginine	
<i>Mycoplasma buccale</i>	+	-	-	+	non-pathogenic
<i>Mycoplasma faucium</i>	+	-	-	+	non-pathogenic
<i>Mycoplasma fermentans</i>	+	± ^a	+	+	detected in joints in inflammatory arthritides and in lungs in HIV infection
<i>Mycoplasma genitalium</i>	±	+	+	-	NGU
<i>Mycoplasma hominis</i>	±	+	-	+	PID
<i>Mycoplasma lipophilum</i>	+	-	-	+	non-pathogenic
<i>Mycoplasma orale</i>	+	-	-	+	non-pathogenic
<i>Mycoplasma penetrans</i>	-	+	+	+	associated with HIV infection
<i>Mycoplasma pirum</i>	?	?	+	+	non-pathogenic
<i>Mycoplasma pneumoniae</i>	+	±	+	-	atypical pneumonia and sequelae
<i>Mycoplasma primatum</i>	-	+	-	+	non-pathogenic
<i>Mycoplasma salivarum</i>	+	-	-	+	arthritis in hypogammaglobulinaemia
<i>Mycoplasma spermatophilum</i>	-	+	-	+	non-pathogenic
<i>Ureaplasma urealyticum</i> ^b	+	+	-	-	NGU and arthritis in hypogammaglobulinaemia
<i>Acholeplasma laidlawii</i>	+	-	+	-	non-pathogenic
<i>Acholeplasma oculi</i>	?	-	+	-	non-pathogenic

^a ± Primary site occasionally.

^b Metabolizes urea

1.1. *Mycoplasma genitalium* as a sexually transmitted pathogen

M. genitalium was firstly isolated in the urogenital tract of two men with non-chlamydial NGU (Tully et al., 1981). Urethra and genital tract have been considered as the primary niche of this mycoplasma (Palmer et al., 1991, Datcu et al., 2013). Prevalence of *M. genitalium* in the global population ranges in different studies from 1 to 4% in men (Manhart and Kay, 2010, Anagnrius et al., 2005, Soni et al., 2010) and from 1 to 6.4% in women (Tosh et al., 2007, Hamasuna et al., 2008, Ross et al., 2009). This prevalence increases to 26.3-38% in populations with high rates of sexually transmitted diseases (Pepin et al., 2005, Casin et al., 2002).

A significantly high prevalence – up to 63% – of this microorganism has been found in people with *M. genitalium*-positive sexual partners (Tosh et al., 2007, Falk et al., 2005, Keane et al., 2000, Falk et al., 2004, Manhart and Kay, 2010). Among these people, *M. genitalium* is rarely detected in women reporting no vaginal intercourse (Manhart et al., 2007, Tosh et al., 2007), but the detection rates increase by nearly 45% for each additional sexual partner (Tosh et al., 2007, Soni et al., 2010). At a molecular level, DNA based typing systems have shown that almost every sex partners with both members infected with *M. genitalium* shared the same phylotype (Hjorth et al., 2006, Ma et al., 2008, Musatovova and Baseman, 2009). All these studies taken together strongly support that *M. genitalium* is an emerging sexually transmitted pathogen (Manhart et al., 2007).

Regarding its sexual transmission, *M. genitalium* has been detected in the rectum of homosexual males (Bradshaw et al., 2009, Taylor-Robinson et al., 2003, Soni et al., 2010). However, rectal infections of this pathogen are asymptomatic, representing an important reservoir for continued spreading (Francis et al., 2008, Taylor-Robinson et al., 2003). Although it was initially found in some throat samples (Baseman et al., 1988), recent studies have repeatedly failed to detect *M. genitalium* in pharynges from people practicing oral sex (Bradshaw et al., 2009, Deguchi et al., 2009). It is noteworthy that this pathogen can also colonize tissues that are not related to the urogenital tract as it has been detected in synovial fluid (Taylor-Robinson et al., 1994, McGowin et al., 2010, Tully et al., 1995a). In a few cases, it has been found in cerebrospinal fluid (Sakata et al., 1993) or respiratory tract (de Barbeyrac et al., 1993), suggesting the haematogenous dissemination of this microorganism (Tully et al., 1986, McGowin et al., 2010).

1.2. Involvement in diseases

Although most *M. genitalium* infections are asymptomatic (Henning et al., 2014), this microorganism has been related to several reproductive tract and systemic diseases. NGU encloses all cases of urethritis in which *Neisseria gonorrhoeae* cannot be detected. In these cases, *Chlamydia trachomatis* is the most common aetiological agent of the disease. It is now known that *M. genitalium* is responsible of 20-35% of Chlamydia-negative NGU (Deguchi and Maeda, 2002, Totten et al., 2001, Horner et al., 1993), a disease that has also been related to other bacteria such as *Ureaplasma urealyticum* (Bowie et al., 1977) and *Trichomonas vaginalis* (Pillay et al., 1994). Urethral infections are usually asymptomatic (Yu et al., 2008). However, it has been demonstrated that symptoms of NGU appear more often when the agent is *M. genitalium* (Falk et al., 2004), and there is also higher risk of balanoposthitis (Horner and Taylor-Robinson, 2011). Finally, *M. genitalium* was also detected by PCR in prostatic biopsies and semen of a small number of patients with abacterial inflammatory prostatitis, but further evidence is needed to confirm this association (Krieger et al., 1996, Mandar et al., 2005).

M. genitalium has also been involved in lower genital tract inflammatory syndromes in women (McGowin and Anderson-Smiths, 2011) as, for example, urethritis (Moi et al., 2009), cervicitis (Uno et al., 1997, Manhart et al., 2003, Falk et al., 2005, Dehon and McGowin, 2014) and vaginal discharge (Tosh et al., 2007). There is also evidence of involvement of this microorganism in PID (Simms et al., 2003, Haggerty and Taylor, 2011, Haggerty, 2008), endometritis (Cohen et al., 2002), salpingitis (Cohen et al., 2005) and pregnancy complications, as preterm birth (Edwards et al., 2006, Hitti et al., 2010) and tubal infertility (Clausen et al., 2001, Svenstrup et al., 2008, Baczynska et al., 2007), showing the capacity of this microorganism to infect upper reproductive tracts. Upper reproductive tract inflammation after experimental infections of *M. genitalium* has been also confirmed in murine (McGowin et al., 2010) and primate animal models (Taylor-Robinson et al., 1987, Moller et al., 1985).

This pathogen has also been related to Sexually Acquired Reactive Arthritis (SARA), as it commonly occurs meanwhile or following an NGU episode (Hannu, 2011), and *M. genitalium* has been recovered from synovial fluid (Taylor-Robinson et al., 1994). Some clinical cases supported the relation of *M. genitalium* in joints with SARA and Reiter's disease (Taylor-Robinson et al., 1994, Henry et al., 2000).

It has been reported that sexually transmitted infections enhance the transmission of human immunodeficiency virus (HIV) (Fleming and Wasserheit, 1999, Cohen, 1998), probably because these pathogens compromise the mucosal epithelial barriers (Das et al., 2014). *M. genitalium* has been identified as one of this AIDS-promoting pathogens (Taylor-Robinson and Jensen, 2011, Manhart et al., 2008, Napierala Mavedzenge and Weiss, 2009, Perez et al., 1998) existing a strong temporal relationship between *M. genitalium* infection and HIV acquisition in women (Mavedzenge et al., 2012, Vandepitte et al., 2014). Furthermore, this pathogen was found more often in HIV-positive men developing AIDS than in HIV-positive men without AIDS (Taylor-Robinson, 2002) and increases the shedding of HIV particles from women cervixes (Manhart et al., 2008). In vitro work supported that *M. genitalium* infection assists HIV movement through epithelium and promotes HIV replication in peripheral blood mononuclear cells (Das et al., 2014). All these data suggest that *M. genitalium* helps in the transmission of HIV and facilitates the development of AIDS.

In the last decades, pathogens causing chronic inflammatory diseases have been considered as initiators or promoters of cancer processes. For example, *Helicobacter pylori* has been linked to gastric cancer (Moss and Blaser, 2005), human papillomavirus (HPV) and *C. trachomatis* to cervical cancer (Anttila et al., 2001) and hepatitis B (HBV) and C virus (HCV) to liver cancer (Moss and Blaser, 2005). Some mycoplasmas have been also related to malignant transformation of mammalian cells (Feng et al., 1999, Tsai et al., 1995) or have been extensively detected in human carcinoma samples (Huang et al., 2001). PCR amplification of mycoplasmal DNA in malignant ovarian cancer samples (Chan et al., 1996)

prompted researchers to consider the possible implication of urogenital mycoplasmas as cancer promoters. *In vitro* studies demonstrated the potential of *M. genitalium* to transform human benign prostatic cells (BPH-1) making infected cells capable to develop tumours when introduced in a nude mice (Namiki et al., 2009). Lately, it was found a modest association between the presence of *M. genitalium* IgG antibodies on ovarian cancer samples in the borderline cases, but the significance of this results is unclear (Idahl et al., 2011).

1.3. Infection and persistence

For many mycoplasmas, the first step for infection and colonization is the adhesion to host cells (Rottem, 2003, Razin and Jacobs, 1992, Krause et al., 1982). It has been demonstrated *in vitro* the adhesion of *M. genitalium* to the surface of several cell types including Vero monkey kidney cells (Tully et al., 1983b, Jensen et al., 1994), Hep-2 (Svenstrup et al., 2002), human spermatozoa (Svenstrup et al., 2003), erythrocytes (Burgos et al., 2006) and lung fibroblasts (Mernaugh et al., 1993), and also to the cilia of human fallopian tube epithelial cells (Collier et al., 1990) and vaginal and cervical epithelial cells (McGowin et al., 2009).

Mycoplasma adhesion is mediated by adhesin proteins (Krause and Baseman, 1982). It has been reported that the protein P140, with the assistance of P110, is the main adhesin of *M. genitalium* (Burgos et al., 2006, Svenstrup et al., 2002, Mernaugh et al., 1993). P140 is homologous to *M. pneumoniae* P1 adhesin (Dallo et al., 1989a, Dallo et al., 1989b, Inamine et al., 1989) and also shows a serological cross-reaction with this adhesin (Morrison-Plummer et al., 1987, Hu et al., 1987). P1 adhesin location is polarized in *M. pneumoniae* cells, clustering at the tip structure (Baseman et al., 1982b, Feldner et al., 1982, Seto et al., 2001). Similarly, P140 is located at the tip structure of *M. genitalium* (Hu et al., 1987), being this structure essential for cytoadhesion (Jensen et al., 1994). This tip structure is also present in many mycoplasmas (Hatchel and Balish, 2008), and is also involved in many other biological functions.

Evidence indicates that the binding target of many mycoplasmas is sialylated oligosaccharides in the surface of host cells (Nagai and Miyata, 2006, Baseman et al., 1982a, Kasai et al., 2013, Roberts et al., 1989). The recognition of particular compounds has been reported as species specific and also has an important role in cell tropism of different mycoplasmas (Kasai et al., 2013). In addition, it has been shown that mycoplasma cells need sialylated oligosaccharides from serum to bind plastic and glass surfaces (Nagai and Miyata, 2006). However, the specific binding target of *M. genitalium* is still unknown.

After adhesion to the host, a subset of *M. genitalium* cells can enter to the cytoplasm and have been found in many intracellular and perinuclear spaces of different cell types (Baseman et al., 1995, Dallo and Baseman, 2000, Mernaugh et al., 1993, McGowin et al.,

2009) including the nucleus (Ueno et al., 2008). However, only a small fraction of cultured cells – about 10% – can be infected *in vitro* (Jensen et al., 1994). Intracellular *M. genitalium* cells have been also found *in vivo* in clinical samples of vaginal swaps (Blaylock et al., 2004). It has been reported that the tip structure is involved in the process of internalization into the cultured cells (Jensen et al., 1994, McGowin et al., 2009). *M. genitalium* internalization is characterized by membrane depressions resembling clathrin-coated pits, in which the tip is always in close contact with the cell membrane, suggesting a site-directed recognition between membrane factors of the eukaryotic cell and tip components of the mycoplasma (Mernaugh et al., 1993).

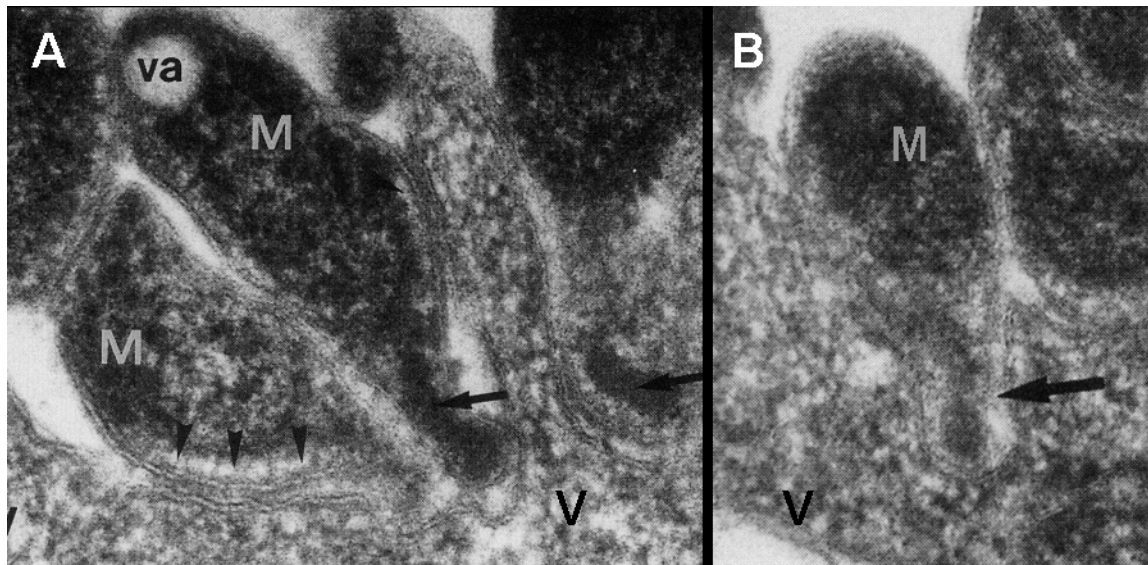


Fig. I.1. (A) *M. genitalium* cells (M) attached to the surface of Vero monkey kidney cells (V). The va denotes vacuole. (B) A *M. genitalium* cell starting the internalization into the Vero cell. Black arrows in (A) and (B) point to the tip structure promoting the adhesion and internalization of this pathogen. Adapted from Jensen et al., 1994.

Potential for intracellular survival grants mycoplasma cells a privileged niche against immunological responses, for example complement-mediated lysis, phagocitation and antibodies recognition (McGowin et al., 2009, Dallo and Baseman, 2000), and also against antibiotic treatments (Wikstrom and Jensen, 2006). This feature also explains the persistence and chronic nature of *M. genitalium* infections (Cohen et al., 2007), the recurrence of the NGU symptoms even after antibiotic treatment and their latent asymptomatic subsistence (Dallo and Baseman, 2000).

1.4. Immune evasion

Immune response against mycoplasmas infection usually requires the recognition of surface exposed proteins by specific antibodies (Bredt et al., 1981, Taylor-Robinson et al., 1966). Many mycoplasmas have developed systems of antigenic variation to evade the immune response. These systems usually involve genetic mechanisms for variant generation in genes coding for surface exposed lipoproteins, including length variations by recombination

of repeated elements (Citti and Wise, 1995, Zhang and Wise, 1996), or phase variations and genome rearrangements (Bhugra et al., 1995, Shen et al., 2000, Citti et al., 2010). The most immunogenic proteins in *M. genitalium* and *M. pneumoniae* are adhesins P140 and P1, respectively (Svenstrup et al., 2006, Jacobs et al., 1991). The genomes of both mycoplasmas contain non-coding regions with sequences homologous to the genes coding for adhesins (Ruland et al., 1990, Wenzel and Herrmann, 1988, Himmelreich et al., 1996, Fraser et al., 1995). By homologous recombination with the adhesin genes, these regions increase the antigenic diversity and contribute to the immune evasion (Rocha and Blanchard, 2002, Su et al., 1993, Peterson et al., 1995).

M. genitalium main adhesins P140 and P110 are coded in genes MG_191 and MG_192, which are located at the MgPa operon together with MG_190 gene, coding for a protein with unknown function (Musatovova et al., 2003). There are 9 regions in *M. genitalium* genome, named MgPa islands or MgPa repeats, that contain sequences homologous to MG_191 and MG_192 genes. MgPa islands are located in non-coding regions and represent the 4.7% of the *M. genitalium* genome. The individual repetitive sequences are known as R1-R6 and each MgPa island contains a different combination of R1-R6 sequences. Recombination events between MgPa sequences and MgPa operon have been detected *in vitro* and *in vivo* and have been related to the antigenic variation of the main adhesins (Iverson-Cabral et al., 2006, Ma et al., 2007). Many of these recombination events are reciprocal, which is not common among the antigenic variation systems in bacterial pathogens (Iverson-Cabral et al., 2007). MgPa islands may recombine between them and with the MgPa operon, providing a system that allows the generation of multiple antigenic variants of P140 and P110 adhesins. Interestingly, MgPa V is located downstream the MgPa operon. Single recombination events between these sequences also allow the deletion of large DNA sequences inside the MgPa operon and are the origin of the mechanism to generate natural cytadherence negative mutant strains of *M. genitalium* (Mernaugh et al., 1993, Burgos et al., 2006). Recently, it has been discovered a novel mechanism in *M. genitalium* to evade the host immune system. This mechanism consists in a membrane-associated protein, MG281, that is able to bind with high affinity the variable regions of κ and λ light chains and broadly block the antigen binding (Grover et al., 2014).

1.5. Inflammation and toxins

Although most of mycoplasma infections are asymptomatic, some of them produce cytopathic effects and diseases. However, only a small amount of toxins and virulence factors of mycoplasmas are currently reported in the literature. The innate immune response to this microorganism has an important role in its pathogenesis. In this way, it has been described that MG309 protein *M. genitalium* induce an strong inflammatory response. This protein is able to activate NF- κ B via Toll-like receptors 2 and 6, resulting in a cytokine secretion from epithelial cells (McGowin et al., 2009). An ADP-ribosyltransferase from *M. pneumoniae* has

a vacuolating cytotoxin activity and produces a pulmonary inflammation responsible of the “Community-Acquired Respiratory Distress Syndrome” (CARDS) (Kannan and Baseman, 2006, Hardy et al., 2009, Medina et al., 2012). CARDS toxin ADP-ribosylates NLRP3 protein, producing a hyperactivation of the inflammasome and the subsequent release of IL-1 β (Bose et al., 2014). It has been demonstrated that hyperactivation of the inflammasome after a pathogen insult can be more damaging than the insult itself (dos Santos et al., 2012).

Mycoplasmas lack key enzymes for peroxide detoxification like catalases and superoxide dismutases. In consequence, high amounts of peroxides are released from mycoplasma cells, generating an oxidative stress in host cells. This oxidative stress has been related to the hemolytic activity detected in some mycoplasmas (Kannan and Baseman, 2000). *M. genitalium* MG408 protein (MsrA) reduces methionine residues and, by this way is also involved in the sensitivity to hydrogen peroxide, resistance to the oxydative stress caused by the inflammatory response and virulence (Dhandayuthapani et al., 2001, Das et al., 2012).

Hence, the combination of the hyperactivation of innate immune response, the mechanisms of evasion to the adaptive immunity, the intracellular persistence and the survival to the oxydative stress make mycoplasmas a significant and still poorly known human and animal pathogen.

1.6. Antibiotic treatment

Treatment of *M. genitalium* with tetracyclines, such as doxycycline, usually failed to eradicate this microorganism (Falk et al., 2003, Wikstrom and Jensen, 2006, Jensen, 2004), probably due to the bacteriostatic activity and the intracellular surveillance of this pathogen. It is established that azytromycin is a better treatment for *M. genitalium* infections (Jensen, 2004, Anagnrius et al., 2013), as well as moxifloxacin (Terada et al., 2012). However, resistant strains to macrolides and fluoroquinolones have been detected worldwide in the last years (Couldwell et al., 2013, Tagg et al., 2013, Kikuchi et al., 2014, Chrisment et al., 2012, Gesink et al., 2012).

2. Mycoplasmas as a model organism for molecular biologists

2.1. Limited genetic tools

The study of the molecular biology of mycoplasmas has been hindered by the availability of limited tools for genetic manipulation of these microorganisms. The presence of nucleases at the cell membrane of mycoplasmas (Minion et al., 1993) and their active restriction systems (Dybvig et al., 1998) stall the transformation of exogenous DNA. First of all, natural plasmids have only been found in *Mycoplasma mycoides subsp. mycoides* (Bergemann et al., 1989,

King and Dybvig, 1992), and its usefulness is limited to *M. mycoides* and *Mycoplasma capricolum*. Artificial plasmids have been engineered using bacterial chromosomal replication origin (OriC) of some species like *M. capricolum subs. capricolum* (Janis et al., 2005), *Mycoplasma agalactiae* (Chopra-Dewasthaly et al., 2005a), *Mycoplasma pulmonis* (Cordova et al., 2002), *Mycoplasma bovis* and *Mycoplasma agalactiae* (Sharma et al., 2015).

Hence, the most widely used technique for genetic manipulation of mycoplasmas is the random insertion mutagenesis (Chopra-Dewasthaly et al., 2005b, Hedreyda et al., 1993, Cao et al., 1994, Reddy et al., 1996). Engineered mini-transposons derived from Tn4001 from *Staphylococcus aureus* (Lyon et al., 1984, Pich et al., 2006b) have allowed the insertion of desired DNA sequences and the inactivation of genes by random disruption (Hasselbring et al., 2005, Hasselbring et al., 2006a, Hasselbring et al., 2006b, Pour-El et al., 2002, Glass et al., 2006, Lluch-Senar et al., 2007, Pich et al., 2006a).

Site directed mutagenesis by homologous recombination techniques is restricted to a few mycoplasma species and gene replacement by double crossover events has only been reported in *M. genitalium* (Dhandayuthapani et al., 1999) and some strains of *M. pneumoniae* (Krishnakumar et al., 2010). Gene replacement is a powerful technique for gene knockout (Burgos et al., 2008, Burgos et al., 2006, Torres-Puig et al., 2015, Pich et al., 2008, Lluch-Senar et al., 2010), and to generate strains bearing mutant alleles (Calisto et al., 2012, Broto, Unpublished).

Since no methods are currently available to generate unmarked mutations in mycoplasmas, antibiotic resistance genes as selectable markers are essential for mycoplasma genome manipulations. Up to date, a limited number of selectable markers are available: *aac(6')*-*aph(2'')* (Mahairas and Minion, 1989), *tetM* (Dybvig and Cassell, 1987), *cat* (Hahn et al., 1999) and *pac* (Algire et al., 2009) genes, conferring resistance to aminoglycosides, tetracycline, chloramphenicol and puromycin, respectively. In *M. genitalium*, the 22 bp promoter sequence from MG_438 gene has been proved to be a useful promoter for expression of antibiotic resistance genes (Pich et al., 2006b, Calisto et al., 2012).

2.2. The minimal genome: a candy for synthetic biologists

The question of which is the minimal subset of genes and functions needed to sustain life in a favourable environment has recently attracted the attention of many researchers (Glass et al., 2006, Xavier et al., 2014). It is assumed that obtaining knowledge about how small, simple cells work will be less complex and easier to understand than complex cells (Glass et al., 2009). Furthermore, it is proposed that a cell with only the essential genes required for metabolism and replication could be modified by adding some extra genes to obtain an organism of desired properties.

M. genitalium possesses one of the smallest genome known for an axenic-cultured bacterium. With only 580 kb and 480 protein-coding genes, represents a natural approach to the minimum cell. For this reason, *M. genitalium* and its close relative *M. pneumoniae* have become the main subjects of study of synthetic biology. *M. genitalium* genome was the second genome of an organism to be sequenced (Fraser et al., 1995) and just a few years later researchers carried on a global transposon random insertion mutagenesis to recognize essential genes (Hutchison et al., 1999, Glass et al., 2006). Global transposon analysis showed that about 265-350 *M. genitalium* ORFs are essential for growth in axenic medium. Further experiments of knock-out and gene disruption have shown that some of these genes could also be disrupted or knocked out (Lluch-Senar et al., 2007). It is noteworthy that, to day, the function of about 100 of these genes is unknown (Glass et al., 2009). These experimental approaches, however, individually disrupt one gene at the same time and no information about which genes are simultaneously dispensable is reported. For this reason, the question of which is the minimal gene set to sustain life has evolved to the search of essential genetic functions (Gibson et al., 2008a). New techniques have allowed the chemical synthesis of a complete *M. genitalium* genome (Gibson et al., 2008a, Gibson et al., 2008b). The transplantation of this genome and reduced variants to empty cells is supposed to help in the search of essential functions (Gibson et al., 2008a). However, the transplantation of the whole genome of *M. genitalium* has not been reported to date. Surprisingly, the transplantation of whole genomes of other mycoplasmas has been described by the same research group (Lartigue et al., 2009, Gibson et al., 2010, Lartigue et al., 2007).

The simplicity of the mycoplasma cells has also encouraged researchers to implement large scale experiments in order to completely understand the functioning of these cells. Although most of these works have been performed using *M. pneumoniae*, nowadays there is an accurate knowledge about the proteome (Kuhner et al., 2009, Parraga-Nino et al., 2012, Maier et al., 2011), transcriptome (Guell et al., 2009, Vivancos et al., 2010, Yus et al., 2012, Maier et al., 2011) and metabolome (Yus et al., 2009, Wodke et al., 2013, Maier et al., 2013) of many of these microorganisms. Protein and DNA modifications have been extensively described as well (Lluch-Senar et al., 2013, van Noort et al., 2012, Schmidl et al., 2010). Even an in silico model of *M. genitalium* has been proposed integrating all the genomic information, which is able to predict the temporal evolution and mean growth rate after the in silico disruption of single genes (Karr et al., 2012).

3. A unique morphology and cell structure

Mycoplasmas are currently considered as simple organism, with very limited cell functions. This paradigm is supported by the presence of small streamlined genomes inside their cells. However, some mycoplasmas possess polar structures with a complexity unparalleled in the bacterial world. These polar structures, commonly referred as tip structures, are

protrusions from the cell body supported by a complex cytoskeleton. The existence of a bacterial cytoskeleton in *M. pneumoniae* (Neimark, 1977, Gobel et al., 1981) was proposed earlier than in other model organisms such as *Escherichia coli*, *Bacillus subtilis*, or *Caulobacter crescentus*. Although mycoplasmas were initially suggested to have an actin-like cytoskeleton, later findings discarded any relation with eukaryotic structures (Balish and Krause, 2006). The singularity of the mycoplasmal cytoskeleton, present only in a few number of organisms, suggest a recent evolution of the whole structure, and therefore, constitute one of a very few examples in phylogeny of the evolution of a completely new cytoskeleton (Balish and Krause, 2006). However, subcellular structures of mycoplasmas remain less understood than those of any other bacteria, probably due to their lack of relation with eukaryotic cytoskeletons, the difference between mycoplasma species and the intrinsic difficulties in working with mycoplasmas (Balish, 2006).

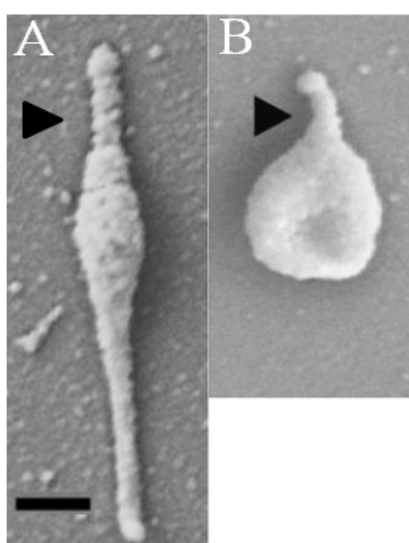


Fig. 1.2. Scanning Electron Microscopy micrographs of (A) *Mycoplasma pneumoniae* and (B) *Mycoplasma genitalium*. Black arrow heads point the respective tip structures. Tip from *M. genitalium* shows a curvature with the cell body axis. *M. pneumoniae* shows a trail at the opposite pole of the tip. Bar is 250 nm. Adapted from Hatchel and Balish, 2008.

The specific tip structure of the organisms from the *pneumoniae* cluster is often referred as terminal organelle (TO) or attachment organelle. This structure confers a flask-shape appearance to the cells. Some singularities can be found in each of the 8 species of the *pneumoniae* cluster, including the size of the protrusion or its curvature with the cell body axis (Hatchel and Balish, 2008). Internally, the terminal organelle is supported by an electron-dense core (Biberfeld and Biberfeld, 1970) which appears to be connected with the cytoskeletal filaments of the cell body (Meng and Pfister, 1980). Terminal organelle has also a pivotal role in many important functions in the lifecycle of mycoplasmas such as the adhesion to host cells, motility and cell division (Mernaugh et al., 1993, Burgos et al., 2006, Henderson and Jensen, 2006, Bredt, 1968, Lluch-Senar et al., 2010) and constitutes an essential structure for virulence (Jordan et al., 2007, Krunkosky et al., 2007). Homologues to the proteins involved in terminal organelle structure and functioning are restricted to the *pneumoniae* cluster, suggesting a common mechanism of working and exclusive to this small set of organisms (Hatchel and Balish, 2008).

3.1. Structure of terminal organelle

Ultrastructure of *M. pneumoniae* terminal organelle has been studied by electron microscopy since the early 70s. First, a rod-like electron-dense structure of around 100 nm by 300 nm surrounded by an electron-lucent layer of cytoplasm was observed by TEM (Biberfeld and Biberfeld, 1970, Wilson and Collier, 1976, Collier and Clyde, 1971). A periodic substructure was also detected to compose the central core of the rod structure. A thin layer of proteins surrounding the terminal organelle was related to the adhesion properties of this organism (Wilson and Collier, 1976). Later, the removal of membrane and cytoplasm using the detergent Triton X-100 allowed to obtain improved images of the rod and other structures including the terminal “knob” or button, as well as the filamentous extensions of cytoskeleton (Gobel et al., 1981, Meng and Pfister, 1980). Ultra-thin sectioning followed by negative staining of *M. pneumoniae* cells allowed the detection of a wheel-like complex at the base of the rod (Regula et al., 2001, Hegermann et al., 2002). Finally, high resolution images of *M. pneumoniae* were taken by electron cryotomography (ECT) and 3D reconstructions of the electron-dense core (Fig. I.3A) are now available (Seybert et al., 2006, Henderson and Jensen, 2006).

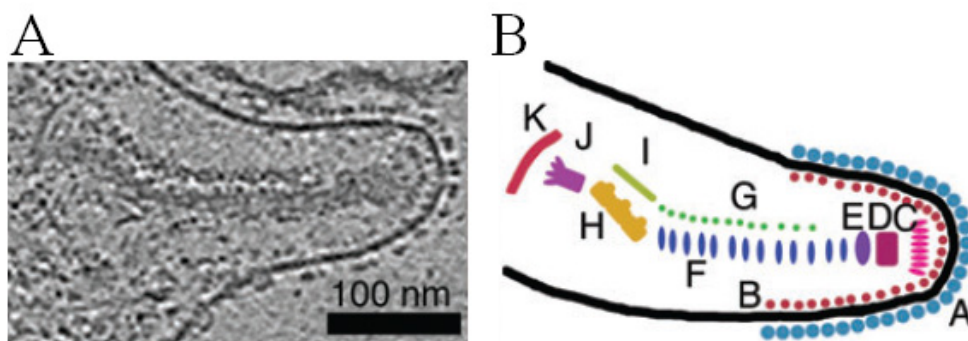


Fig. I.3. Ultrastructure of the terminal organelle of *M. pneumoniae* by electron cryotomography. (A) Tomogram showing the electron-dense core of this microorganism. (B) Schematic of the terminal organelle showing 11 protein structures labelled A-K. Adapted from Henderson and Jensen, 2006.

3.2. Proteins involved in the terminal organelle structure

Up to eleven different protein structures in *M. pneumoniae* terminal organelle were distinguished by ECT (Fig. I.3A). But, specific proteins cannot be already assigned to these structures. However, several mutant strains of *M. pneumoniae* and *M. genitalium* showing deficiencies in terminal organelle structure and functioning have been isolated, thus providing a list of proteins involved in this structure (Pich et al., 2008, Burgos et al., 2008, Jordan et al., 2007, Hasselbring et al., 2006b, Pich et al., 2006a, Burgos et al., 2007). Furthermore, these proteins have been localized with fluorescent fusions or immunofluorescence and assigned to the nap, wheel-like complex, rod or terminal button substructures in one or both species (Seto et al., 2001, Seto and Miyata, 2003, Kenri et al., 2004, Balish et al., 2003, Burgos et al., 2008, Calisto et al., 2012).

The nap

Surrounding the surface of the terminal organelle of *M. genitalium* and *M. pneumoniae*, adhesins are clustered in a nap-like layer (Baseman et al., 1982b, Mernaugh et al., 1993, Seybert et al., 2006, Henderson and Jensen, 2006). P1 and P40/P90 in *M. pneumoniae* and its orthologues P140 and P110 in *M. genitalium* compose their respective naps (Hu et al., 1987, Baseman et al., 1982b). The correct assembly and localization of the nap needed from the participation of many of the cytoskeletal proteins (Pich et al., 2008, Burgos et al., 2007, Willby and Krause, 2002, Willby et al., 2004, Hahn et al., 1998, Cloward and Krause, 2009). Besides being essential for cytoadhesion (Mernaugh et al., 1993, Baseman, 1993, Krause and Baseman, 1983, Krause, 1996), these adhesins have been related to cell invasion and infection (Tully et al., 1983a). Furthermore, they are necessary for the terminal organelle formation and regulate the initiation of new terminal organelles in *M. genitalium* (Burgos et al., 2006, Pich et al., 2009). Whether the nap has an active role in motility or merely participates attaching the cells to the surface is still controversial (Henderson and Jensen, 2006, Seybert et al., 2006, Seto et al., 2005a, Miyata, 2008).

The terminal button or “knob”

This substructure is located at the distal end of the electron-dense core. *M. pneumoniae* P30 protein is a transmembrane protein that localizes at the distal end of the terminal organelle (Seto and Miyata, 2003) and is involved in adherence, motility and terminal organelle development (Relich and Balish, 2011, Dallo et al., 1996, Hasselbring et al., 2005, Romero-Arroyo et al., 1999). Although its *M. genitalium* orthologue P32 (Reddy et al., 1995) has not been studied previously, it localizes also at the terminal button when the coding gene is introduced in a *M. pneumoniae* P30 null mutant by transposition and restores the WT phenotype. Hence, a very similar function of these proteins is expected in both mycoplasmas (Relich and Balish, 2011).

M. genitalium MG217 and its *M. pneumoniae* orthologue protein P65 also localize at the distal end of the terminal organelle (Burgos et al., 2008, Kenri et al., 2004, Seto and Miyata, 2003). The stability and proper localization of P65 require a full complement of P30 and HMW3 (Willby and Krause, 2002, Jordan et al., 2001). Although P65 has been located at the outer side of cell membrane (Jordan et al., 2001), MG217 is found completely inside *M. genitalium* cells (Burgos et al., 2008). P65 mutants of *M. pneumoniae* show a dramatic decrease in cell motility (Hasselbring et al., 2012). In contrast, MG217 has been related to the curvature of the terminal organelle and the direction of movement (Burgos et al., 2008).

It is reported that MG317 and HMW3 orthologue proteins, respectively in *M. genitalium* and *M. pneumoniae*, also localize at the terminal button (Stevens and Krause, 1992, Seto et al., 2001). These proteins anchor the terminal button to the electron-dense core (Pich et

al., 2008) and stabilize both the terminal button and the rod (Pich et al., 2008, Stevens and Krause, 1992, Willby and Krause, 2002).

The rod or core

M. genitalium MG218 protein and *M. pneumoniae* HMW2 are the main components of their respective rods (Pich et al., 2008, Balish et al., 2003, Kenri et al., 2004, Bose et al., 2009). The rod is located at the central part of the electron-dense core and consists in two segmented paired plates (Fig.1.3). These proteins are crucial in the development of the respective terminal organelles and a properly assembled core prevents the proteolytic degradation of many cytoskeletal proteins (Pich et al., 2008, Fisseha et al., 1999, Popham et al., 1997, Krause and Balish, 2004). For this reason, they also have been related to cytodherence and motility (Pich et al., 2008, Krause et al., 1997, Dhandayuthapani et al., 1999, Dhandayuthapani et al., 2002).

A small version of MG218 and HMW2 of approximately 25 kDa corresponding in sequence to the C-terminal of these proteins has been reported in both species (Krause et al., 1997, Fisseha et al., 1999, Pich et al., 2008). These small proteins are translated from a transcript directed by two internal promoters located inside the MG_218 and MPN310 genes, respectively (Boonmee et al., 2009, Broto, Unpublished). It has been suggested that these proteins are involved in the structure of the protein network of the rod (Balish et al., 2003).

HMW1 protein is also a main component of the rod in *M. pneumoniae* (Seto and Miyata, 2003). HMW1 is a membrane-associated protein (Balish et al., 2001) essential for rod assembly by stabilizing HMW2 protein (Willby et al., 2004, Krause and Balish, 2001). Hence, HMW1 is essential for terminal organelle development and normal cell morphology (Layh-Schmitt et al., 1995, Willby et al., 2004) and is a key component for cytodherence as it is involved in adhesin trafficking to the cell membrane (Hahn et al., 1998). The HMW1 ortholog in *M. genitalium* MG312 is also involved in rod assembly and cytodhesion but it has also been reported that its N-terminal is involved in locomotion (Burgos et al., 2007). In this way, both MG312 and HMW1 possess an Enriched in Aromatic and Glycine Residues (EAGR) box close to the N-terminus, a domain that has been found in proteins related with cell motility (Balish et al., 2001, Burgos et al., 2007, Calisto et al., 2012, Pich et al., 2006a). *M. genitalium* MG312 has not been found associated to the cell membrane (Parraga-Nino et al., 2012).

The wheel-like complex

Wheel-like complex is a structure located at the proximal end of the terminal organelle. *M. pneumoniae* P200 protein was localized in this area of the terminal organelle and was related to motility and cell invasion (Jordan et al., 2007). Similarly, its *M. genitalium* ortholog

MG386 is involved in cell motility (Pich et al., 2006a) and, interestingly, both proteins include several EAGR boxes.

Proteins MG200 and TopJ are orthologue proteins in *M. genitalium* and *M. pneumoniae*, respectively, located at the wheel-like complex (Cloward and Krause, 2009, Calisto et al., 2012), which also contain EAGR boxes (Cloward and Krause, 2010, Pich et al., 2006a). These multidomain proteins are involved in cytodherence and motility (Cloward and Krause, 2009, Pich et al., 2006a, Calisto et al., 2012, Broto, Unpublished) and contain a J domain at the N-terminus suggesting that they have a role as co-chaperones (Cloward and Krause, 2010). It has been proposed that TopJ protein is related to adhesin folding and trafficking, which could explain the involvement of these proteins in cytodherence and motility (Cloward and Krause, 2011).

Protein P41 of *M. pneumoniae* has been localized also at the wheel-like complex (Kenri et al., 2004). A mutant strain of *M. pneumoniae* lacking this protein showed motile terminal organelles that detach from the cell body and move for short periods of time, indicating that P41 is essential for anchoring the terminal organelle to the cell body (Hasselbring and Krause, 2007a). Also, P41 is one of the earliest proteins that localizes in developing terminal organelles (Hasselbring et al., 2006a). Up to date, the role of P41 *M. genitalium* ortholog, MG491 protein, remains unknown.

Finally, protein P24 of *M. pneumoniae* also participates in the wheel-like complex (Kenri et al., 2004). This protein participates in gliding motility by regulating the activation of the motor after cell division (Hasselbring and Krause, 2007b). No orthologs have been found in *M. genitalium*. However, MG_219 gene is located at the same locus in the cytodherence regulatory operon *crl* (Hedreyda and Krause, 1995, Reddy et al., 1996, Kenri et al., 2004) and codes for the MG219 protein, which shows a similar function in the regulation of motility than P24 (González-González, Unpublished).

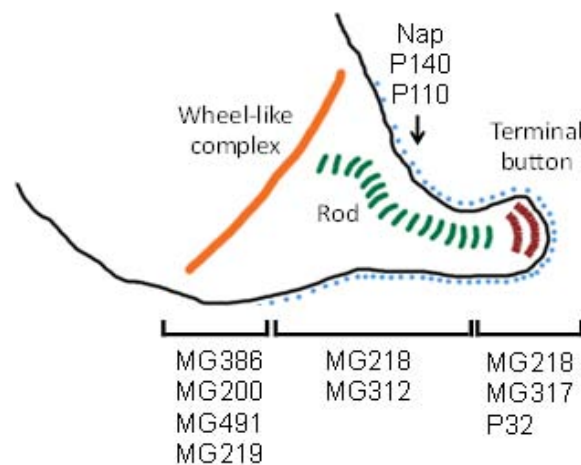


Fig. I.4. Outline with the ultrastructure of the terminal organelle in *M. genitalium*.

Table I.2. Table of orthologue correspondences between terminal organelle proteins of *M. genitalium* and *M. pneumoniae* and their role.

<i>M. genitalium</i>			<i>M. pneumoniae</i>		Sequence	
Locus Tag ^a	Locus Tag ^b	Protein	Locus Tag ^c	Protein	identity (%)	Role
MG_191	MG_RS01075	P140	MPN141	P1	45.4	Adhesion
MG_192	MG_RS01080	P110	MPN142 ^d	P40/P90	50.2	Adhesion
MG_200	MG_RS01130	MG200	MPN119	TopJ	34.9	Motility
MG_217	MG_RS01275	MG217	MPN309	P65	41.6	Motility
MG_218	MG_RS01280	MG218	MPN310	HMW2	57.0	Motility/Adhesion
MG_219	MG_RS01285	MG219	MPN312	P24 ^e	15.9	Unknown
MG_312	MG_RS01865	MG312	MPN447	HMW1	32.9	Motility/Adhesion
MG_317	MG_RS01890	MG317	MPN452	HMW3	33.5	Motility/Adhesion
MG_318	MG_RS01895	P32	MPN453	P30	43.2	Adhesion
MG_386	MG_RS02355	MG386	MPN567	P200	29.7	Motility
MG_491	MG_RS01285	MG491	MPN311	P41	53.7	Unknown

^a Names according to the *M. genitalium* G37 genome sequence with accession number L43967.2

^b Names according to the *M. genitalium* G37 genome sequence with accession number NC_000908.2

^c Names according to the *M. pneumoniae* M129 genome sequence with accession number NC_000912.1

^d Protein product of MPN142 is post-translationally cleaved in *M. pneumoniae*

^e MG_219 gene cannot be considered an ortholog of MPN312.

3.3. Motility of mycoplasmas

As discussed above, the terminal organelle of *M. genitalium* and related mycoplasmas is involved in cytoadherence and host cell invasion, which are central functions regarding their parasitic lifestyle. Furthermore, the terminal organelle is essential for the locomotion of many mycoplasma species (Hasselbring and Krause, 2007a, Miyata, 2010). Besides an obvious role in the spreading of mycoplasma cells, cell motility has also an important role in the infection of host cells (Jordan et al., 2007, Prince et al., 2014) and cell division (Hasselbring et al., 2006a, Seto et al., 2001, Lluch-Senar et al., 2010).

Motile mycoplasmas slide over solid surfaces without using flagella, pili or other motile machineries common in the bacterial world (McBride, 2001, Jarrell and McBride, 2008). This movement is highly dependent on adhesion to a solid surface. This sliding movement is known as gliding motility and is not restricted to the mycoplasma genus, i.e. *Flavobacterium johnsoniae*, *Myxococcus xanthus* or *Synechocystis* sp. also glide on solid surfaces (McBride, 2001). However, the mechanisms by which mycoplasmas glide are different from any of these species. Even, different engines for gliding motility have been proposed in the different species of mycoplasma (Miyata, 2008).

Gliding motility has been detected in 13 mycoplasma species, including 7 out of the 8 mycoplasma species of the *pneumoniae* cluster, with the only non-motile bacterium *Mycoplasma alvi*. Mean speeds of this cluster range from 28 nm s⁻¹ for *Mycoplasma pirum* to 2 970 nm s⁻¹ of *Mycoplasma testudinis* (Hatchel and Balish, 2008). It has been reported that mycoplasma cells glide towards the direction of the terminal organelle (Miyata, 2010, Burgos et al., 2008) and that this tip structure contains the entire motile machinery (Hasselbring and Krause, 2007a).

The motile machinery of *Mycoplasma mobile* is the best characterized for any mycoplasma species. This fish pathogen belongs to the *sualvi* cluster and proteins involved in motion share no homology with those of the *pneumoniae* cluster (Nakane and Miyata, 2007). Furthermore, *M. mobile* glides faster (4.5 μm s⁻¹) than any other known mycoplasma (Miyata, 2010). The tip structure of *M. mobile* is supported by a jellyfish-like cytoskeleton (Nakane and Miyata, 2007) and is also involved in gliding motility (Nakane and Miyata, 2012, Uenoyama et al., 2004). Four proteins are involved in *M. mobile* gliding: Gli521, Gli349, Gli123 and P42, which are located together at the base of the tip structure, called the neck. These proteins arrange as spike-like structures of approximately 50 nm long that are responsible of the cell adhesion (Miyata and Petersen, 2004). It has been reported that Gli123 is the responsible for the proper localization of the trimeric complex composed by Gli123, Gli349 and Gli521 (Uenoyama and Miyata, 2005b). Gli349 is the main adhesin of this microorganism and the different conformations shown by this protein suggest that Gli349 propel the cells by repeated catching, binding and releasing sialylated compounds

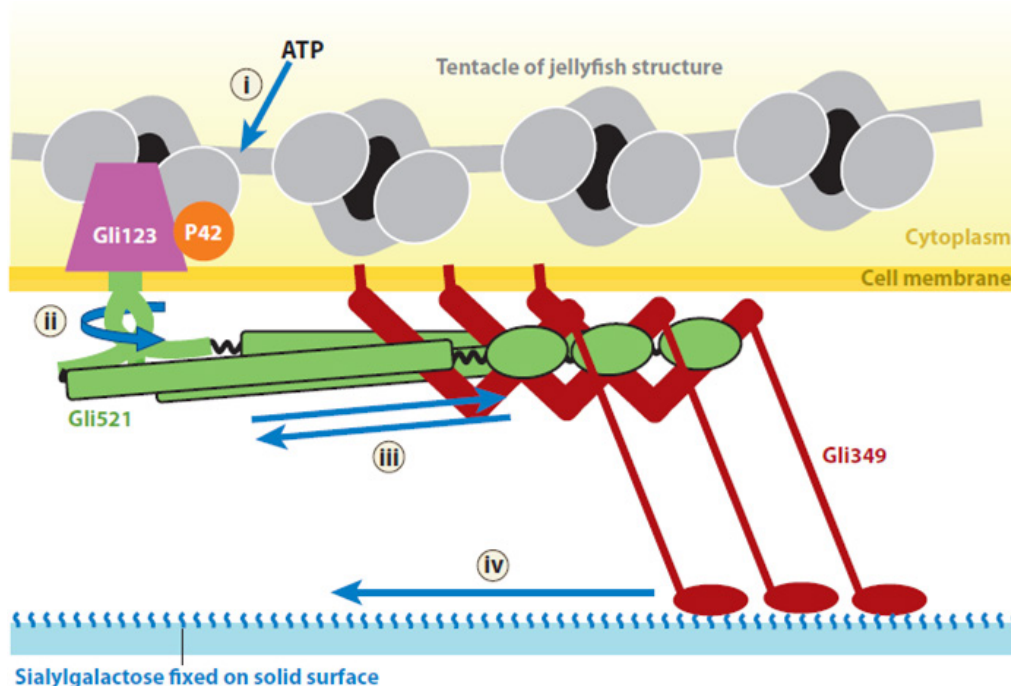


Fig. I.5. Schematic of the assembled gliding machinery of *M. mobile*. (i) ATP is hydrolysed by P42 to generate movement. (ii) Gli521 changes its conformation. (iii) The conformational change is transmitted to Gli349. (iv) Gli349 is attached to the sialylgalactose fixed on the surface and propels the cell through its conformational changes. This schematic was obtained from Miyata, 2010.

found at the gliding surface (Kasai et al., 2013, Adan-Kubo et al., 2006, Nagai and Miyata, 2006, Lesoil et al., 2010, Uenoyama et al., 2009). For this reason, Gli349 is known as the leg protein of *M. mobile*. Within this model, Gli521 act as a gear protein and is the responsible of the Gli349 conformational changes (Seto et al., 2005b, Uenoyama et al., 2009). Finally, the P42 nucleoside triphosphatase is a good candidate to be the motor for gliding motility (Ohtani and Miyata, 2007, Uenoyama and Miyata, 2005a, Tulum et al., 2014).

An adhesin-driven mechanism has also been suggested to explain motility of mycoplasmas from the *pneumoniae* cluster. In agreement with this “centipede” model, *M. pneumoniae* cells stopped in presence of P1 adhesin antibodies just before they were released from the glass surface (Seto et al., 2005a). This evidence is weak as gliding motility is highly dependent on adhesion.

Alternative models for motility of *M. pneumoniae* and related mycoplasmas highlight the role of the cytoskeletal proteins in the generation of movement. Firstly, it was proposed that the rod component of the terminal organelle drives the motion of the cell by repeated longitudinal shortenings and extensions (Wolgemuth et al., 2003). Further studies of *M. pneumoniae* electron-dense cores by ECT revealed different stages of rod bending (Seybert et al., 2006), and different conformation of the segments composing the rod (Henderson and Jensen, 2006) rather than different rod lengths. This supports an “inchworm” model for mycoplasma gliding motility, by which the rod component propels the cell by repeated bending changes (Seybert et al., 2006, Henderson and Jensen, 2006, Miyata, 2008). The “inchworm” model is currently accepted among the mycoplasma community to explain gliding motility for *M. pneumoniae* and *M. genitalium*, but the evidence supporting this model is weak as it does not demonstrate whether rod bending is in the origin, or alternatively, is the consequence of gliding motility. Mycoplasmas from the *pneumoniae* cluster possess rods with different lengths that are not correlated with the velocity of the respective mycoplasmas, which argues against this model (Hatchel and Balish, 2008).

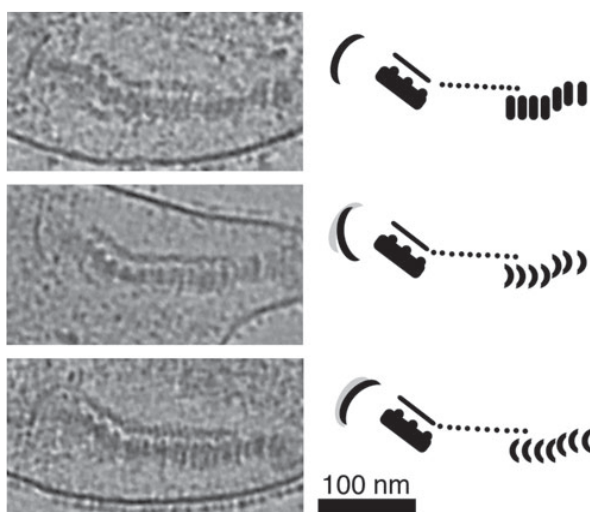


Fig. 1.6. Electron cryotomography pictures and schematic of the different conformations of the segments in the rod. This figure was obtained from Henderson and Jensen, 2006.

In conclusion, the mechanism of gliding motility in both *M. pneumoniae* and *M. genitalium* is still unclear and controversial. The complex interplay between the proteins involved in cytoadhesion and motility and the mutual co-stabilization of these proteins preclude the easy understanding of the motile mechanism. For example, the stability, trafficking and localization of adhesins are highly dependent on proteins of the cytoskeleton (Pich et al., 2008, Burgos et al., 2007, Willby and Krause, 2002, Hahn et al., 1998, Cloward and Krause, 2011). Similarly, these adhesins are needed to assemble the terminal organelle by stabilizing the cytoskeleton and attaching the cells to the surface (Burgos et al., 2006).

3.4. Implication of the terminal organelle in cell division

Cell division in mycoplasmas with terminal organelle is initiated by the duplication of this structure (Bredt, 1968). In this way, *M. pneumoniae* cells with more than one terminal organelle show increased DNA content (Seto et al., 2001). Cell division begins when a new terminal organelle is developed close to the pre-existing one and gliding motility ceases (Hegermann et al., 2002, Hasselbring et al., 2006a, Bredt, 1968). Newly synthesized terminal organelle proteins assemble the new electron-dense core in a hierarchical order by a still poorly understood mechanism (Hasselbring et al., 2006a, Krause and Balish, 2004). It has been reported that P41 protein from *M. pneumoniae* appears early in terminal organelle development, even before the cell stops gliding movement (Hasselbring et al., 2006a) and also plays a role in the localization of the nascent terminal organelle (Hasselbring and Krause, 2007a). Contrary, *M. pneumoniae* P30 and P65 appear late during the terminal organelle development (Hasselbring et al., 2006a), suggesting that the assembly of new electron-dense cores begins by the wheel-like structure.

Once the terminal organelle is duplicated and the new structure attaches to the surface, the pre-existing terminal organelle recovers the gliding ability, thus separating the two terminal organelles at the different poles of the cell (Hasselbring et al., 2006a). Finally, the new terminal organelle becomes motile and it has been suggested that this gliding motility at opposite directions may help in segregation of daughter cells favouring cytokinesis (Lluch-Senar et al., 2010).

M. pneumoniae is able to produce more than one terminal organelle before cytokinesis and gliding restoration (Hasselbring et al., 2006a), suggesting that this microorganism may initiate multiple cell division cycles simultaneously. In contrast, cells bearing multiple terminal organelles are rarely observed in *M. genitalium*. Even in gliding deficient strains with impaired cytokinesis, the frequency of cells showing multiple terminal organelles is very low, suggesting the presence of a mechanism regulating the development of nascent terminal organelles (Pich et al., 2009). This temporal regulation in *M. genitalium* that prevents the presence of multiple terminal organelles seems to be coordinated by P110 adhesin (Pich et al., 2009).

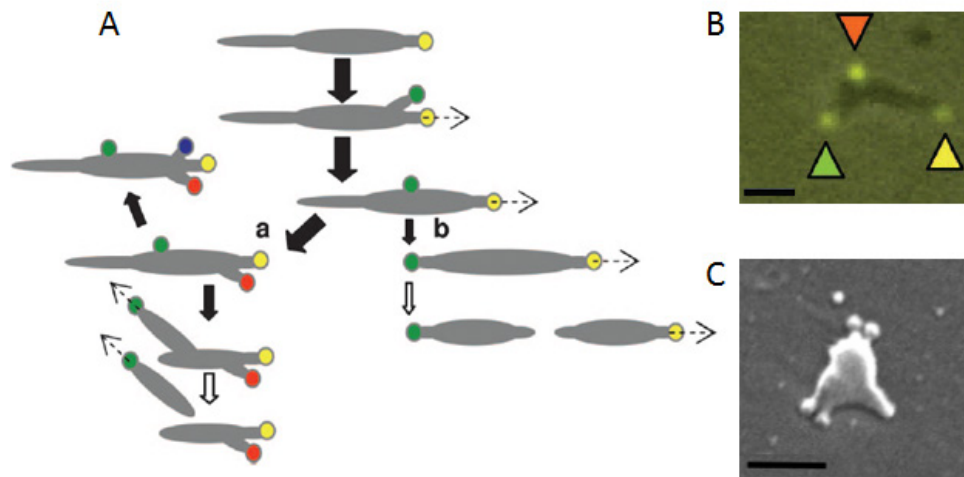


Fig. 1.7. (A) Cell division in *M. pneumoniae*. More than one terminal organelle might appear before cytokinesis (a) or undergo a complete cell cycle before starting a new one (b). (B) *M. pneumoniae* cell showing three different P41 foci (arrow heads) revealing the presence of three terminal organelles. (C) *M. genitalium* mutant strain T192 lacking P110 adhesin and showing four terminal organelles. Bar is 1 μ m in (B) and 0.5 μ m in (C). Adapted from Hasselbring 2006a and Pich, 2009.

However, mutant strains of both *M. genitalium* and *M. pneumoniae* showing strong deficiencies in gliding motility and even lacking the terminal organelle structure have been isolated (Willby et al., 2004, Hasselbring et al., 2005, Pich et al., 2006a, Burgos et al., 2006), indicating that gliding motility is not essential for cytokinesis.

Chapter 1

1. Obtaining a MG_491 null mutant strain of *M. genitalium* and perform a phenotype analysis of this strain.
2. Confirm the presence and localize remaining cytoskeletal elements inside this strain by using a fluorescence fusion of P32 as a marker protein.
3. Gain a better understanding of the mechanism of *M. genitalium* gliding motility.

Chapter 2

4. Examine the role of MG491 several domains in the structure of the terminal organelle and gliding motility.
5. Investigate the biological role of the MG491 organization by characterizing *M. genitalium* strains carrying mutations in residues with special relevance in MG491 3D structure.
6. To investigate the role of the MG491-MG200 interactions in gliding motility and terminal organelle structure.

Chapter 3

7. Develop a new method to quantitatively and precisely measure the hemadsorption activity of mycoplasma strains.
8. Provide a mathematical model for the attachment of mycoplasma cells to erythrocytes.
9. Determine how the binding kinetic constants are related to specific binding deficiencies in mycoplasma strains.
10. Compare the adhesion properties of several mycoplasma strains.

Chapter 1: Gliding Motility in Electron-Dense Deficient Mutants of *Mycoplasma genitalium*

The cell-wall less bacterium *Mycoplasma genitalium* uses specialized adhesins located at the terminal organelle to adhere to host cells and surfaces. The terminal organelle is a polar structure protruding from the main cell body that is internally supported by a cytoskeleton and also has an important role in cell motility. We have engineered a *M. genitalium* null mutant for MG491 protein showing a massive downstream destabilization of proteins involved in the terminal organelle organization. This mutant strain exhibited striking similarities with the previously isolated MG_218 null mutant strain. Upon introduction of an extra copy of MG_318 in both strains, the amount of main adhesins dramatically increased. These strains were characterized by microcinematography, fluorescent microscopy and cryo-electron microscopy, revealing the presence of motile cells and filaments in the absence of many proteins previously considered essential for proper cell adhesion and motility. These results indicate that adhesin complexes play a major role in the motile machinery of *M. genitalium* and demonstrate that the rod element of the cytoskeleton core is not the molecular motor propelling mycoplasma cells. These strains containing a minimized motile machinery also provide a valuable cell model to investigate the adhesion and gliding properties of this human pathogen.

Chapter 2: *Mycoplasma genitalium* Strains with Relevant Mutations in the Structure and Function of MG491 Protein

The crystal structure of *M. genitalium* MG491 protein has been recently determined. The MG491 molecule is a tetramer presenting a unique organization as a dimer of structural heterodimers. The asymmetric arrangement results in two very different intersubunit interfaces, which can explain the formation of only 50% of the disulphide bridges between Cys87 residues. *M. genitalium* cells with a point mutation in the MG_491 gene causing the change Cys87 to Ser present a drastic reduction in motility, while preserving normal levels of terminal organelle proteins. Similarly, other *M. genitalium* strains with mutations affecting the quaternary structure as well as the C-terminal peptide involved in the interaction with MG200 have also shown significant changes in gliding motility. However, the *M. genitalium* strain with MG491 N-terminal deletion showed a massive downstream destabilization of terminal organelle proteins. The results in this work indicate that MG491 protein is involved in the stability and anchoring of the *M. genitalium* terminal organelle and plays a particular role in gliding motility.

Chapter 3: Quantitative Hemadsorption Assay for Mycoplasma Species using Flow Cytometry

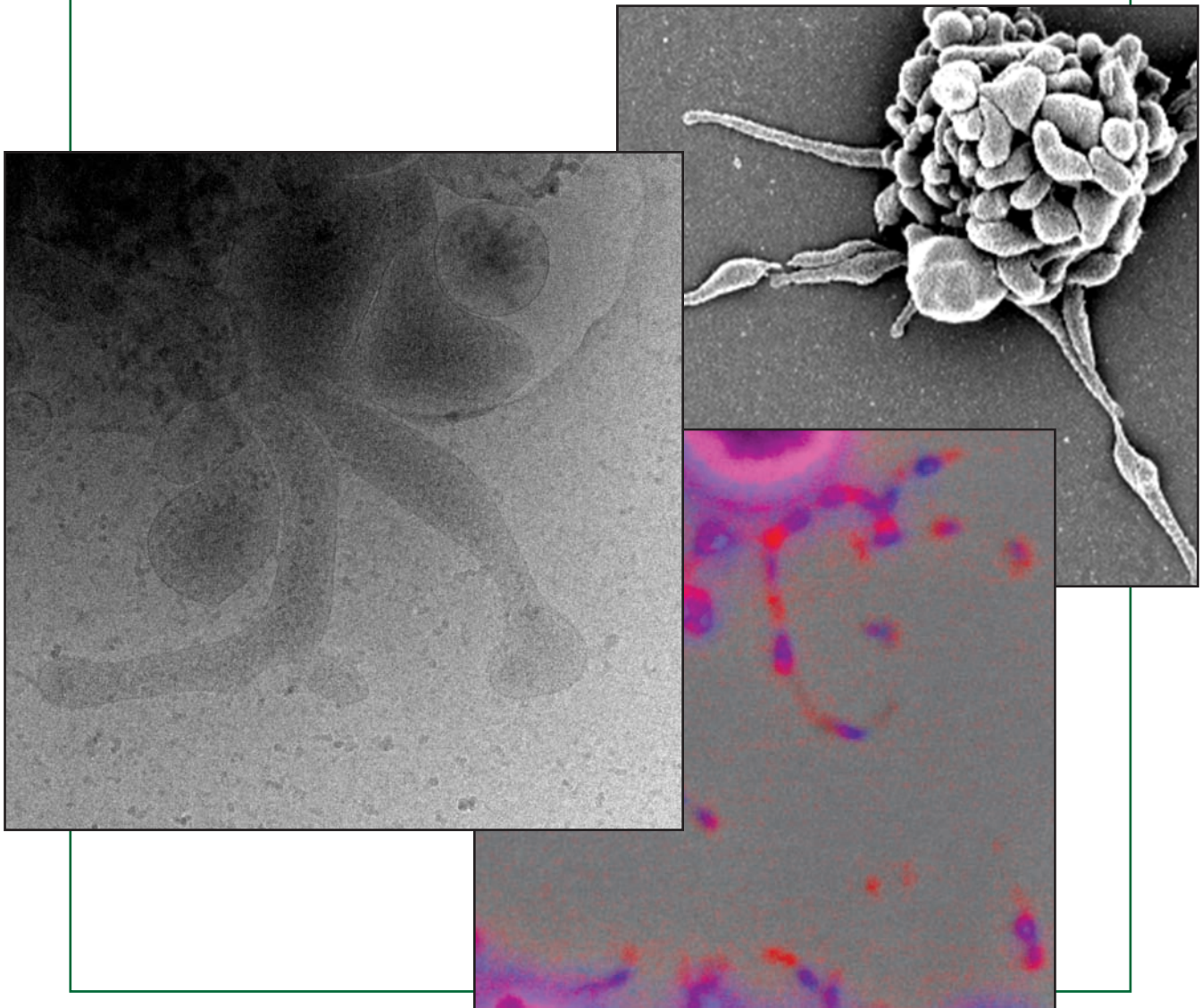
A number of adherent mycoplasmas have developed highly complex polar structures that are involved in diverse aspects of the biology of these microorganisms and play a key role as virulence factors by promoting adhesion to host cells in the first stages of infection. Attachment activity of mycoplasma cells has been traditionally investigated by determining their hemadsorption ability to red blood cells and it is a distinctive trait widely examined when characterizing the different mycoplasma species. Despite the fact that protocols to qualitatively determine the hemadsorption or hemagglutination of mycoplasmas are straightforward, current methods when investigating hemadsorption at the quantitative level are expensive and poorly reproducible. By using flow cytometry, we have developed a procedure to quantify rapidly and accurately the hemadsorption activity of mycoplasmas in the presence of SYBR Green I, a vital fluorochrome that stains nucleic acids, allowing to resolve erythrocyte and mycoplasma cells by their different size and fluorescence. This method is very reproducible and permits the kinetic analysis of the obtained data and a precise hemadsorption quantification based on standard binding parameters such as the dissociation constant K_d . The procedure we developed could be easily implemented in a standardized assay to test the hemadsorption activity of the growing number of clinical isolates and mutant strains of different mycoplasma species, providing valuable data about the virulence of these microorganisms.

Gliding Motility in Electron-Dense Deficient Mutants of *Mycoplasma genitalium*

Part 1: Characterization of MG_491 null mutant strain.

Part 2: Gliding motility in Δ mg491-P32Ch cells.

Part 3: Characterization of Δ mg218-P32Ch cells.



Introduction

Mycoplasmas are small cell wall-less bacteria that have arisen from Gram-positive ancestors by genome reduction (Woese et al., 1980, Sirand-Pugnet et al., 2007). Due to their small genomes, these microorganisms possess limited metabolic pathways and have adopted a parasitic lifestyle, obtaining most of the essential nutrients from the host (Pollack et al., 1997, Razin et al., 1998b). Many mycoplasmas are also pathogens of a wide range of animals and plants, and a number are characterized by the presence of polar structures exhibiting uncommon complexity in the bacterial world. These polar structures, which have received a panoply of different names in the different mycoplasma species (e.g. bleb, tip structure, attachment organelle, terminal organelle, membrane protrusion), have a pivotal role in the virulence of these microorganisms. They assist the cells in adhesion and further invasion of the host cells (Jensen et al., 1994, Krunkosky et al., 2007, Krause et al., 1982), play a relevant function in cell division (Lluch-Senar et al., 2010, Bredt, 1968, Hasselbring et al., 2006a) and contain the molecular motor that propels and directs the cells to glide on solid surfaces (Miyata, 2010, Hasselbring and Krause, 2007a, Burgos et al., 2008).

Mycoplasma genitalium is the causative agent of non-chlamydial and non-gonococcal urethritis (Deguchi and Maeda, 2002, Horner et al., 1993, Totten et al., 2001) and other genital inflammatory diseases (Dehon and McGowin, 2014, Haggerty and Taylor, 2011, Manhart et al., 2003). Belonging to the *pneumoniae* cluster, *M. genitalium* is indeed an excellent model to study the molecular mechanisms involved in virulence and pathogenicity. Besides the interest as a human pathogen, this small flask-shaped bacterium with a genome of only 580 kb has attracted the interest of many researchers as a natural approach to a minimal cell (Fraser et al., 1995, Hutchison et al., 1999). Unlike many mycoplasma species, methods for targeted gene deletion are available in *M. genitalium* (Burgos et al., 2006, Dhandayuthapani et al., 1999) making it possible to obtain well characterized mutant strains showing gliding deficiencies, loss of the adhesion properties and structural changes in the terminal organelle (Burgos et al., 2007, Burgos et al., 2008, Calisto et al., 2012, Pich et al., 2008). Besides this, two terminal organelle proteins, MG386 and MG200, involved preferentially in cell motility but not in cell adhesion were identified by transposon mutagenesis (Pich et al., 2006a). Moreover, *M. genitalium* genes show high identity degree with their orthologues in the closely related human pathogen *Mycoplasma pneumoniae*, suggesting many similarities in virulence mechanisms such as gliding motility (Hatchel and Balish, 2008).

Several proteins of *M. pneumoniae* and *M. genitalium* have been localized in the terminal organelle using immunochemistry and fluorescent fusions (Calisto et al., 2012, Hasselbring et al., 2006a, Kenri et al., 2004, Seto et al., 2001). Terminal organelles are internally supported by a complex electron-dense cytoskeleton (Hegermann et al., 2002, Meng and Pfister, 1980, Regula et al., 2001). Several distinctive components of *M. pneumoniae* cytoskeleton have

been identified and characterized by electron cryotomography: a terminal knob or terminal button at the distal end of the internal cytoskeleton; a rod containing segmented paired plates in the central part of the internal cytoskeleton; and a wheel-like or bowl complex at the proximal end of the cytoskeleton close to the cell body (Hegermann et al., 2002, Henderson and Jensen, 2006, Miyata, 2008, Seybert et al., 2006). Furthermore, it was also identified a nap structure containing the main adhesins surrounding the cell membrane. Since conformational variants of the rod component were detected by electron cryotomography, it was suggested that repeated changes between the different conformations might generate the cell movement by an inchworm like mechanism (Henderson and Jensen, 2006, Miyata, 2008, Seybert et al., 2006). However, blocking *M. pneumoniae* P1 adhesin with antibodies stopped cell movement just before those cells were detached from the surface (Seto et al., 2005a). Moreover, no correlation has been found between electron-dense core size and gliding properties when comparing different mycoplasma species (Hatchel and Balish, 2008). These views support that movement could be achieved in a similar way as a centipede, which is the movement model proposed for *Mycoplasma mobile* gliding. In this mycoplasma species it is thought that leg proteins move the cells by repeated catching, binding and releasing the substrate (Adan-Kubo et al., 2006, Kasai et al., 2013, Miyata, 2010). However, no direct evidence is currently available supporting any movement model for mycoplasmas belonging to the *pneumoniae* cluster.

In this work, we have engineered a null *M. genitalium* mutant strain for the MG_491 gene, coding for a protein which is expected to localize in the wheel-like component of the cytoskeleton (Kenri et al., 2004). The phenotype of this strain showed a massive downstream destabilization of structural proteins involved in the terminal organelle organization and shared many similarities with a previously isolated MG_218 deficient strain (Pich et al., 2008). Upon the introduction in both strains of an extra copy of MG_318 gene, coding for the cytoadherence related protein P32 (Reddy et al., 1995), the levels of the main adhesins increased dramatically. These strains also generated motile filaments and cells in the absence of the major cytoskeletal proteins, highlighting the role of the adhesins in gliding motility and revealing that many cytoskeletal proteins, previously considered critical for terminal organization and motility, are not essential for movement generation in this otherwise minimalized microorganism. These results also provide the first direct evidence that the rod component of the terminal organelle is not essential for gliding motility.

Results

Part 1: Characterization of MG_491 null mutant strain

1.1. Isolation of Δ mg491 strain by homologous recombination

M. genitalium Δ mg491 null mutant strain was obtained by gene replacement using the *tetM438* selectable marker (Fig. 1.1A). We isolated four transformant colonies, all showing a single 6.3 kb band by Southern blot consistent with the presence of the intended replacement (Fig. 1.1B,C). One of these transformants (C2) was selected for further analyses. To confirm the replacement, flanking regions sequences of *tetM438* were determined by direct Sanger sequencing of genomic DNA of this mutant (data not shown).

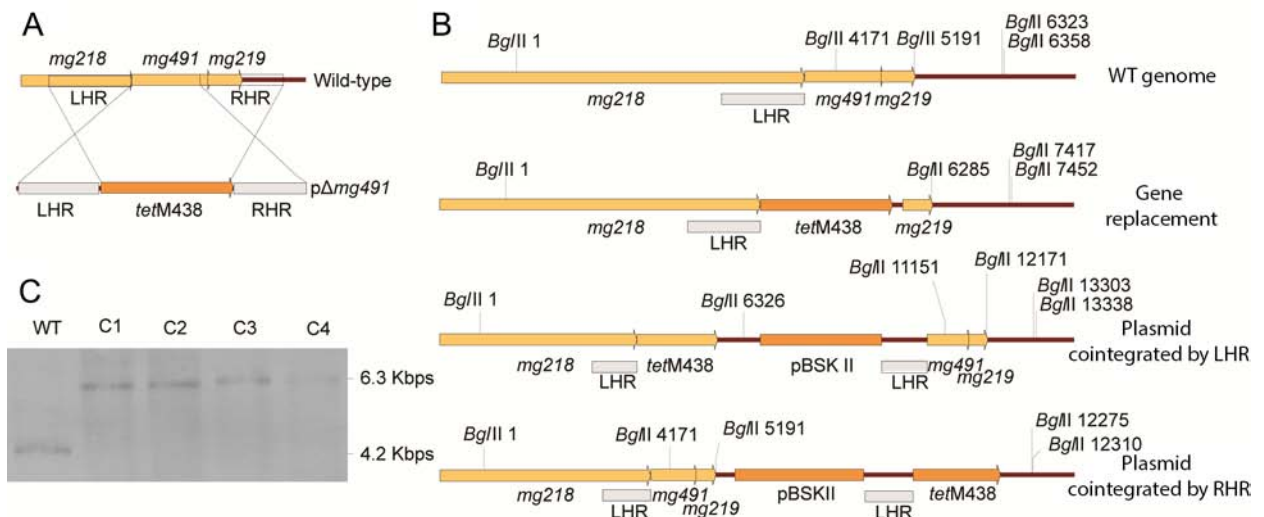


Fig 1.1. Transformation of *pΔmg491* plasmid and analysis of the transformant colonies. (A) Double cross-over recombination events causes *mg491* deletion and *tetM438* insertion. (B) A single 4171-bp band is expected when *Bgl*III digested G37 WT genomic DNA is probed by LHR fragment in a Southern blot. A 6285-bp band is expected when *mg491* is replaced by *tetM438* marker. Two bands of 4825 and 6326 bp would appear in plasmid cointegrates by LHR while two bands of 4171 and 7084 bp would appear in plasmid cointegrates by RHR region. (C) Southern blot showing the presence of the intended deletion in all 4 isolated mutant colonies.

1.2. Additional mutations in the MgPa operon

All four Δ mg491 clones grew in suspension showing big aggregates of cells. This phenotype prompted us to investigate the presence of spontaneous mutations inside the MgPa operon coding for the main adhesins (Burgos et al., 2006, Mernaugh et al., 1993). Genomic DNA from these clones was amplified by three PCRs using R1-R4, R5-R6, and R1-R6 primers, respectively (Fig. 1.2A). These oligonucleotides were designed to detect recombination events between the repetitive sequences found in MgPa operon and in MgPa islands (RC1-6), modifying the length of the amplicons. C2-C4 clones showed amplicons of WT length in the three PCR tests, indicating that no spontaneous recombination in MgPa operon had

happened (Fig. 1.2B). In contrast, C1 clone showed differences in the size of the fragments resulting from amplification with R1-R6 and R1-R4 primers, and no band was detected from the PCR with R5-R6 primers. The analysis of this PCR profile reveals that a double cross-over recombination had occurred in the C1 clone between the RC3 and RC5 regions of the MgPa operon and their homologous regions in MgPa island V, located immediately downstream the MgPa operon (Fig. 1.2C). Hence, non-adhesion growing in clones C2-C4 are only consequence of the intended deletion of MG_491 gene.

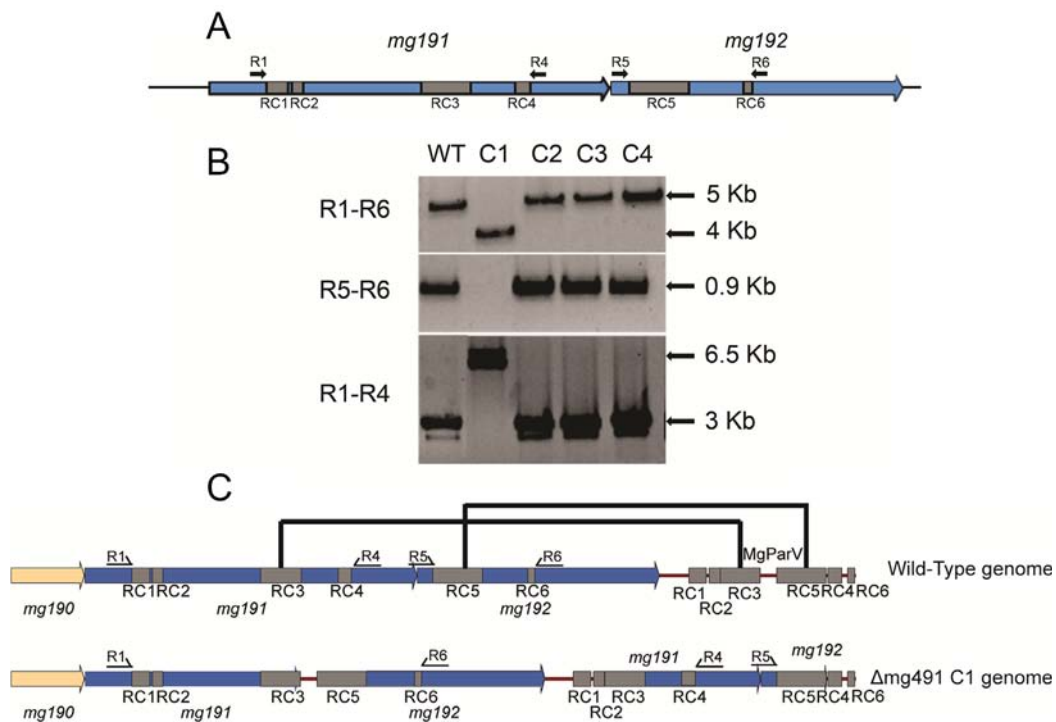


Fig. 1.2. Detection of additional mutations in MgPa operon by PCR. (A) Localization of primers R1, R4, R5 and R6 in *mg191* and *mg192* genes. RC1-RC6 are DNA sequences found also in MgPa islands (B) Amplification of WT G37 and C1-C4 genomic DNA with primers R1-R6, R5-R6 and R1-R4 show a mutation in MgPa operon only in C1 clone. (C) Recombination events between RC3 and RC5 and the corresponding regions in MgPa island V explain the differences in the PCR fragments from C1 clone.

1.3. Downstream destabilization of adhesion related proteins

The absence of MG491 protein in Δ MG491 strain was confirmed by Western Blot using an anti-P41 polyclonal antiserum (Fig. 1.3B). Protein profiles of cells from Δ mg491 strain showed a drastic decrease in the amounts of P110 and P140 adhesins and MG218, MG312 and P32 proteins, and also reduced levels of MG386 protein (Fig. 1.3). These proteins have been found previously involved in the terminal organelle organization of *M. genitalium* (Burgos et al., 2006, Burgos et al., 2007, Pich et al., 2008) and they are, respectively, the orthologs of the *M. pneumoniae* cytoskeletal proteins P1, P40 and P90, HMW2, HMW1, HMW3, P30 and P200 (Burgos et al., 2007, Pich et al., 2008, Willby et al., 2004, Seto and Miyata, 2003). Δ MG491 also showed a decrease of the MG218Ct and MG217 proteins

under the levels of detection (Fig. 1.3). MG218Ct is a 28 kDa polypeptide corresponding to the C-terminal region of MG218 coded by a small ORF located at the 3' end of MG_218 gene (Boonmee et al., 2009). MG217 protein homologous to *M. pneumoniae* P65 is located, together with MG317 and P32, at the distal end of the tip structure (Burgos et al., 2008, Hasselbring et al., 2006a, Jordan et al., 2001, Kenri et al., 2004). MG200, a TopJ orthologous protein, was detected at WT levels in Δ mg491 cells. This protein has a specific role in gliding motility and might be involved in adhesin folding and translocation to the cell membrane (Calisto et al., 2012, Cloward and Krause, 2011, Pich et al., 2006a). MG219 protein was also found at WT levels in Δ mg491 cells indicating that the deletion of MG_491 had no polar effects on the expression of the downstream MG_219 gene (Fig. 1.3).

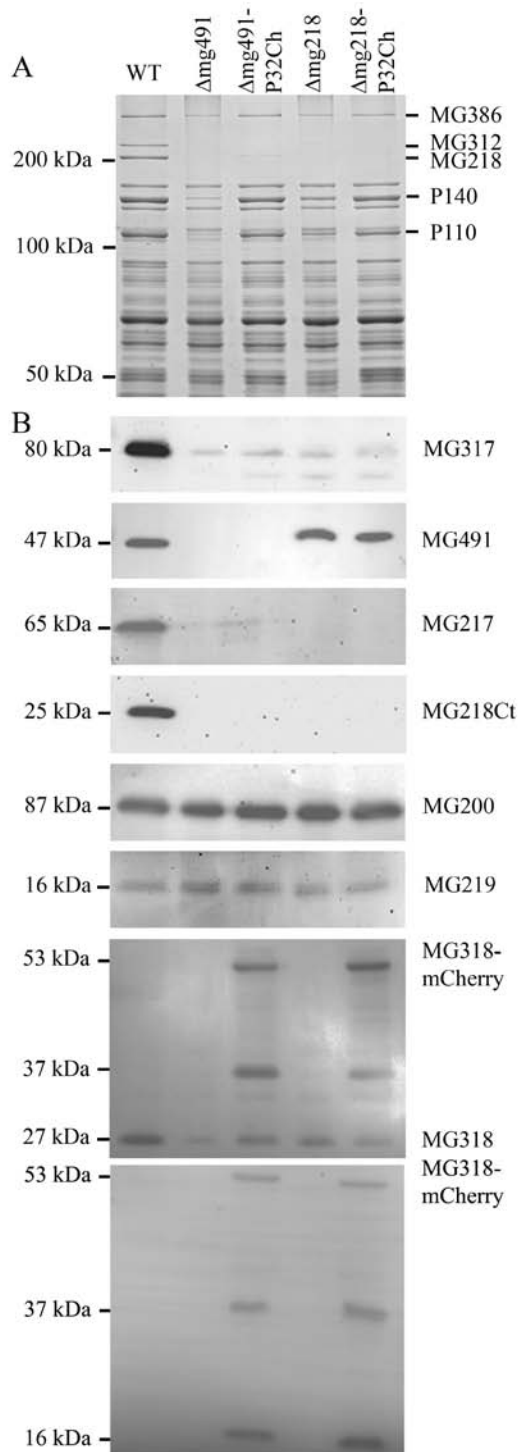


Fig. 1.3. Protein profile and Western immunoblot analysis of the *M. genitalium* G37 WT strain, MG491 null mutants and MG218 null mutants used in this work. (A) Protein profiles of G37 WT strain and mutant strains Δ mg491, Δ mg491-P32ch, Δ mg218 and Δ mg218-P32ch. Bands corresponding to MG386, MG312, MG218 proteins and P110 and P140 adhesins were assessed by their electrophoretic mobility as previously described in (Pich et al., 2008). Size standards are given in the left. Levels of proteins MG312 and MG218 were highly reduced or absent in all mutant strains. P110 and P140 adhesin levels were also very reduced in Δ mg491 and Δ mg218 strains. Δ mg491-P32ch and Δ mg218-P32ch strains showed P110 and P140 adhesin levels about 50% of those found WT G37 strain by densitometric tracings. (B) Western immunoblot analysis to determine the levels MG317, MG491, MG217, MG218Ct, MG200, P32 and MG219 proteins. Levels of most proteins in mutant strains were reduced or absent when compared to those exhibited by the G37 WT strain. Levels of MG491 protein in Δ mg218 and Δ mg218-P32ch strains were similar to those found in the WT G37 strain. MG200 and MG219 levels were similar in all the tested strains. Three bands were detected in Δ mg491-P32ch and Δ mg218-P32ch when tested with a polyclonal anti-P32 serum, being the upper band corresponding to the P32:mCherry fusion and the lower band to the endogenous P32 protein; an intermediate band corresponding to a proteolytic product of the P32:mCherry fusion was also detected. P32-mCherry fusion was also investigated by using anti-mCherry antibodies confirming the presence of two proteolytic bands of 37 kDa and 16 kDa originated by a proteolytic cleavage inside the mCherry protein.

Given the strong impact in the stability of many cytoskeletal proteins upon deletion of MG_491, we examined the adhesion and gliding motility properties of Δ mg491 strain. In agreement with the low amount of the main adhesins, cells from this strain bound poorly to plastic surfaces and red blood cells (Fig. 1.4). In addition, these cells grew as filaments and forming large cell aggregates, making difficult the visualization of single cells by phase contrast microscopy.

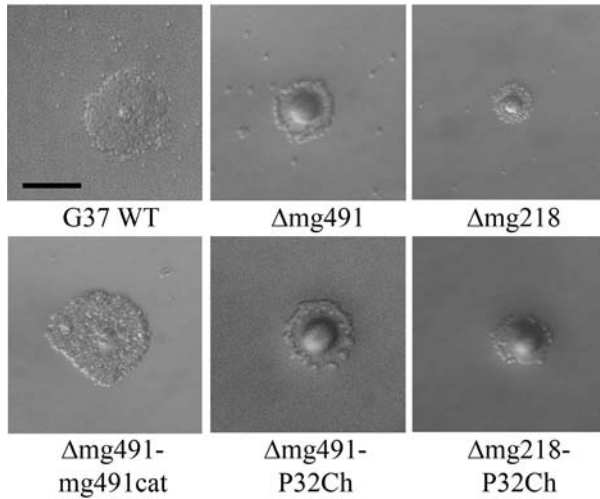


Fig. 1.4. Qualitative hemadsorption assay of *M. genitalium* G37 WT strain and derivative mutant strains. Colonies from G37 WT strain and one isolate of Δ mg491 strain transformed with plasmid pMTnMG491 plasmid were uniformly covered by erythrocytes. In contrast, all the remaining mutant strains showed few or no erythrocytes attached to the colonies. Bar is 100 μ m.

1.4. Filamentous morphology and motility

Upon extended incubation times, some filaments and cell aggregates of Δ mg491 cells were eventually bound to the slides, allowing their examination (Fig. 1.5). No individual cells resembling the WT morphology were observed. Some of these filaments grew by the extension of one of their ends at extremely slow rates and several hours of time lapse cinematography were needed to demonstrate the elongation of these filaments (Fig. 1.6). Cell filaments could be originated by protrusions from the main cell aggregates or, alternatively, by the presence of a rudimentary motile machinery at at one of the ends. In contrast to previous observations in *M. pneumoniae* MPN311 mutant (Hasselbring & Krause, 2007a) no cell particles escaping from the filaments and cell aggregates were detected.

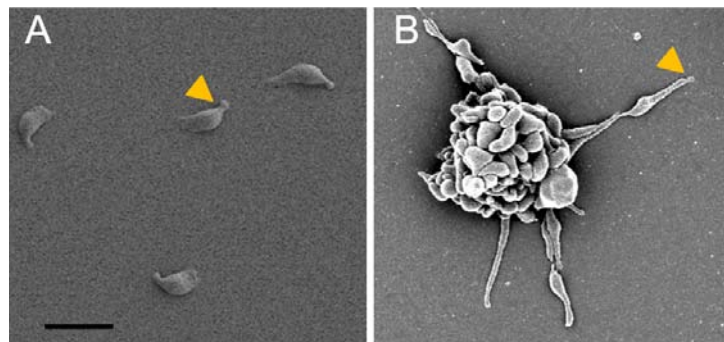


Fig. 1.5. Scanning Electron Microscopy (SEM) images from *M. genitalium* G37 WT and Δ mg491 mutant strain. (A) Cells from G37 WT strain; arrow head points to the terminal organelle of one cell. (B) Cells from Δ mg491-P32ch strain showing the filamentous morphology; arrow head points to the end of one filament. Bar is 1 μ m.

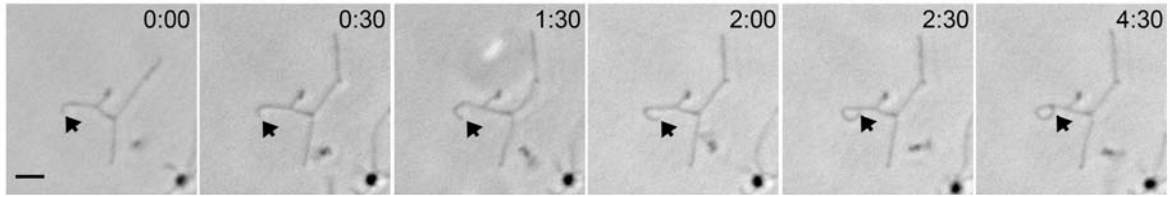


Fig. 1.6. Microcinematography of Δ mg491 strain. Frames were captured at 30 min intervals for 16 h. The arrow points to a filament extension. Time is h:min, bar is 2 μ m.

1.5. Complementation of Δ mg491 null mutants

To exclude the presence of genetic defects in the Δ mg491 strain other than the intended deletion, we engineered a pMTn cat mg491 containing a wild-type copy of MG_491 gene under the control of the MG_438 promoter. This promoter was previously used for efficient expression of genes in *M. genitalium* and for complementation assays (Burgos et al., 2006, Lluch-Senar et al., 2010). Protein profiles were the same as those exhibited by WT cells (Fig. 1.7A) and, consistent with the normal amounts of the cytoskeletal proteins, this transformant also recovered the hemadsorption activity at the same levels than WT G37 strain (Fig. 1.4). Cells of Δ mg491-mg491 cat complemented strain recovered the flask-shape morphology when visualized by scanning electron microscopy (Fig. 1.7B). When examined by phase contrast and time lapse microcinematography, most of the cells glide as single, individual cells with velocities and frequencies similar to those found in the G37 strain. Thus, complementation with a WT MG_491 allele demonstrates that the complex phenotype of Δ mg491 cells is triggered only by the absence of MG491 protein.

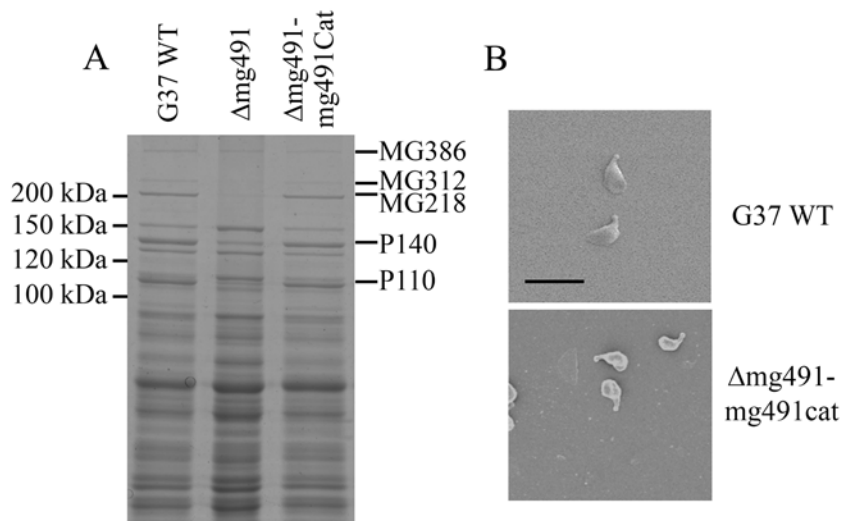


Fig. 1.7. Complementation of Δ mg491 strain by transformation with pMTn cat mg491. (A) Protein profiles of *M. genitalium* G37 WT, Δ mg491 and Δ mg491-mg491 cat showing the reduced levels of the main cytoskeleton proteins and adhesins in Δ mg491 strain and the recovery to normal levels in Δ mg491-mg491 cat strain. (B) Cells from G37 WT and Δ mg491-mg491 cat strains show the same flask-shape appearance by SEM.

Part 2: Gliding motility in Δ MG491-P32Ch cells

2.1. Characterization of the motile machinery in the filaments

The observed growing filaments might be originated by the presence of a rudimentary motility machinery at one of their ends. To address this hypothesis, we were prompted to investigate the presence of that machinery by using a fluorescent mCherry-P32 fusion as a marker protein. Similar fluorescent fusions have been used as markers for terminal organelle development in *M. pneumoniae* (Hasselbring et al., 2006a, Hasselbring and Krause, 2007a, Hasselbring and Krause, 2007b). After introducing an extra copy of P32 fused to mCherry, protein profile of Δ mg491-P32ch cells was assessed by SDS-PAGE and Western blot (Fig. 1.3). Two new bands of 53 kDa and 37 kDa were detected by using anti-P32 antibodies. While the 53 kDa band is in agreement with the expected mass of P32:mCherry fusion protein, the 37 kDa band could be a proteolysis product, indicating that this fusion is not completely stable when introduced to *M. genitalium*. Remarkably, it was also detected an increase in the amounts of P32 protein, suggesting that the fusion may stabilize the P32 protein in cells or alternatively that the P32 protein was itself one of the proteolysis products of the fluorescent fusion. By using anti-mCherry antibodies, we excluded that the increased levels of P32 in Δ mg491-P32ch were the consequence of a limited proteolysis of the fusion protein (Fig. 1.3B). Interestingly, the protein profile of this strain also showed the recovery of the adhesins P110 and P140 to levels approximately 50% of those found in WT G37 cells, indicating that the main adhesin complex P140-P110 is, at least in part, stabilized by the presence of the P32 protein (Fig. 1.3A).

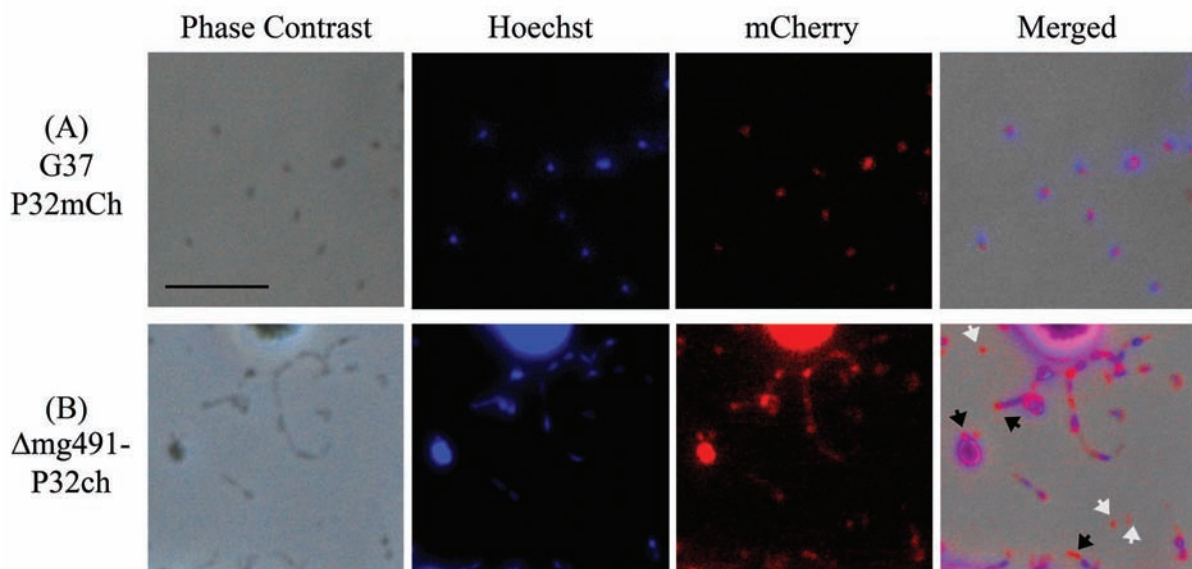


Fig. 1.8. Phase contrast/fluorescence microscopy to locate P32 in *M. genitalium* G37 P32mCh and Δ mg491-P32ch strains. Phase contrast, Hoechst 33342 and mCherry epifluorescence pictures of representative fields are shown for each strain. These pictures are merged in the left panels. Black arrows point to several P32:mCherry foci found in the filament stems and at the tip of these filaments. White arrows point to P32:mCherry foci observed in very small cells with no Hoechst 33342 fluorescence signal. Bar is 10 μ m.

G37-P32ch cells exhibited a strong mCherry epifluorescence signal and in several cells this signal was overlapping with the phase contrast and fluorescent foci from Hoechst 33342 stained DNA (Fig. 1.8A). This pictures may suggest that P32 is localized scattered over a substantial part of the mycoplasma cell, being less polarized than the orthologous protein in *M. pneumoniae* (Hasselbring et al., 2006a). However, we cannot exclude the presence of a fluorescent mCherry background as a consequence of the limited proteolysis of P32-mCherry fusion detected by Western-blot (Fig. 1.3B). Alternatively, P32 might be in excess in these cells, precluding the proper localization of all P32 molecules. When analyzing the Δ mg491-P32ch strain, all cell aggregates and filaments showed a fluorescent background. Fortunately, some discrete foci were also visible in several points of the cell filaments, especially at their ends (Fig. 1.8B, black arrows). Since P32 is involved in terminal organelle organization (Hasselbring et al., 2005, Reddy et al., 1995), this result reinforces the notion that a residual motile machinery persists in Δ mg491 cells. Interestingly, it was also noticeable the presence of particles smaller than mycoplasma cells showing an intense mCherry fluorescence but no Hoechst 33342 fluorescence (Fig. 1.8B, white arrows). These particles may correspond to cell detachments as previously reported (Hasselbring and Krause, 2007a) and their presence is also in agreement with the existence of a minimized motile machinery in Δ mg491 cells.

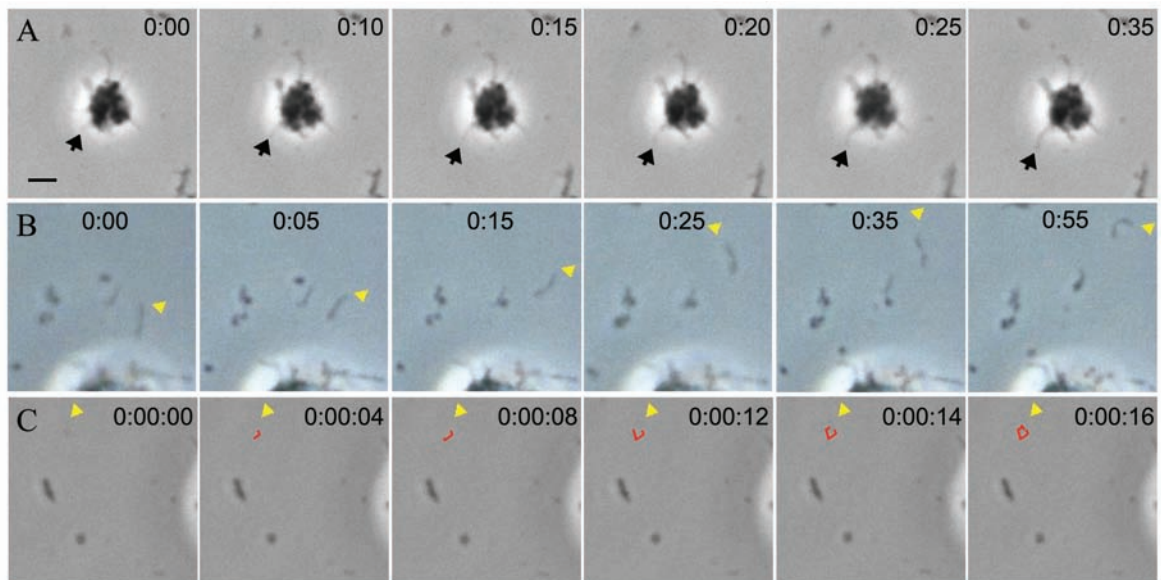


Fig. 1.9. Time-lapse phase contrast microcinematographies of cells from Δ mg491-P32ch strain. Frames were taken every 5 min in (A-B) and every 2 sec in (C). (A) A filament extending at its end is pointed by a black arrow. (B) A motile filament is pointed by a yellow arrow head. (C) A motile small cell showing a circular track (marked in red) and a velocity similar to that exhibited by G37 WT cells is pointed by a yellow arrow head. Bar is 2 μ m. Time is hour:min in (A-B) and hour:min:sec in (C).

Cells from Δ mg491-P32ch strain grew forming large cell aggregates and filaments similar to those exhibited by the cells from the Δ mg491 parental strain. In agreement with the increased levels of P140 and P110 adhesins, Δ mg491-P32ch cells attached easily to plastic slides. However, the hemadsorption activity of this strain was not restored (Fig. 1.4), indicating that a full P140-P110 complement is required for proper cell adhesion (Pich

et al., 2009). Surprisingly, when the Δ mg491-P32ch strain was analyzed by time-lapse microcinematography (Fig. 1.9), cell filaments grew faster than those of Δ mg491 strain. In addition, small filaments, single cells and small particles gliding on the plastic surface were also evident. Although filaments extended at very slow velocities ($0.6 \pm 0.07 \text{ nm s}^{-1}$), the small particles moved at velocities ($0.056 \pm 0.014 \text{ } \mu\text{m s}^{-1}$) comparable to those of WT G37 cells. Consequently, the increased amounts of P32 and the main adhesin complex in Δ mg491-P32ch cells are well correlated with the improved motility of this mycoplasma strain.

2.2. Ultrastructure of the cytoskeleton in Δ mg491-P32ch cells

Cells from G37 WT and Δ mg491 P32mCh strains were examined by SEM to characterize the external cell morphology (Fig. 1.10A,B) and by cryo-electron microscopy (Cryo-EM) to detect internal structures (Fig. 1.10C-H). An electron-dense core supporting the terminal organelle was found inside most of WT cells. In particular, a curved, segmented rod and the terminal button were easily visualized (Fig. 1.10C,D. arrows). Moreover, WT cells showed an electron-lucent area surrounding the electron-dense core, as it has been previously reported in *M. pneumoniae* (Henderson and Jensen, 2006, Seybert et al., 2006). A large amount of

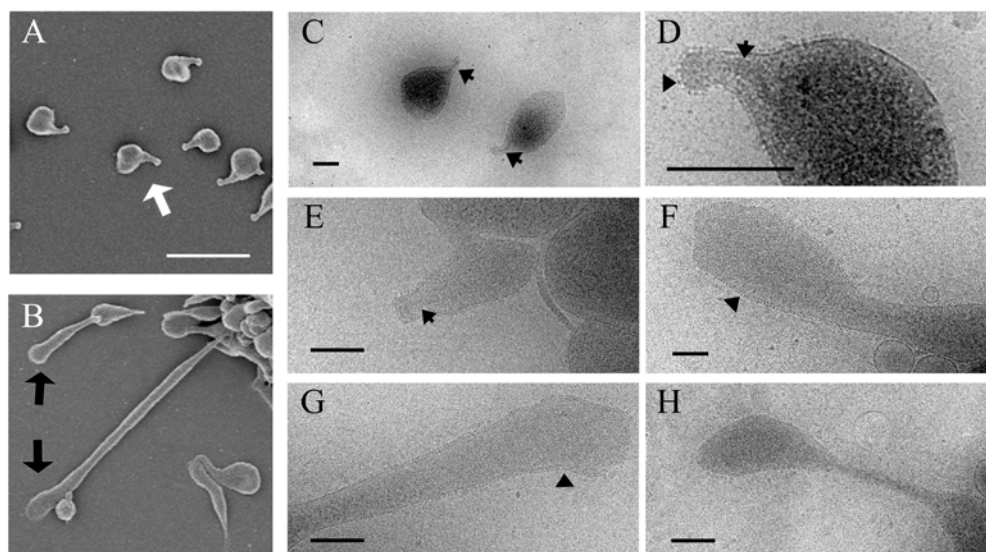


Fig. 1.10. Analysis of the morphology and ultrastructure of cells and filaments from G37 WT and Δ mg491-P32ch strain by SEM and cryo-electron microscopy (Cryo-EM). (A) SEM micrograph of cells from *M. genitalium* G37 WT strain; white arrow points to the terminal organelle of one cell. (B) SEM micrograph of cells from Δ mg491-P32ch strain showing the filamentous morphology with pleomorphic tips, pointed with black arrows. Bar in SEM micrographs is 1 μm . (C-D) Cryo-EM images of G37 WT cells showing the terminal organelle and the distinctive elements of the external and internal cytoskeleton. Black arrows point to the internal electron-dense cores supporting the terminal organelle architecture. Arrow head points to the nap structure anchored to the cell membrane surrounding the terminal organelle. (E-H) Cryo-EM images of filaments from Δ mg491-P32ch strain showing a thickened tip. No internal structures could be observed in filaments from pictures F-H. Only a single cell exhibiting an electron-dense core-like structure (black arrow) was detected and is showed in panel E. Arrow heads point to the nap structure that was visualized in the enlarged pictures E-G. Bars in cryo-EM pictures are 0.3 μm .

particles were also observed at the external side of the cell membrane surrounding the terminal organelle (Fig. 1.10C,D; arrow head). These particles are formed by the adhesin complexes and comprise the nap structure of *M. genitalium* and *M. pneumoniae* (Baseman et al., 1982b, Henderson and Jensen, 2006, Seto et al., 2001, Seybert et al., 2006).

Only few cells from the Δ mg491-P32Ch strain showed electron-dense cores. In these cells, structures resembling the terminal button and the rod could be identified (Fig. 1.10E). However, no internal structures were observed inside the profuse filaments produced by this strain (Fig. 1.10F-H). These filaments were pleomorphic extensions of the cell bodies with a variable size but often finished by a thickened end, which was connected in many cases by a thin segment to the cell body (Fig. 1.10F-H). Probably, further elongation of these thin segments may result in the breaking of the filament and this could be in the origin of the cell detachments observed by epifluorescence microscopy (Fig. 1.8B). Interestingly, a significant number of nap structures were detected along the filaments. Nap structures were always observed at the thickened end of the filaments and also decorating some segments of the filament stem. However, no nap structures were identified when examining the longest filaments in the regions closer to the cell body (Fig. 1.10G).

Part 3: Characterization of Δ mg218-P32Ch cells

3.1. Role of the cytoskeletal proteins in the motile machinery of *M. genitalium*

The above results suggesting an active role of P32, P140 and P110 in cell motility were unexpected. To date, MG218 has been considered a protein essential for mycoplasma movement. Previous analyses of MG218 null mutants demonstrated that in the absence of this protein, mycoplasma cells are not motile (Pich et al., 2008). According to the current inchworm model for mycoplasma motility, movement is generated by the rod component of the terminal organelle (Henderson and Jensen, 2006, Miyata, 2008, Seybert et al., 2006), and MG218 is the main protein involved in the rod architecture (Balish et al., 2003, Pich et al., 2008). However, an unequivocal demonstration of the precise role of MG218 in motility has been precluded by the fact that in the absence of this protein there is also a concomitant

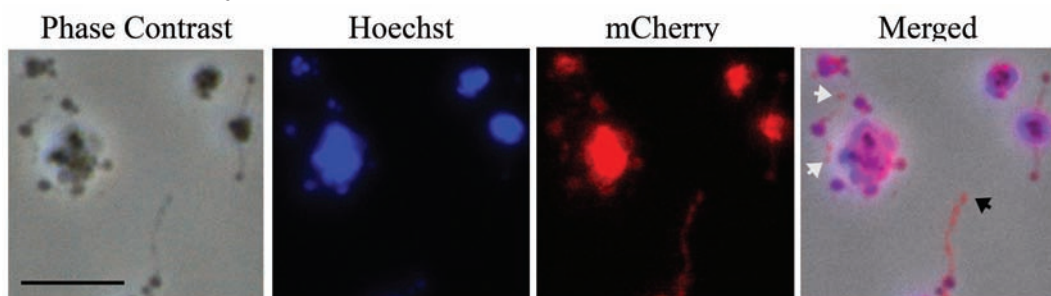


Fig. 1.11. Phase contrast/fluorescence microscopy to locate P32 in *M. genitalium* Δ mg218-P32ch strain. Phase contrast, Hoechst 33342 and mCherry epifluorescence pictures of a representative field are shown and merged in the left panel. Black arrow points to P32:mCherry foci found in filament stems and tips. White arrows point to P32:mCherry foci observed in very small cells with no Hoechst 33342 fluorescence signal. Bar is 10 μ m.

loss of many cytoskeletal proteins including P32, P140 and P110 (Fig. 1.3). Based on the motile properties of Δ mg491-P32ch cells, we addressed the question if a similar rescue of the motile activity could be also achieved in cells completely lacking of MG218. To this end, pmTnGmP32:mCherry construct was electroporated on the Δ mg218 *M. genitalium* strain deficient for MG_218 previously obtained in our laboratory (Pich et al., 2008). Δ mg218-P32ch transformant cells exhibited normal levels of MG491 protein, similar to those found in the parental strain and WT G37 strain. Noteworthy, protein profiles of Δ mg218-P32ch transformant cells showed increased levels of P140, P110 and P32 similar to those detected in Δ mg491-P32ch cells (Fig. 1.3). The hemadsorption status was also very similar to that of the Δ mg491-P32ch strain (Fig. 1.4). When this strain was examined by epifluorescence, filaments and cell aggregates showing some mCherry fluorescence background and several discrete foci were observed (Fig. 1.11) indicating preferential sites for P32 clustering even in the absence of MG218. Interestingly, phase contrast and time lapse microcinematography analysis revealed the presence not only of growing filaments, but isolated motile filaments were also evident and gliding at velocities similar to those exhibited by Δ mg491-P32ch cells (Fig. 1.12). Consequently, the detection of motile structures in cells lacking MG218 confirmed our previous expectations indicating that this protein is not an essential component of the motile machinery of *M. genitalium*.

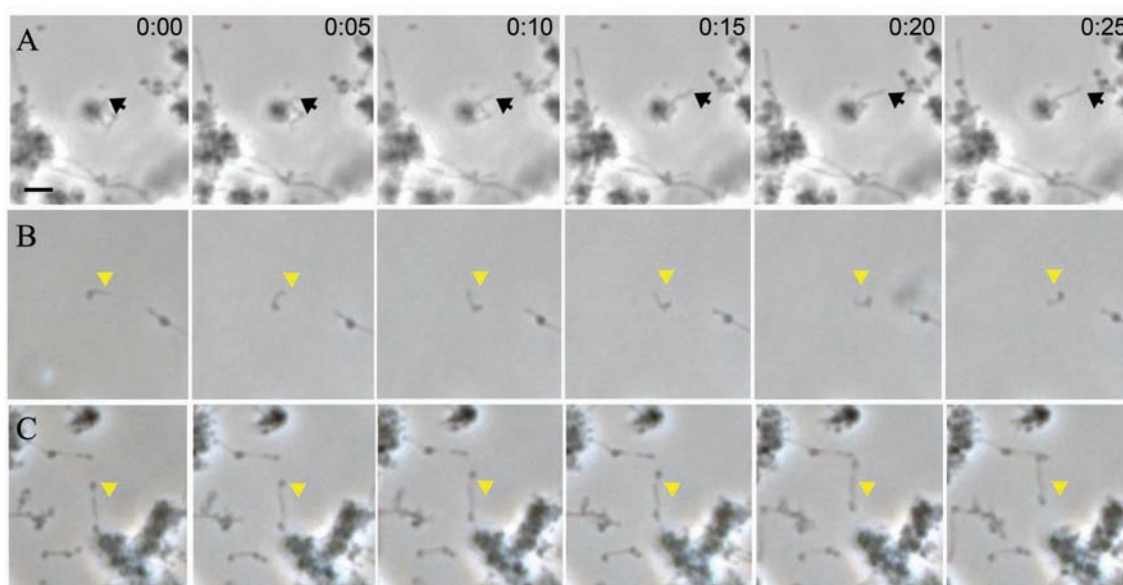


Fig. 1.12. Time lapse phase contrast microcinematographies of cells from Δ mg218-P32ch strain. Frames were taken at 5 min intervals. (A) A filament extending at its end is pointed by a black arrow. (B-C) Motile filaments are pointed by a yellow arrow head. Time is h:min. Bar is 2 μ m.

3.2. Rearrangements of the cytoskeleton in the Δ mg218-P32Ch strain

Cells from Δ mg218-P32ch also exhibited a large amount of filament extensions from the main cell body when examined by SEM and Cryo-EM (Fig. 1.13). As it was observed in Δ mg491-P32ch, these filaments had a pleomorphic appearance, showing also thin segments in the region closer to ends, which consistently had a rounded shape (Fig. 1.13).

Remarkably, a novel electron-dense structure was detected inside the rounded ends of the filaments (Fig. 1.13C-F). This new cytoskeletal structure had a circular shape with a diameter between 120-150 nm. Nap structures were also found consistently localized at the outer side of the cell membrane surrounding this rounded structure (Fig. 1.13F), suggesting a close association between the adhesin complexes and the distinctive cytoskeleton of these cells. We were unable to obtain reproducible preparations of Δ mg491 and Δ mg218 mutant cells. These strains are prone to form large aggregates, which led to the presence of very thick ice layers during the vitrification step, precluding that these samples could be properly visualized and analyzed by Cryo-EM.

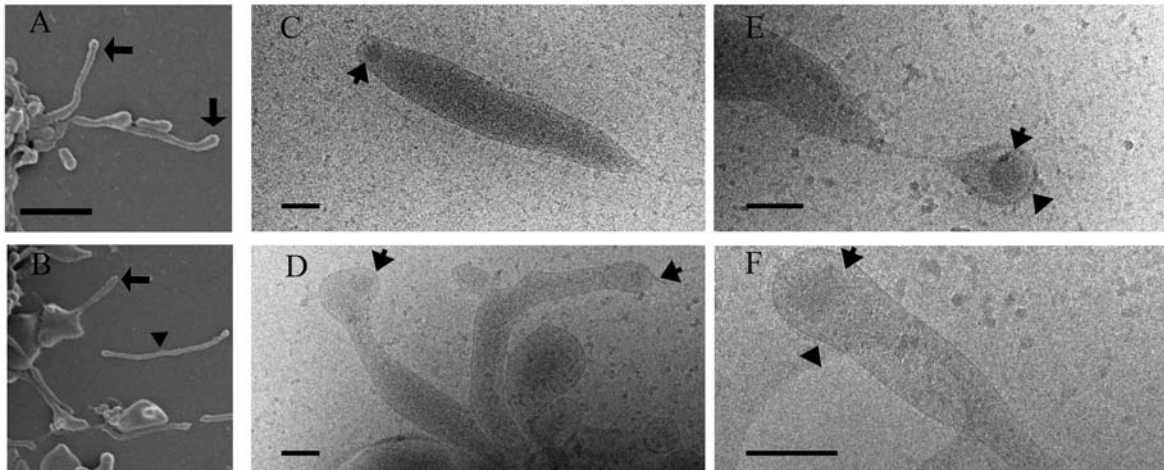


Fig. 1.13. Analysis of the morphology and ultrastructure of cells and filaments from Δ mg218-P32ch strain by SEM and Cryo-EM. (A-B) SEM micrographs of cells from Δ mg218-P32ch strain showing the filamentous morphology. Cell filaments are pointed with black arrows. A detached filament is pointed by a black arrow head. Bar is 1 μ m. (C-F) Cryo-EM images of cells from Δ mg491-P32ch strain showing a rounded structure at the end of the filaments (black arrows). Nap structures are localized at the membrane surrounding the rounded structure. Bars are 0.3 μ m.

Discussion

Motile mycoplasmas glide on solid surfaces by unique and largely unknown mechanisms and display cytoskeleton structures of unprecedented complexity in the bacterial world. Motility is also in close connection with the virulence of these mucosal pathogens (Jordan et al., 2007, Prince et al., 2014). Therefore, we choose to examine the contribution of different cytoskeletal proteins to the gliding motility of the mucosal pathogen *M. genitalium* to gain insight into the function of these proteins when generating the cell movement. Our results highlight the role of P32 protein and the P110-P140 main adhesin complex in the motile machinery of *M. genitalium* and also suggest that MG312 and MG218 proteins are not essential for motility. These findings add a new knowledge about the motile machinery of this microorganism and, contrary to previous views (Henderson and Jensen, 2006, Seybert et al., 2006), indicate that the rod element of the cytoskeleton core is not the molecular motor propelling mycoplasma cells.

The isolated mutant strain deficient for MG491 protein presented extremely low levels of several proteins involved in the terminal organelle structure and functioning. Downstream events in additional proteins are common when engineering mutant strains lacking cytoskeletal proteins. Most of these events have a posttranslational origin since many proteins are stabilized once entered into the terminal organelle structure (Popham et al., 1997). We have found that downstream events in Δ mg491 cells are very similar to those found in Δ mg218 cells (Fig. 1.3), suggesting that most of changes detected in Δ mg491 cells might be a direct consequence of the low levels of MG218. Consistent with the low levels of MG218 and MG312 proteins, Δ mg491 cells also showed low amounts of the main adhesins P110 and P140 and failed in cytoskeleton development (Fig. 1.10) (Pich et al., 2008). However, a small number of these cells possessed structures reminiscent of the terminal button and rod (Fig. 1.10E), which is in agreement with the low levels of the main cytoskeletal proteins remaining in this strain. Although the high identity levels between MG491 and P41, the phenotype of Δ mg491 cells is remarkably different from that exhibited by *M. pneumoniae* MPN311 mutant cells lacking P41, which produce functional terminal organelles with a composition similar to those of WT cells (Hasselbring and Krause, 2007a). This suggests that the interplay and mutual stabilization of the terminal organelle elements is very different in these two closely related mycoplasma species. In addition, the structure and composition of the cytoskeleton cores of *M. genitalium* and *M. pneumoniae* are nearly identical (Fig. 1.10C-D) (González-González, Unpublished, Henderson and Jensen, 2006, Seybert et al., 2006). Rather than a different functional role for MG491 and P41, our findings suggest that the dissimilar protein complement in both mutant strains is probably a consequence of the particular stability of MG218 and HMW2 orthologues in both mycoplasma species. Supporting this view, the low levels of most cytoskeletal proteins in Δ mg491 cells is consistent with previous expectations suggesting that MG491 is incorporated early in terminal organelle assembly (Hasselbring et al., 2006a, Hasselbring and Krause, 2007a).

Cells from Δ mg491 strain grew forming large cell aggregates and long filaments. To investigate the origin of these filaments, a minitransposon containing a translational fusion P32:mCherry was introduced in the genome of Δ mg491 cells by transposition. Upon the introduction of the extra copy of MG_318 gene, the amount of the P110-P140 adhesin complexes increased to values around 50% of those found in WT cells indicating that P32 protein has a role in stabilizing P110-P140 adhesins. This result is in agreement with previous findings indicating that *M. pneumoniae* P30 is not essential for adhesin trafficking but is required to form properly functional adhesin complexes (Romero-Arroyo et al., 1999). However, our results also suggest that additional protein/s are required to fully stabilize P140 and P110 complexes and are consistent with an earlier work reporting that MG317 is required for normal levels of these adhesins (Pich et al., 2008). It is also noteworthy that P110-P140 complexes exhibited a clustered distribution, and nap structures were evident at the tip of the filaments and in discrete locations of the filament stems. In a previous work, TopJ protein of *M. pneumoniae* was suggested to be essential for adhesin translocation to the outer side of the cell membrane (Cloward and Krause, 2011). Interestingly, normal levels of the TopJ homologue protein MG200 were detected in all filamentous strains of this work (Fig. 1.3B). Since no cytoskeletal structures were visualized in these filaments, this finding suggests that MG200 protein has a role in adhesin trafficking by a mechanism independent of most of supporting cytoskeletal proteins. On the other hand, nap structures were the single distinctive elements remaining in most of the visualized cells from Δ mg491-P32ch strain. The clustered distribution of P110-P140 complexes specially at the tip of the filaments suggests that nap structure is involved in the filament elongation by pulling the cell membrane out of the main body and, in the absence of a functional cytoskeleton, the main body remains anchored to the solid surface. Having a nap structure stretching the tip in different directions may also explain the pleomorphic thickened ends of these filaments (Fig. 1.10F-H). Our pictures are also consistent with the notion that the thickened ends may eventually detach from the growing filament, generating in this way a motile particle (Fig. 1.10H) (Hasselbring and Krause, 2007a). In this scenario, the improved motile activity exhibited by Δ mg491-P32ch cells was very well correlated with an increased amount of P32 protein and P110-P140 adhesins. These findings, together with the fact that levels of the remaining cytoskeletal proteins were unaffected, provide the first evidence that P110-P140 adhesin complexes stabilized with P32 protein have a pivotal role on the movement generation of *M. genitalium* cells.

Cell filaments from Δ mg218-P32ch strain extended at velocities similar to Δ mg491-P32ch filaments and interestingly, a number of isolated filamentous cells were also observed to glide. These motile filamentous cells are strong evidence about the existence of a gliding machinery independent of MG218 protein and the rod structure. These observations also support the notion that the extension of filaments from either Δ mg491-P32ch and Δ mg218-P32ch cells are a direct consequence of the presence of minimized motile machinery at the tip of the filaments. Filaments from Δ mg218-P32ch strain showed a rounded electron dense

structure in the filament tips (Fig. 1.13C-F). This structure was much bigger than a regular terminal button and nap structures were restricted to the cell membrane surrounding this area, indicating that this core is fully proficient when organizing the adhesins. Consequently, these cells showed more compact tips and more regular morphologies than those observed in Δ mg491-P32ch cells. The composition of this new cytoskeletal core is unknown. However, Δ mg218-P32ch strain, which is derived from Δ mg218 strain, lacks MG218 but has a full complement of MG491 protein (Fig. 1.3B) (Pich et al., 2008). Since no additional changes in the levels of the other cytoskeletal proteins were detected after introducing the extra copy of MG_318 gene, we conclude that MG491 protein plays a decisive role in the architecture of the cytoskeleton in Δ mg218-P32ch cells. In addition to MG491 protein, it is also plausible that some of the remaining cytoskeletal proteins in Δ mg218-P32ch cells are also participating in this new macromolecular assembly. The recent finding that the C-terminal end of MG491 protein interacts with MG200 by the EAGR box (Chapter 2) reinforces this view. Based on the presence of a stable cytoskeleton, a properly localized nap structure and the presence of DNA in many gliding filaments and cells, we could define a minimized set of proteins essential for the motile machinery of *M. genitalium*: MG491, MG219, MG386 and MG200, participating in the inner cell core and P110-P140 complexes together with P32 anchored to the cell membrane, in close connection to inner cell core. This motile machinery set may be also reminiscent of that existing in an earlier evolutionary step while mycoplasmas were developing mechanisms to propel cells. The remaining cytoskeletal proteins also involved in gliding motility that are found in modern mycoplasmas (MG218, MG312, MG317 and MG217) seem to provide additional mechanisms for an improved transmission of the movement to the main cell body, an increased stability of adhesin complexes or modulate the direction of the cell movement, which could be critical for host invasion.

In conclusion, we provide the first direct evidence supporting that the motor structure of *M. genitalium* does not lie within the rod element of the cytoskeleton core and discards the current inchworm model to explain the movement generation in the terminal organelle of mycoplasma cells. In addition to highlight the role of the adhesin complexes in the origin or transmission of cell movement, we also provide a valuable minimized cell system to elucidate the intricacies of the complex motile machinery and cytoskeleton architecture of mycoplasma cells.

Mycoplasma genitalium Strains with Relevant Mutations in the Structure and Function of MG491 Protein

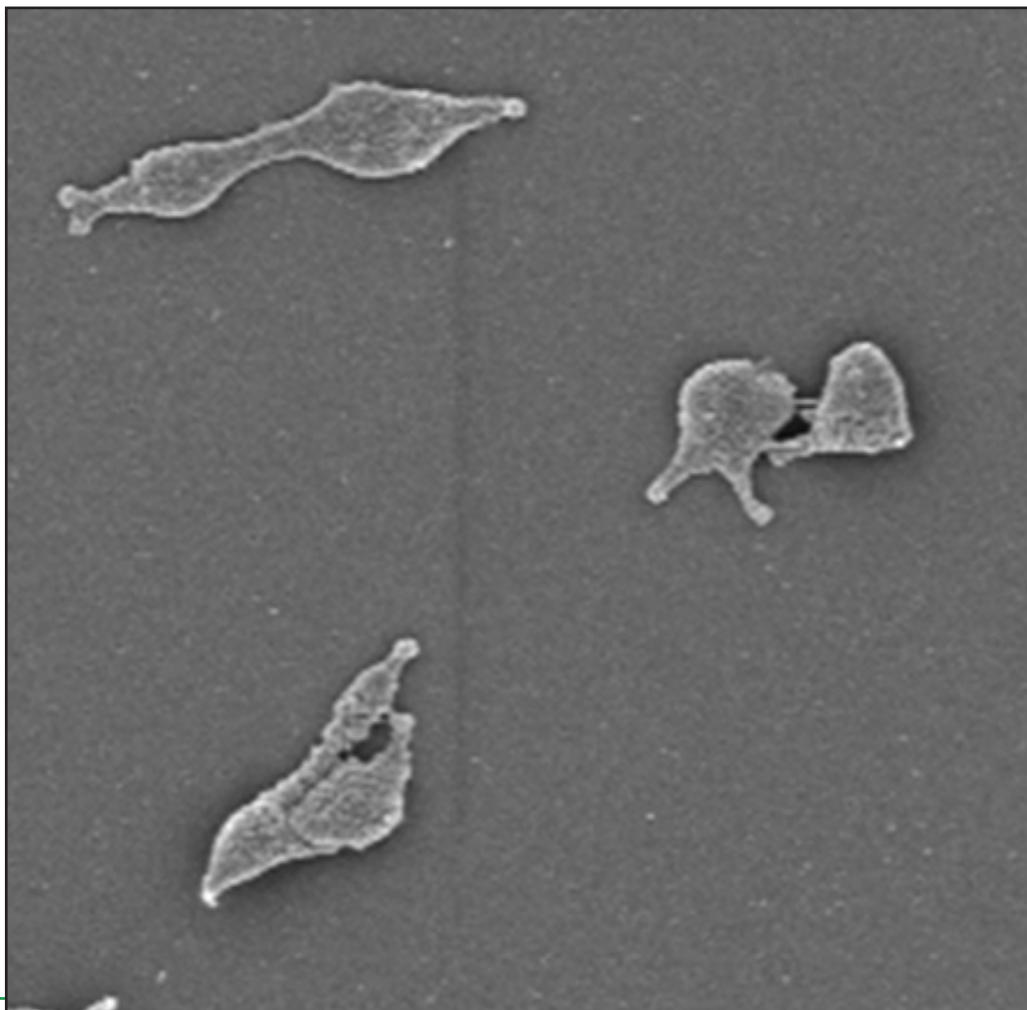
Part 1: Characterization of mg491- Δ p1 strain.

Part 2: Characterization of mg491-C87S strain.

Part 3: Characterization of mg491-F157A-F158A strain.

Part 4: Characterization of mg491- Δ loopL2 strain.

Part 5: Characterization of mg491- Δ Nt strain



This work has been partially published in:

Martinelli L¹, Lalli D¹, García-Morales L¹, Ratera M, Querol E, Piñol J, Fita I, Calisto BM (2014) A Major Determinant for Gliding Motility in *Mycoplasma genitalium*: the Interaction between the Terminal Organelle proteins MG200 and MG491. J Biol Chem. doi: 10.1074/jbc.M114.594762

¹ Authors contributed equally.

Introduction

Mycoplasma genitalium, as well as many mycoplasmas of the *pneumoniae* group, glides through surfaces in the direction of a cell protrusion called terminal organelle (Miyata, 2010), which is also relevant in adhesion, cell division and host cell invasion (Jensen et al., 1994, Burgos et al., 2006, Mernaugh et al., 1993, Bredt, 1968, Lluch-Senar et al., 2010). The terminal organelle is internally supported by an electron-dense core structure composed by proteins with no homologues outside the *pneumoniae* cluster. Cryo-EM studies have revealed the existence of eleven protein complexes composing the electron-dense core (Henderson and Jensen, 2006, Seybert et al., 2006). These studies have also shown that the terminal organelle is organised in three main structures: the terminal button, at the distal end; the rod or segmented paired plates, at the center; and the wheel-like complex, at the proximal end to the cell body. Some terminal organelle proteins of *M. pneumoniae* have been localized into these three structures using immunofluorescence or translational fusions with fluorescence proteins (Kenri et al., 2004, Seto et al., 2001, Seto and Miyata, 2003, Hasselbring and Krause, 2007b, Calisto et al., 2012).

Due to the close phylogenetic relation between mycoplasmas of *pneumoniae* cluster and the proteins conforming the electron-dense core, it is often accepted a common mechanism of movement between these species (Hatchel and Balish, 2008). However, many functional differences have been found when studying the wheel-like proteins of *M. genitalium* and *M. pneumoniae*. First of all, *M. pneumoniae* MPN_312 gene coding for P24 protein is important in the terminal organelle formation and gliding motility (Hasselbring and Krause, 2007b), but the corresponding orthologue in *M. genitalium* has not been identified. Nevertheless, *M. genitalium* MG_219 gene is located at the same place as *M. pneumoniae* MPN_312 gene in the P65 operon, and is also essential for normal terminal organelle development and gliding motility (González-González, Unpublished). *M. pneumoniae* TopJ protein is involved in gliding motility and cytoadherence (Cloward and Krause, 2011, Cloward and Krause, 2009), but its *M. genitalium* orthologue MG200 is only involved in gliding motility (Pich et al., 2006a). Also, *M. pneumoniae* P41 protein is essential in the anchoring of the terminal organelle to the main cell body (Hasselbring and Krause, 2007a), while the *M. genitalium* orthologue MG491 protein is essential to develop the electron-dense core (chapter 1). In contrast, orthologue proteins P200 of *M. pneumoniae* and MG386 of *M. genitalium* have a similar role in gliding motility (Jordan et al., 2007, Pich et al., 2006a). All together indicates that the wheel-like structure is involved in both terminal organelle development and gliding motility.

Despite the overall structural information obtained by cryo-EM and the localization of the terminal organelle proteins into the electron-dense core, there is still very limited information about molecular details in the organisation of the terminal organelle. In particular, the 3D structure of the terminal organelle constituent proteins as well as their molecular

interactions are essential to understand the assembling of the whole electron-dense core and the mechanism of gliding motility. This lack of structural information is probably due to technical issues resulting from the nature of the terminal organelle proteins, which are highly hydrophobic and rich in disordered regions. Nevertheless, researchers from I. Fita group (IBMB-CSIC, Barcelona) together with the structural biology group at the European Synchrotron Radiation Facility (ESRF, Grenoble) have recently determined the 3D structure of some domains of the wheel-like proteins MG200 and MG491.

M. genitalium MG200 protein, as well as *M. pneumoniae* orthologue protein TopJ, is involved in motility and terminal organelle function (Cloward and Krause, 2009, Pich et al., 2006a). This protein of 601 residues is predicted to be a multi-domain polypeptide (Cloward and Krause, 2010, Cloward and Krause, 2009, Balish et al., 2001). TopJ N-terminal region is composed by a J-like domain. Briefly, J-domains are usually found in DnaJ family of co-chaperones, where these domains stimulate DnaK (Hsp70) chaperone to hydrolyze ATP, thus inducing a conformational change in DnaK that allows the binding to the presented polypeptide and inhibiting premature protein folding (Hendrick and Hartl, 1995, Frydman, 2001). *M. pneumoniae* TopJ mutants in J-domain fail to properly assemble the terminal organelle having strong effects on cytoadherence and motility. This suggests that TopJ J-domain is actually a co-chaperone activating DnaK for terminal organelle maturation (Cloward and Krause, 2011, Cloward and Krause, 2010, Cloward and Krause, 2009). Following the J-domain, MG200 and TopJ proteins have an Enriched in Aromatic and Glycine Residues (EAGR) box (Balish et al., 2001). EAGR boxes have been found exclusively in the terminal organelle proteins MG200, MG312 and MG386 in *M. genitalium* and the corresponding orthologues TopJ, HMW1 and P200 in *M. pneumoniae* (Balish et al., 2001). Mutants of both EAGR boxes in MG312 and MG200 proteins interfere in cell motility confirming a relevant contribution of this box in the gliding mechanism. Crystals of MG200 EAGR box (Gln149 to Glu203) revealed a new protein fold (Calisto et al., 2012). This structure consists in three antiparallel β -sheets (β 1- β 6- β 5) flanked by the helix α 1 that bury an hydrophobic core including most of the aromatic residues. Strands β 5- β 6 form a hairpin that is similar in

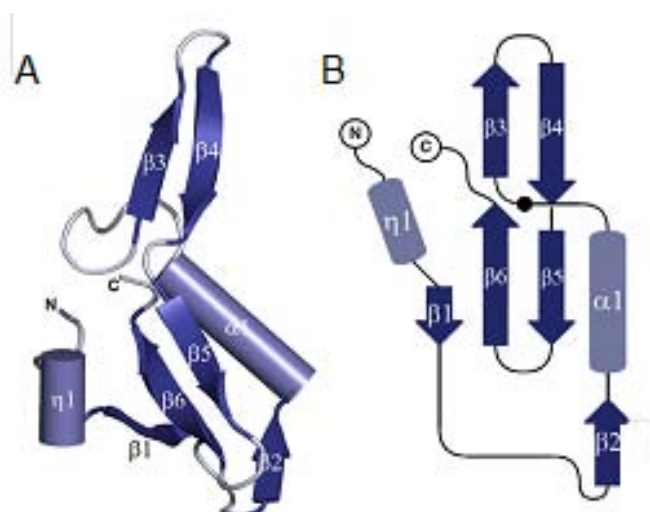


Fig.2.1. Crystal structure of MG200 EAGR box. (A) Cartoon representation. (B) Scheme of the subunit topology with helices depicted as light blue cylinders and β -strands as dark blue arrows.

sequence and structure to β 3- β 4 hairpin. While the first hairpin is involved in dimerization, β 3- β 4 hairpin is solvent exposed and highly reactive, suggesting that EAGR boxes can be a platform for interactions. MG200 and TopJ EAGR boxes are followed by an Acidic and Proline Rich (APR) domain and a long C-terminal domain. APR is also present in the other EAGR-containing proteins as well as in MG317 and MG217 proteins and in the respective orthologues HMW3 and P65 of *M. pneumoniae* (Balish et al., 2001). The function of both APR and C-terminal domain in TopJ protein are still unclear, but are needed for the correct localization of TopJ protein, having a strong effect in gliding motility (Cloward and Krause, 2010).

Protein MG491 from *M. genitalium* has also been studied in vitro using structural biology approaches. Crystal structure of the central fragment from Asn67 to Ala203 has been recently solved (Martinelli, Submitted). Both in crystals and in solution, MG491 forms a tetramer organized as an homodimer of heterodimers. Each monomer folds into an antiparallel three-helix-bundle (α 1-3) with α 1 and α 2 helices connected by a small loop L1, while a longer and more flexible loop L2 connects α 2 and α 3 helices (Fig. 2.2). Helix α 1 is kinked in its central part due to the presence of a π -helix turn that starts in Cys87 residue.

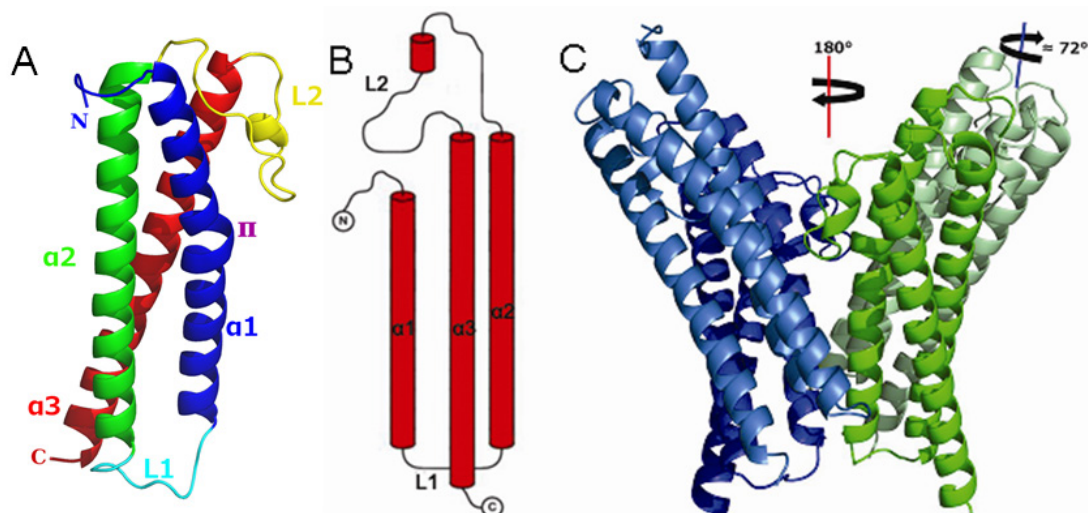


Fig. 2.2. Crystal structure of MG491 from residues 67 to 203. (A) MG491 monomer coloured as follow: helix α 1, α 2 and α 3 and loops L1 and L2 in blue, green, red, cyan and yellow, respectively. (B) Scheme of the subunit topology with helices depicted as red cylinders. (C) Quaternary structure of the MG491 tetramer showing the 72° rotation between subunits of the tight dimer and the 180° relation between dimers. Adapted from Martinelli L. et al (Unpublished).

Two tight dimers are formed between A – D and B – C subunits (Fig. 2.3A). The two subunits of the dimer have a contact surface of $1\,183\text{ \AA}^2$ (tight interface) and are related by a 72° rotation axis. Subunits A – B and C – D interact to form the final tetramer with an average interface area between subunits of 530 \AA^2 (loose interface). The loop L2 presents two different conformations (Fig. 2.3B), one present in subunits A and C, and the other in subunits B and D, and are related with its involvement in the tight or the loose interface. The interactions of the residues in L2 with the residues of other monomers are different in

subunits A – C from subunits B – D, due to the conformational differences in this loop. In subunits B and D, residues Gln155, Phe157 and Phe158 face the other subunit in the tight dimer and become part of the tight interface. In subunits A and C, L2 face the other tight dimer, being involved in the loose interface.

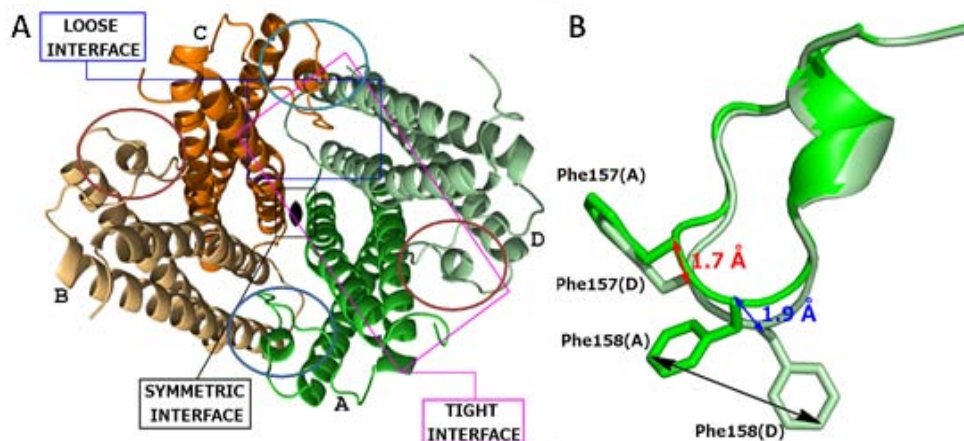


Fig. 2.3. Organization of MG491 monomers (A) Quaternary structure of MG491 tetramer. Subunits A-D and B-C are organized in tight dimers, respectively, and are confronted with the opposite dimer by loose interfaces. Loops L2 in loose interfaces are circled in blue, loops L2 in tight dimers are circled in dark red. (B) Different L2 conformations in the A subunit, at the loose interface, and in the D subunit, at the tight interface.

It is also noteworthy that Cys87 in $\alpha 1$ helices of monomers A and C are located close in the quaternary structure at both sides of the symmetric interface (Fig. 2.3A). The eventual formation of a disulphide bond in these monomers would prevent the π -helix turn formation by promoting an α -helix turn and stabilizing in this way the overall structure. However, the cysteines are not participating in disulphide bonds in the crystal structure due to the presence of reducing compounds in the crystallization conditions. Some in vitro assays have suggested that half of the protein monomers in solution are linked by disulphide bonds (Martinelli, Submitted), which is in agreement with the formation of a disulphide bond only between the Cys87 of A and C subunits.

An interaction between the wheel-like complex proteins MG200 and MG491 was identified by SPR with a K_D around 80 nM. The implication in the interaction of the MG200 EAGR box, which was predicted to be a platform for protein-protein interactions, was also confirmed by SPR (Fig 2.4). MG491 protein was found to interact with this domain through a 25 residues peptide T298-P322 (peptide_1) located at the C-terminal end. The sequence of this peptide is TDLKKQKKKPLNFITRPVFKSNLP. NMR was used to examine the CSPs occurring in the HSQC spectra of the ^{15}N -EAGR box when titrated with increasing concentrations of MG491 protein. This allowed to determine the residues from the MG200 EAGR box that interact in the complex (Fig 2.4). Surprisingly, MG491 peptide_1 does not interact with the solvent-exposed $\beta 3$ - $\beta 4$ hairpin from EAGR box, but interacts with the N-terminal end of the domain including the solvent-exposed face of helix $\alpha 1$ and strand $\beta 2$, which are part of the dimerization interface.

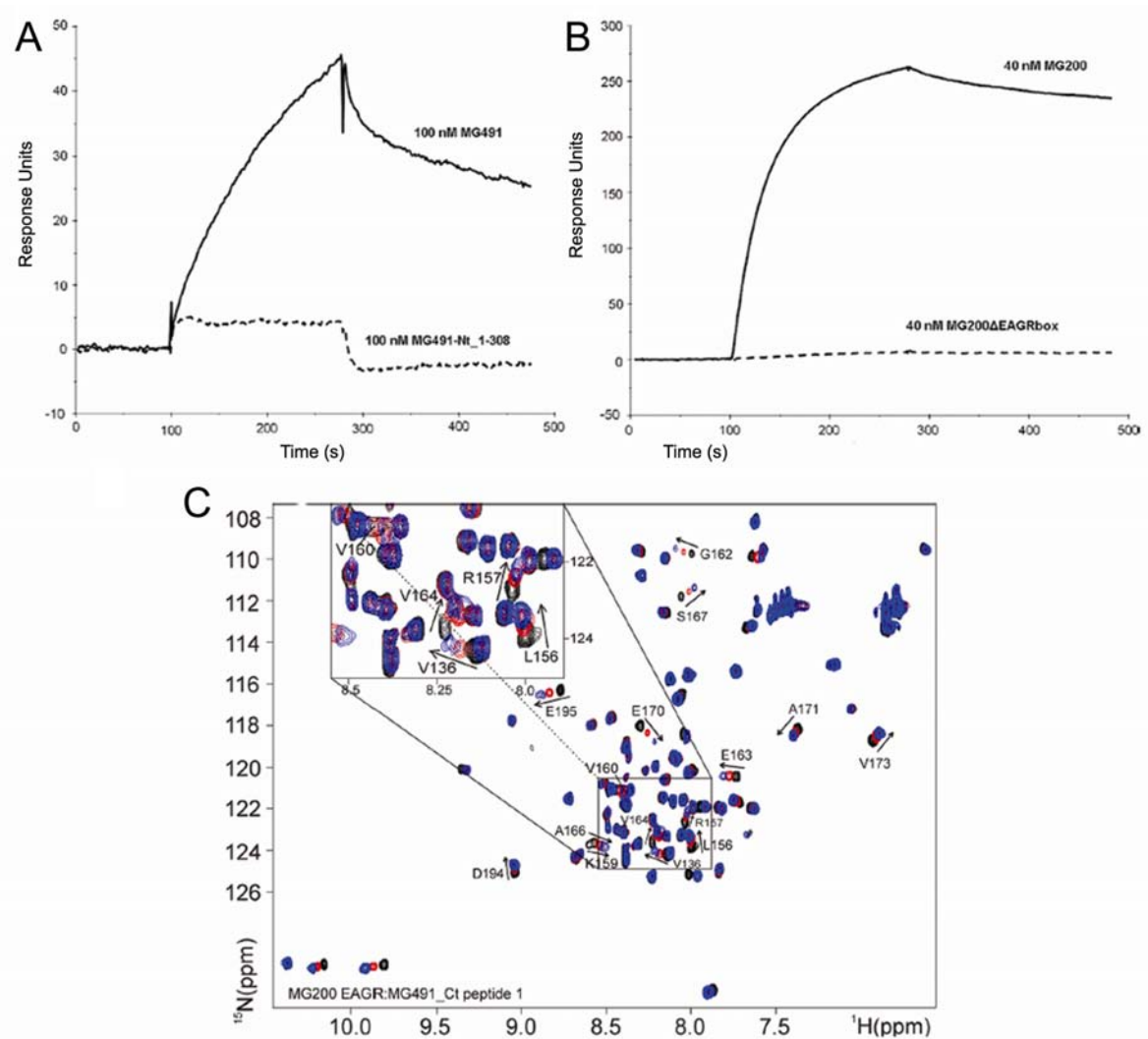


Fig. 2.4. Interaction between MG200 EAGR box and MG491 peptide₁. (A) SPR sensorgrams of 100 nM MG491 and 100 nM MG491-Nt (residues 1-308) injected over the MG200-immobilized flow cell. (B) SPR sensorgrams of 40 nM MG200 and 40 nM MG200ΔEAGR box injected over the MG491 peptide₁ flow cell. (C) Superimposition of ^1H , ^{15}N HSQC spectra of MG200 EAGR box at 1:0 (black), 1:3.5 (red) and 1:7 (blue) MG200 EAGR box/MG491 peptide₁ ratios. Labeled residues show an average CSP higher than 0.03 ppm.

The work in the present study focuses on the biological relevance of the structural information available for MG491 protein. To this end, five different mutant strains of *M. genitalium* were obtained and examined for the presence of defects in terminal organelle structure and function. Our results revealed that besides being involved in terminal organelle assembly, MG491 protein has a pivotal role in gliding motility and in the anchorage of the terminal organelle to the main cell body. Furthermore, we have identified key regions in MG491 protein that are involved in each of these functions. As a result, and for the first time, we have obtained significant information relating the structure and function of a terminal organelle protein.

Results

Part 1: Characterization of mg491- Δ p1 strain

1.1. Isolation of mg491- Δ p1 mutant strain

A *M. genitalium* mutant strain lacking the C-ter peptide₁ (Δ p1 mutation) involved in the interaction with the EAGR domain of MG200 protein was engineered by targeted gene replacement, by using the vector p Δ p1cat (Fig. 2.5A). Since MG₄₉₁ overlaps the 5' end of MG₂₁₉, chloramphenicol acetyl transferase (*cat*) gene marker was placed at the 3' end of MG₂₁₉ gene in p Δ p1cat. This design, which was aimed to avoid polar effects on MG₂₁₉ gene, may result in a high background of non-mutant clones after the transformation experiments (Fig. 2.5A, dashed lines). For this reason, a PCR-based screening was designed to test the presence of the Δ p1 mutation among the transformant colonies. Three

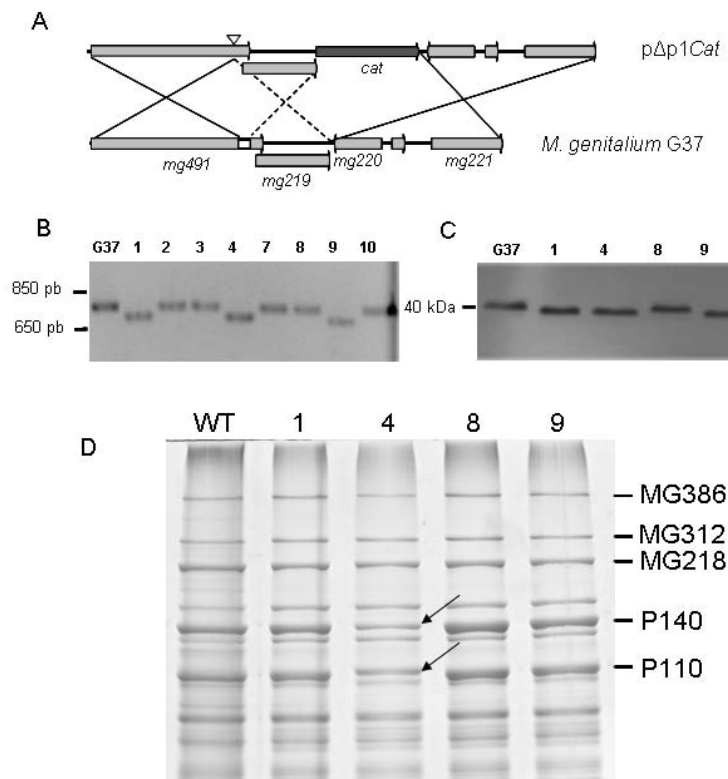


Fig. 2.5. Engineering of mg491-p Δ 1cat mutant strain. (A) Possible crossover events between the WT G37 genome and the p Δ p1cat plasmid. Solid lines indicate crossover events resulting in the deletion of peptide₁ coding region and in the insertion of *cat* gene. Dashed lines indicate a crossover event resulting also in the insertion of *cat* gene but not in the deletion of peptide₁. (B) Screening of p Δ p1cat transformant colonies by PCR using genomic DNA as template. The deletion of the region coding for peptide₁ was identified by the presence of a PCR smaller than that of the WT strain (clones 1, 4, and 9). (C) Western blot analysis of G37 WT and Δ p1 clones 1, 4, 8, and 9 using a polyclonal antiserum against the *M. pneumoniae* P41 protein. Clones 1, 4, and 9 show a shift in the MG491 band, consistent with the deletion of the 25 residues of the peptide₁. Clone 8 was analyzed as control of a non-mutagenic recombination. (D) Protein profile of G37 WT and transformant clones 1, 4, 8 and 9. Normal amounts of the TO proteins MG386, MG312, MG218 and P140 and P110 adhesins were detected in clones 1, 8 and 9. Clone 4 shows reduced levels of P140 and P110 adhesins.

out of the eight recovered clones showed a PCR fragment consistent with the deletion of the 75-bp fragment corresponding to the peptide₁ coding sequence (Fig. 2.5B). The presence of the intended mutation in these clones was further confirmed by direct sequencing of MG₄₉₁ gene. Finally, a Western Blot analysis of the three recombinant clones using anti-P41 antiserum showed a shift in the electrophoretic mobility of the MG491 protein band also confirming the presence of the mutation (Fig. 2.5C). Protein profiles of p Δ p1cat transformants were examined by SDS-PAGE (Fig. 2.5D) and no differences were found in the amounts of the terminal organelle-related proteins MG200, MG218, MG312, MG317 and MG386 or the P110 and P140 adhesins. Cells from clone 4 showed reduced levels of the P110 and P140 adhesins, suggesting that this clone had additional mutations and was discarded. Clone 1 was selected for further analysis and named mg491- Δ p1. To discard the presence of polar effects on the expression of MG₂₁₉ downstream gene, a Western Blot using polyclonal anti-MG219 antibodies was performed. Cells from mg491- Δ p1 strain exhibited a similar amount of MG219 than WT cells, demonstrating that the Δ p1 mutation has no impact on MG219 expression (Fig 2.6A).

1.2. Complementation assay of mg491- Δ p1 mutant strain

We engineered a pMTnGmMG491 plasmid carrying a mini-transposon with a WT copy of the MG₄₉₁ gene under the control of MG₄₃₈ promoter and the gentamycin resistance gene. This plasmid was electroporated into cells of mg491- Δ p1 strain and one transformant colony, named mg491- Δ p1TC6, was selected for phenotype analysis. This strain possess the mutated and the WT alleles of MG₄₉₁ gene and the two variants of the protein were expressed at the same level (Fig. 2.6B). The mg491- Δ p1TC6 strain was used to confirm that the mg491- Δ p1 phenotype can be complemented in the presence of the WT MG₄₉₁ allele.

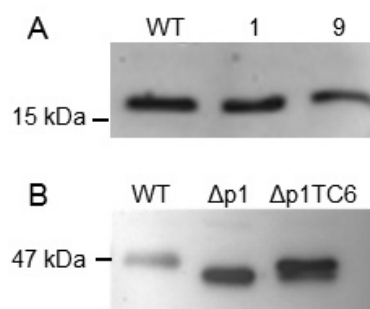


Fig. 2.6. Confirming the phenotype of the Δ p1 mutation. (A) Western blot using MG219 polyclonal antibodies of G37 WT and mg491- Δ p1 clones 1 and 9 showing the same amount of MG219 protein. The Δ p1 mutation has no polar effects in the expression of MG₂₁₉ gene. (B) Western blot using P41 polyclonal antibodies of G37 WT, mg491- Δ p1 and mg491 Δ p1TC6 showing the expression of a shorter MG491 in mg491- Δ p1 and both full-length and shorter MG491 in mg491- Δ p1TC6 cells.

1.3. Gliding motility and cell morphology of mg491- Δ p1

The motile properties of the mg491- Δ p1 and mg491- Δ p1TC6 cells were investigated by time-lapse microcinematography. The frequency of motile cells, the mean gliding velocity, and the diameter of the circular tracks were compared with those of G37 WT cells (Fig. 2.7, Table 2.1). The mean velocity and the ratio of motile cells from the mg491- Δ p1 strain

were similar to those found for WT cells. However, a significant reduction in the diameter of the circular tracks performed by mg491- Δ p1 motile cells was found. In contrast, mg491- Δ p1TC6 cells draw wider tracks showing a recovery of the diameter of the circular tracks to WT levels.

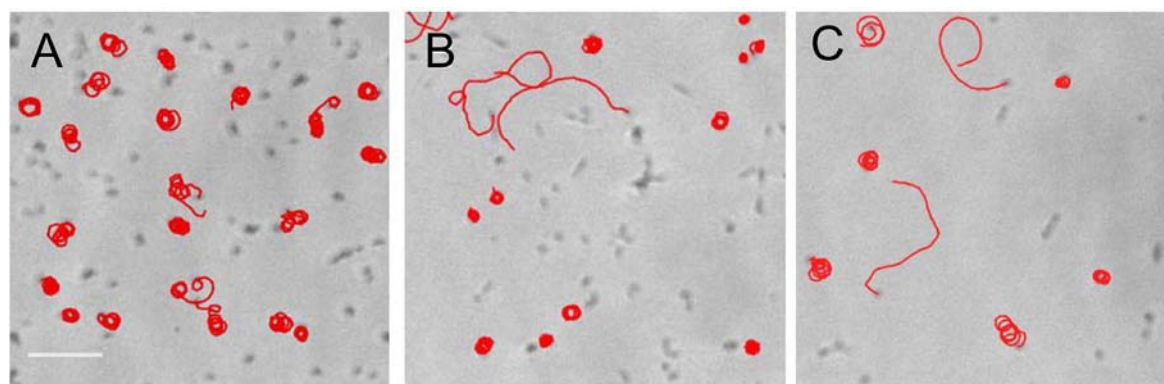


Fig. 2.7. Gliding motility of G37 WT, mg491- Δ p1 and mg491- Δ p1TC6 cells. (A) Representative tracks of *M. genitalium* G37 WT cells. (B) Representative tracks of mg491- Δ p1 cells. (C) Representative tracks of mg491- Δ p1TC6. Bar is 5 μ m.

Table 2.1. Gliding parameters of G37 WT, mg491- Δ p1 and mg491- Δ p1TC6 cells.

Strain	Percentage of motile cells (%)	Velocity (μ m/s) ^a	Diameter of circular tracks (μ m) ^a
G37 WT	85.0	0.125 \pm 0.002	1.05 \pm 0.02
mg491- Δ p1	78.2	0.124 \pm 0.004	0.81 \pm 0.03*
Δ p1TC6	80	0.128 \pm 0.010	1.05 \pm 0.04

^a Values shown include S.E.

* Statistical difference with G37 WT cells (p -value < 0.05).

Many mycoplasmas, including *M. genitalium*, have curved terminal organelles and draw circular tracks (Hatchel and Balish, 2008). It is described that the curvature of *M. genitalium* terminal organelle correlates well with the diameter of the circular tracks (Burgos et al., 2008). Hence, the presence of cells showing altered patterns of gliding motility in mg491- Δ p1 strain prompted us to investigate the cell and terminal organelle morphology by scanning electron microscopy. Although no significant differences were found in the terminal organelle-cell body axis angle between cells of the three strains, it was noticeable the presence of cells showing bipartite cell bodies in mg491- Δ p1 strain. These cells exhibited a strong curvature inside the cell body, probably reflecting the presence of changes in the structure of the cytoskeleton (Fig. 2.8, Table 2.2). These bipartite cells provide an explanation to the narrow tracks drawn by cells of m491- Δ p1 strain. Micrographs of mg491- Δ p1 strain suggest that terminal organelles in bipartite cells are not well attached to the main cell body and form prominent protrusions, which are in many cases dramatically retracted onto the cell body. It was also noticeable the presence of a significant amount of minute cells with a size <0.35 μ m. Minute cells are very uncommon in G37 WT cells and are thought to be terminal organelle detachments from the cell body. These terminal organelle detachments

were originally described in the MPN311 mutant of *M. pneumoniae*, which is a null mutant for the MG491 orthologue protein, P41 (Hasselbring and Krause, 2007a). In the *mg491-Δp1* mutant strain, minute cells could be originated also as detachments of the terminal organelle. Accordingly, many motile minute cells were detected in microcinematographies. The frequency of bipartite and minute cells was strongly reduced in *mg491-Δp1TC6* strain, but did not reach G37 WT amounts (Fig. 2.8, Table 2.2), indicating that the reintroduction of WT MG_491 allele does not fully complement the mutant phenotype. This is probably due to the presence of both WT and mutated forms of MG491 protein in this strain.

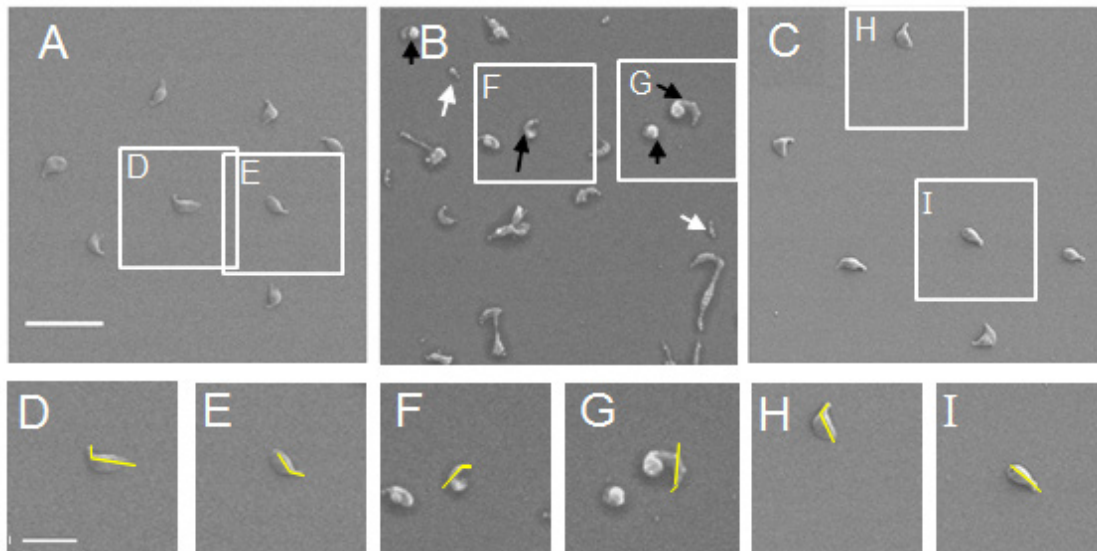


Fig. 2.8. Cell morphology of G37 WT, *mg491-Δp1* and *mg491-Δp1TC6* cells. (A,D,E) SEM micrograph of G37 WT cells. (B,F,G) SEM micrographs of *mg491-Δp1* cells. (C,H,I) SEM micrographs of *mg491-Δp1TC6* cells. Bar is 2 μm in A and 1 μm in D.

Table 2.2. Cell morphology of G37 WT, *mg491-Δp1* and *mg491-Δp1TC6* cells.

Strain	TO-Body axis angle (degrees) ^a	Bipartite cells (%)	Minute cells (<0.35 μm) (%)
G37 WT	136 \pm 2	2	1
<i>mg491-Δp1</i>	142 \pm 2	21*	17.5*
$\Delta p1TC6$ cells	142 \pm 2	8	4

^a Values shown include S.E.

* Statistical difference with G37 WT cells (p value < 0.05).

Part 2: Characterization of *mg491-C87S* strain

To assess the importance of the Cys87 in MG491 function and to find out the role of an eventual disulphide bond in the quaternary MG491 structure, we engineered a mutant strain of *M. genitalium* with a Cys87 \rightarrow Ser mutation in this protein. This change represents a single atom mutation (sulfur by oxygen) in MG491 protein. The mutant strain was obtained by random transposon insertion of the mutated allele in the $\Delta mg491$ null strain lacking

the MG_491 gene (chapter 1). The Δ mg491-mg491cat strain (chapter 1) was used as control because also has a WT allele of MG_491 gene randomly inserted by transposition in the Δ mg491 null strain. One transformant colony with pMTncatC87S suicide plasmid was randomly selected and named mg491-C87S. The transposon insertion was examined and was found disrupting the MG_414 locus, which codes for an hypothetical protein not involved in gliding motility or terminal organelle organization (Glass et al., 2006).

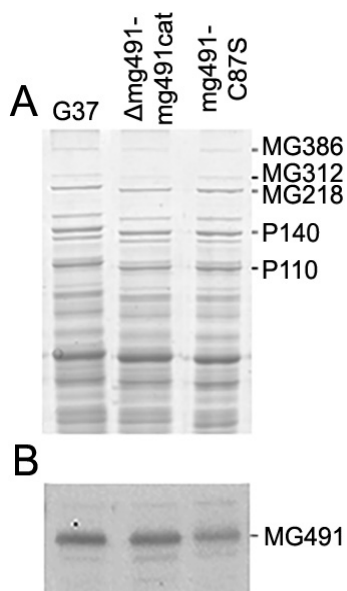


Fig. 2.8. Protein profile of *M. genitalium* G37, Δ mg491-mg491cat and mg491-C87S strains. (A) SDS-PAGE showing a full recovery of the main terminal organelle proteins in both mutant strains. (B) Western Blot using anti-P41 antiserum showing reduced levels of MG491 protein in mg491-C87S.

Strain mg491-C87S expressed the MG491-C87S mutant protein, but the protein amount was below the levels of the WT allele when compared by Western Blot (Fig 2.9B). In contrast, the amount of MG491 in Δ mg491-mg491cat was very similar to the amount of this protein in WT cells. This suggests that Cys87 is involved in MG491 stability or folding. Interestingly, the low levels of many terminal organelle proteins reported in Δ mg491 strain (chapter 1) were fully restored upon introduction of the mg491-C87S allele (Fig. 2.9A), indicating that the Cys87 is not required for the stability of the terminal organelle proteins and that the reduced amounts of MG491 protein in this strain are enough to restore this function.

In agreement with the rescue of the full complement of terminal organelle proteins, the characteristic flask-shape morphology of *M. genitalium* cells (Fig 2.10A) was also recovered in mg491-C87S strain, which also showed a normal terminal organelle ultrastructure as revealed by Cryo-EM (Fig. 2.10B). However, an increased frequency of cells bearing multiple terminal organelles (12.5%) when compared to G37 WT cells (4.9%) was detected by SEM. The development of terminal organelles is synchronized with cell division in many mycoplasmas (Seto et al., 2001, Hasselbring et al., 2006a, Bredt, 1968, Pich et al., 2008), in a process that is highly dependent on gliding motility (Pich et al., 2009, Hasselbring et al., 2006a, Lluch-Senar et al., 2010). For this reason, many previously isolated mutant strains of *M. genitalium* with gliding deficiencies also show the presence of multiple terminal organelles (Lluch-Senar et al., 2010, Pich et al., 2009). Time-lapse microcinematographies of mg491-C87S cells confirmed the existence of gliding motility deficiencies characterised

by the presence of a low number of motile cells (19%) and a decreased mean velocity of gliding cells ($0.098 \mu\text{m s}^{-1}$, Table 2.3). However, the frequency of motile cells is more altered than the mean velocity or the number of cells bearing multiple terminal organelles. When examining time-lapse cinematographies of G37 WT cells, around 18% of the motile cells show one or more resting periods. These resting periods are short and seem not to be related to cell division. Hence, these stopped cells are not expected to show multiple terminal organelles when examined by SEM. The frequency of motile cells showing resting periods in time-lapse cinematographies of mg491-C87S strain was 49%, indicating that the high frequency of non-motile cells might be a consequence of these cell division-independent cell stoppings. The significant increase in the amount of resting periods mg491-C87S suggests that MG491 has a role in the regulation of gliding motility and that Cys87 is a key residue for this function.

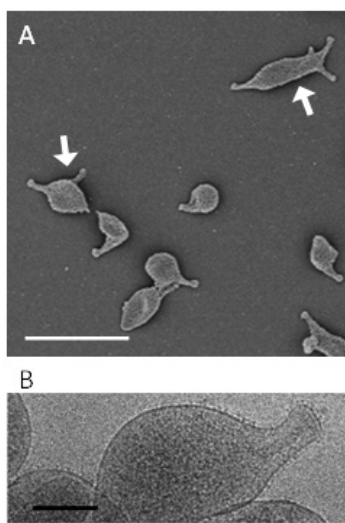


Fig. 2.10. (A) SEM micrograph showing the multiple terminal organelle phenotype of *M. genitalium* mg491-C87S cells. White arrows point multiple TO cells. Bar is $1 \mu\text{m}$. (B) Cryo-EM image of an mg491-C87S cell showing a normal cytoskeleton. Bar is $0.2 \mu\text{m}$.

Part 3: Characterization of mg491-F157A-F158A strain

Residues Phe157 and Phe158 are pivotal for the stabilization of the quaternary structure of MG491 protein and the two benzyl side chains can adopt two conformations in the different MG491 monomers. To find out the biological significance of this, we engineered a mutant strain with the two Phe substituted to Ala, to remove both benzyl side chains. To this purpose, the two codons TTT coding for Phe157 and Phe158 were substituted by two codons GCT coding for Ala. This mutant strain was obtained by random transposon insertion of the mutated allele in the Δmg491 null strain lacking the MG_491 gene (chapter 1). The Δmg491 -mg491cat strain (chapter 1) was used also as control. One transformant colony with pMTncatF157A-F158A suicide plasmid was randomly selected and named mg491-F157A-F158A. The transposon insertion was found to disrupt the MG_032 gene, a conserved hypothetical protein not involved in the terminal organelle structure and function (Glass et al., 2006).

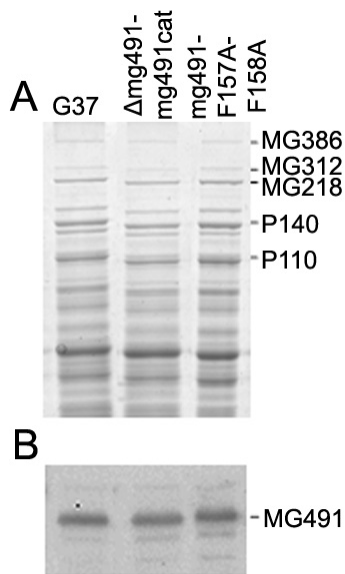


Fig. 2.11. Protein profile of *M. genitalium* G37, Δ mg491-mg491cat and mg491-F157A-F158A strains. (A) SDS-PAGE showing a full recovery of the main TO proteins in both mutant strains. (B) Western Blot using anti-P41 antiserum showing steady-state levels of MG491 in the mutant strains.

The transposon delivery of the mg491-F157A-F158A allele resulted in a full restoration of MG491 protein levels (Fig. 2.11A). The protein levels in the main terminal organelle proteins were also restored in mg491-F157A-F158A strain (Fig. 2.11B). This indicates that the two Phe mutations in this strain do not affect the stability of the MG491 protein or the whole terminal organelle.

Accordingly, these cells recovered the WT morphology and the terminal organelle ultrastructure (Fig 2.12). Even the frequency of cells bearing multiple terminal organelles (5.5%) was also similar to that found in G37 WT strain (4.9%). However, EM studies on this strain revealed the presence of a large amount of cells (13.6%) with sizes smaller than 0.35 μ m (Fig. 2.12A). These minute cells are similar to those found in *M. pneumoniae* MPN311 mutant strain (Hasselbring and Krause, 2007a) and in the *M. genitalium* mg491- Δ p1 strain. Given these similarities, minute cell are thought to be consequence of terminal organelle detachments from the cell body, reinforcing the idea that MG491 has a role in the anchoring of the terminal organelle in a similar way as its *M. pneumoniae* ortholog protein P41.

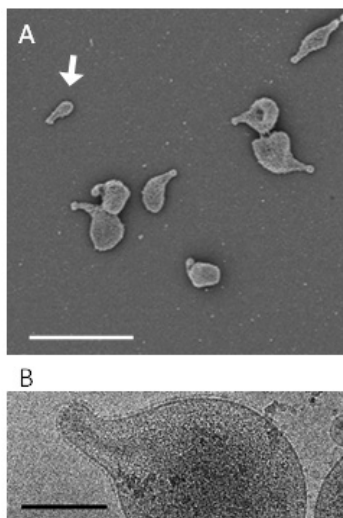


Fig. 2.12. (A) SEM micrograph showing the flask-shaped morphology of *M. genitalium* mg491-F157A-F158A cells. White arrow points a minute cell. Bar is 1 μ m. (B) Cryo-EM image of an mg491-F157-F158A cell showing a normal electron-dense core. Bar is 0.2 μ m.

Strain mg491-F157A-F158A did not exhibit deficiencies in gliding motility. The frequency of non-motile cells in this strain (80.7%) was similar to the frequency of non-motile cells in the G37 WT cell population (85%). Also the velocity of mg491-F157A-F158A cells ($0.100 \mu\text{m s}^{-1}$) represented the 83% of the velocity of G37 WT cells. This phenotype is in agreement with the low frequency of mg491-F157A-F158A cells bearing multiple terminal organelles.

Part 4: Characterization of mg491- Δ loopL2 strain

As described before, the loop L2 has a pivotal role stabilizing the MG491 quaternary structure and adopt two conformations in the different monomers. To further investigate the role of loop L2 in the function of MG491 protein, we engineered a mutant strain lacking the residues N155-K160. This mutant strain was obtained as by random transposon insertion of the mutated allele in the Δ mg491 null strain lacking the MG_491 gene (chapter 1). The Δ mg491-mg491cat strain (chapter 1) was used also as control.

One colony obtained after transform pMTncat Δ loopL2 suicide plasmid in Δ mg491 cells was selected and the transposon insertion was determined. Transposon insertion was located at 3' end of MG_460 gene coding for L-lactate dehydrogenase. Usually, transposon insertions close to the 3' end of a gene are not considered to disrupt gene function (Glass, 2006). This clone was named mg491- Δ loopL2 and used for phenotype examination. The protein levels of MG491 were restored in mg491- Δ loopL2 strain (Fig. 2.13B), suggesting that defects in quaternary structure caused by the deletion in loop L2 do not affect the stability of MG491 monomers. Also, the levels of terminal organelle proteins showed a recovery in this strain were very similar to those found in WT cells (Fig. 2.13A).

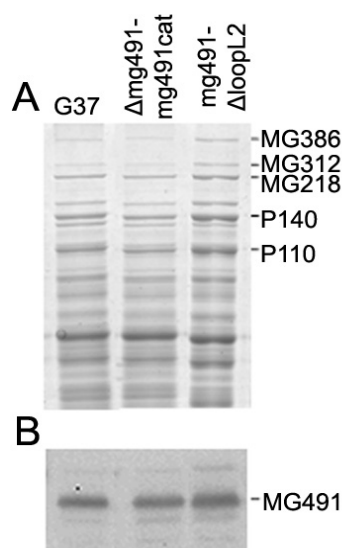


Fig. 2.13. Protein profile of *M. genitalium* G37, Δ mg491-mg491cat and mg491- Δ loopL2 strains. (A) SDS-PAGE showing a full recovery of the main TO proteins in both mutant strains. (B) Western Blot using anti-P41 antiserum showing normal levels of MG491 in the mutant strains.

One colony obtained after transform pMTncat Δ loopL2 suicide plasmid in Δ mg491 cells was selected and the transposon insertion was determined. Transposon insertion was located at 3' end of MG_460 gene coding for L-lactate dehydrogenase. Usually, transposon insertions

close to the 3' end of a gene are not considered to disrupt gene function (Glass, 2006). This clone was named mg491- Δ loopL2 and used for phenotype examination.

The protein levels of MG491 were restored in mg491- Δ loopL2 strain (Fig. 2.13B), suggesting that defects in quaternary structure caused by the deletion in loop L2 do not affect the stability of MG491 monomers. Also, the levels of terminal organelle proteins showed a recovery in this strain were very similar to those found in WT cells (Fig. 2.13A).

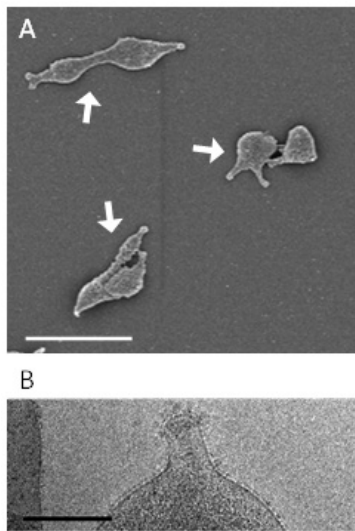


Fig. 2.14. (A) SEM micrograph showing the multiple TO phenotype of *M. genitalium* mg491- Δ loopL2 cells. White arrows point cells with multiple terminal organelles. Bar is 1 μ m. (B) Cryo-EM image of an mg491- Δ loopL2 cell showing a normal cytoskeleton. Bar is 0.2 μ m.

Electron microscope analysis of mg491- Δ loopL2 cells showed the presence of normal terminal organelles (Fig. 2.14). However, the frequency of cells bearing multiple terminal organelles was found unusually high (26.2%) when compared to G37 WT cells (4.9%). As described for mg491-C87S, this multiple terminal organelle phenotype is correlated with the presence of gliding motility deficiencies. By time-lapse microcinematography, only 29.6% of mg491- Δ loopL2 cells were found motile and the mean velocity of the motile cells was highly reduced ($0.033 \mu\text{m s}^{-1}$) when compared to G37 WT.

Part 5: Characterization of mg491- Δ Nt strain

MG491 N-ter domain shows a high identity with N-ter end of *M. pneumoniae* P41 protein. The crystal structure of this domain is still unsolved. To have a complete characterization of the MG491 protein, we were interested in the function of the N-ter domain of MG491. To this purpose, we engineered a mutant strain with a deletion of residues Met1-Gln61 by random transposon delivery of the mutated allele in the Δ mg491 null mutant strain (chapter 1). Strain Δ mg491-mg491cat was used as control.

The mutated allele was obtained by PCR amplification of the C-terminal of MG_491 gene from *M. genitalium* genome. The amplicon was excised and cloned into a pMTncat plasmid and the resulting pMTncat Δ Nt was electroporated into Δ mg491 cells. Transposon insertion of one transformant colony was examined and found to disrupt the MG_414 gene, which is

coding for a conserved hypothetical protein not involved in terminal organelle structure and function (Glass et al., 2006). This clone was named mg491- Δ Nt.

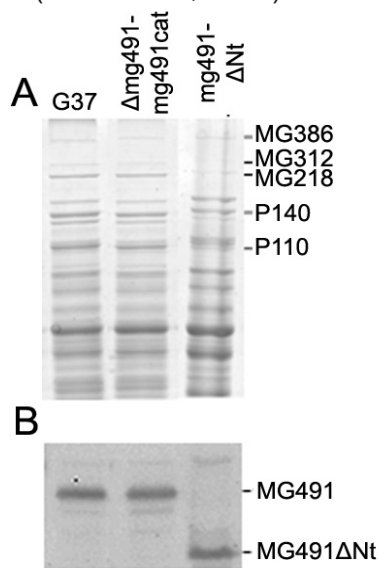


Fig. 2.15. Protein profile of *M. genitalium* G37, Δ mg491-mg491cat and mg491- Δ Nt strains. (A) SDS-PAGE showing reduced levels of MG312, MG218, P140 and P110 in mg491- Δ Nt strain. (B) Western Blot using anti-P41 antiserum showing normal levels of MG491 in the mutant strains and the shorter version of this protein in mg491- Δ Nt strain.

The introduction of pMTncat Δ Nt transposon in Δ mg491 cells restored the expression of MG491 to WT levels (Fig. 2.15B). The Western blot using anti-P41 polyclonal antibodies showed a protein band with a molecular weight consistent with the presence of the intended deletion (Fig. 2.15B). However, the main terminal organelle proteins showed reduced levels similar to those found in the parental Δ mg491 strain (Fig. 2.15A, chapter 1). This result confirms that MG491 has an important role in the stability of the terminal organelle, and indicates that its N-ter domain is essential for this function.

Cells from mg491- Δ Nt cells showed a filamentous morphology when examined by SEM (Fig. 2.16A) similar to that exhibited by Δ mg491 cells (chapter 1). In agreement with the low amounts of terminal organelle proteins, a few filaments end with a structure resembling the terminal organelle (Fig. 2.16A, arrow). Cryo-EM images showed no cytoskeletal structures inside the filaments of mg491- Δ Nt strain (Fig. 2.16B). Similar to Δ mg491 cells, standard 2 min time-lapse microcinematographies of mg491- Δ Nt strain did not show motile cells. All these results taken together suggest that N-ter domain of MG491 is essential for protein function.

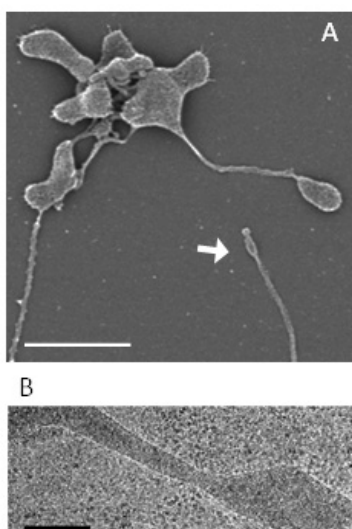


Fig. 2.16. (A) SEM micrograph showing the filamentous morphology of *M. genitalium* mg491- Δ Nt cells. White arrow points a cell filament ending in a terminal organelle-like structure. Bar is 1 μ m. (B) Cryo-EM image of an mg491- Δ Nt cell showing the absence of internal cytoskeleton. Bar is 0.2 μ m.

Table 2.3. Summary of the phenotype of mutant strains used in this work

Strain	Protein profile		Scanning Electron Microscopy			Time Lapse Microcinematographies		
	MG491	TO proteins	Shape	Multiple TO (%)	Minute Cells (%)	Motile cells (%)	Velocity ($\mu\text{m s}^{-1}$)	Resting Periods (%)
G37	+++	+++	Flask	4.9	1	85	0.121 ± 0.006	18
Δmg491	-	+	Filamentous	0	N/D	0	0	N/A
$\Delta\text{mg491-mg491cat}$	+++	+++	Flask	5.5	1.5	82.3	0.125 ± 0.003	19
$\text{mg491-}\Delta\text{p1}$	+++	+++	Flask	20.1	17.5	78.2	0.124 ± 0.004	22
Δp1TC6	+++	+++	Flask	16	4	80	0.128 ± 0.010	25
mg491-C87S	++	+++	Flask	12.5	2.5	19	0.098 ± 0.005	49
mg491-F157A-F158A	+++	+++	Flask	5.6	13.6	80.7	0.100 ± 0.005	24
$\text{mg491-}\Delta\text{loopL2}$	+++	+++	Flask	26.2	1	29.6	0.033 ± 0.004	29
$\text{mg491-}\Delta\text{Nt}$	+++	+	Filamentous	0	N/D	0	0	N/A

(+++) means WT protein levels, (++) means reduced protein levels, (+) means very low protein levels, (-) means undetectable protein levels.

N/D: although some minute cells were detected in Δmg491 and $\text{mg491-}\Delta\text{Nt}$, it is not possible to calculate a percentage due to the aggregative phenotype.

N/A: Not applicable, resting periods were calculated on motile cells.

Discussion

Because of the wide range of biological functions associated with the terminal organelle of mycoplasmas, this structure has been considered to play a central role in the lifestyle and pathogenesis of these microorganisms. Protein MG491 is required for the assembly of the *M. genitalium* terminal organelle (chapter 1), but its particular functioning in gliding motility has not been characterized yet. In this work, we have taken advantage of the current structural data obtained from MG491 protein to generate several *M. genitalium* strains with mutations in key residues and regions of this protein. Our results reveal that MG491 is a multitask protein required for proper terminal organelle functioning.

M. genitalium MG491 protein shares a high sequence identity (54%) with the *M. pneumoniae* P41 protein, located at the wheel-like complex. However, P41 is not required for the assembly of the *M. pneumoniae* terminal organelle (Hasselbring and Krause, 2007a). Surprisingly, our results suggested that the N-ter domain of MG491, which is strongly conserved in P41 (56% of sequence identity), is essential for terminal organelle assembly. The lack of N-ter domain in MG491 might also alter the folding and/or proper localization of this protein in mg491- Δ Nt cells, which would lead in a terminal organelle destabilization as observed in a MG491 null mutant strain.

P41 protein is involved in anchoring the *M. pneumoniae* terminal organelle and a null mutant strain for this protein showed terminal organelles detaching from the cell body (Hasselbring and Krause, 2007a). Strains mg491- Δ p1 and mg491-F157A-F158A revealed that MG491 protein is also responsible for the anchoring of the terminal organelle to the cell body of *M. genitalium*. These mutant variants were designed to impede the interaction between MG491 and MG200 proteins or hinder the quaternary organization of MG491, respectively. The mutations in these strains did not lead to severe motility deficiencies, but many isolated terminal organelles were detected in both strains. Minute cells similar to these detached terminal organelles were also detected in *M. genitalium* MG491 and MG218 null mutant strains when motility of these strains was partially restored upon introduction of an extra copy of MG_318 gene (chapter 1). These observations suggest that an accurate transmission of the movement generated at the terminal organelle to the cell body by the rod and wheel-like structures is needed to prevent terminal organelle detachments. In particular, our results propose that MG218 protein at the rod and MG491, together with MG200 at the wheel-like complex, are the major determinants for this function.

The role of MG491 in gliding motility could not be determined when examining cells from MG491 null mutant strain because of the presence of extensive downstream events in most of the terminal organelle proteins (chapter 1). The MG491 crystal structure has revealed a unique monomer organization. Loop L2, a small fragment of 20 residues, is involved in the interactions between the interfaces of the different subunits. We designed a *M. genitalium*

mutant strain with a deletion of six key residues from MG491 loop L2 in order to disrupt the MG491 quaternary interactions. Cells from mg491- Δ loopL2 strain exhibited significant gliding motility deficiencies, but this mutation did not lead to downstream events on other terminal organelle proteins or defects in the assembly of the terminal organelle overall structure. These results reveal an active role of MG491 protein in gliding motility similar to other *M. genitalium* wheel-like complex proteins such as MG200, MG386 and MG219 (Pich et al., 2006; Calisto et al., 2012; L. González-González et al., unpublished).

Gliding motility was also found affected when examining cells from the mg491-C87S mutant strain with a Cys87Ser substitution. Cells from this strain exhibited WT levels of all terminal organelle proteins and also showed normal cytoskeleton architecture, but the frequency of motile cells was found significantly reduced. Gliding motility is involved in the segregation of the terminal organelles to opposite poles during cell division and in cytokinesis (Hasselbring et al., 2006a; Seto et al., 2001, Pich et al., 2009, Lluch-Senar et al., 2010). In this way, gliding motility defects often result in the presence of cells bearing multiple terminal organelles probably as consequence of the long cytokinesis undergone by these cells (Pich et al, 2009, Lluch-Senar et al., 2010). However, the frequency of non-motile cells and the frequency of cells bearing multiple terminal organelles were not well correlated in mg491-C87S strain. Similar to *M. pneumoniae*, *M. genitalium* cells exhibit resting periods of different lengths and frequency (Radestock and Bredt, 1977; Pich et al., 2006; Calisto et al., 2012). The origin of these resting periods is unknown and they might be consequence of a temporal limitation in the energy sources. Alternatively, the regulatory mechanisms that stop gliding motility in dividing cells (Hasselbring et al., 2006a) could also be in the origin of these resting periods. The low frequency of cells showing multiple terminal organelles suggest that the high frequency of non-motile cells in mg491-C87S strain is probably the result of long resting periods exhibited by the cells of this strain. Interestingly, the frequency of cells showing resting periods was similarly increased in the *M. genitalium* mutant strains lacking the EAGR box from MG200 (Calisto et al, 2012), being the EAGR box from MG200 responsible of the interaction with MG491 Ct peptide_1. This suggests a close relationship between the resting periods and the interactions among both proteins.

It is noteworthy that the severe gliding motility defects in mg491-C87S mutant strain are consequence of a mutation in a single residue and suggest a major role for Cys87 in MG491 monomers. Cysteine residues might act as molecular switches in protein function because the redox state of thiol groups can be reversed by different ways (Lipton et al., 2002; Loi et al., 2015, Leichert and Jacob, 2004). Although cytoplasm is normally reduced due to the presence of low molecular weight thiols (e.g. cysteine) and enzymatic oxidoreductases (Fahey et al. 2013; Loi et al., 2015; Das et al., 2012), some events, such as the release of reactive oxygen species (ROS) by the host's innate immune response, might lead to an oxidative stress (Zhang and Baseman, 2014, Pritchard and Balish, 2015). Cysteine thiol groups can be easily oxidized by the presence of ROS, reactive electrophile species

(RES) and reactive nitrogen species (RNS) generated during oxidative stresses. Common modifications include oxidation to sulfenic acid, S-nitrosylation or formation of a disulfide bond (Lipton et al., 2002). Recently, it has been reported that cysteine residues from many bacterial proteins –such as OxyR from *Salmonella typhimurium*, rsrA from *Streptomyces coelicolor* or Spx and ohrR from *Bacillus subtilis*– are modified as a consequence of oxidative stress, normally by the formation of a disulfide bond or by oxidation to sulfenic acid. These modifications act as ‘redox switches’ in protein function being sensors of oxidative stress. These oxidized proteins can activate the transcription of genes involved in oxidative stress response, including those encoding for peroxidases or thioredoxin reductases (Antelmann and Helmann, 2011; Giles, 2003). The presence of a single Cys residue in MG491 raises the possibility that the activity of this protein could be regulated. The formation of a disulfide bond between two subunits in MG491 oligomer promotes the transition of the π -helix turn into a more stable α -helix turn. Since cells from mg491-C87S mutant strain showed a high frequency of resting periods, it is tempting to propose that disulfide formation could act as a switch in gliding motility and suggest that the oxidative stress might be an important regulator of gliding motility.

Gliding motility also ceases and reinitiates during cell division in a coordinated way (Hasselbring et al., 2006a; Seto et al., 2001), suggesting that mycoplasmas possess a regulatory mechanisms for gliding motility. In fact, it has been suggested that P41 may co-ordinate gliding cessation in *M. pneumoniae* (Hasselbring and Krause, 2007a). It is noteworthy that P41, as well as other proteins of the terminal organelle such as HMW1, HMW2 and P1, are phosphorylated by protein kinase C PrkC and dephosphorylated by the protein phosphatase PrpC (Schmidl et al., 2010, Page and Krause, 2013). In this way, PrkC mutants exhibit gliding motility deficiencies while PrpC mutant show an enhanced motile properties (Page and Krause, 2013). This suggests that gliding motility in *M. pneumoniae* is regulated by phosphorylation of some of the terminal organelle proteins, probably including P41. In *M. genitalium*, MG491 is a good candidate to be a modulator of gliding motility by both phosphorylation and disulfide bond formation. However, the phosphorylation status of MG491 has not been determined yet.

In conclusion, this work provides a substantial insight into the role of MG491 in the structure and function of the *M. genitalium* terminal organelle. Besides being a fundamental component of the terminal organelle structure, this protein promotes the motility of these cells and anchors the terminal organelle to the cell body. Finally, the presence of several residues with a potential regulatory role makes this protein an excellent candidate to integrate the signals from different biological processes and to provide a response by modulating the gliding motility of mycoplasma cells.

Quantitative Hemadsorption Assay for Mycoplasma Species Using Flow Cytometry

Flow cytometry is a laser-based technology that allows simultaneous multiparametric analysis of the physical and chemical characteristics of up to thousands of particles per second. In a flow cytometer, cells are suspended in a stream of fluid and passed individually through some lasers and detectors. Physical characteristics of the cell particles affect light dispersion. Traditionally, the forward scatter (FSC) is correlated with the volume of the cell particle, and the side scatter (SSC) is correlated with internal complexity, but also with the volume of the particle. Flow cytometers also are able to detect different fluorescent molecules. Hence, in a single experiment, cells can be classified by their size, by their complexity and by their fluorescence.

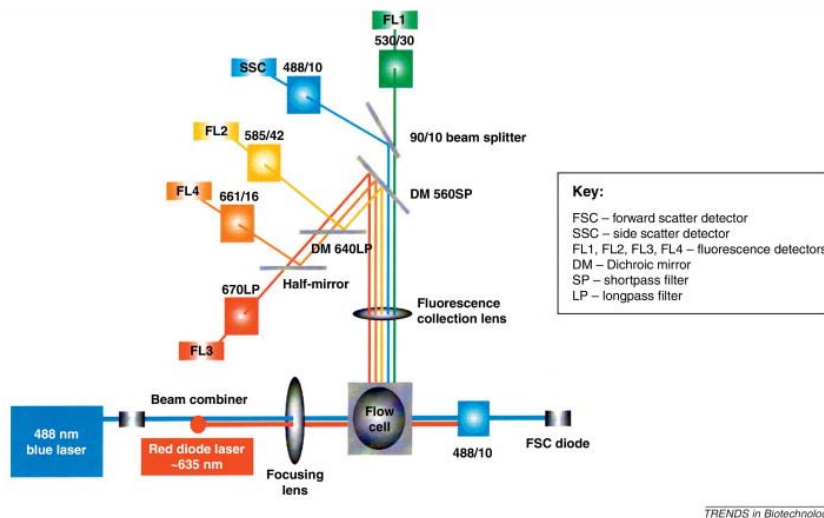


Fig. 3.1. BD FACSCalibur Optical Path Configuration, from Da silva et al., 2012.

In the experiment presented in this study, three different populations need to be distinguished. First, it is expected that erythrocytes show high values for FSC and SSC, but a low fluorescence when staining nucleic acids with SYBR green I. In contrast, mycoplasmas are expected to show low values for FSC and SSC due to their small size, but higher values for SYBR green fluorescence. Finally, erythrocytes with attached mycoplasmas must show high values for FSC, SSC and SYBR fluorescence.

This work has been published in:

García-Morales L, González-González L, Costa M, Querol E, Piñol J (2014) Quantitative Assessment of Mycoplasma Hemadsorption Activity by Flow Cytometry. PLoS ONE 9(1): e87500. doi:10.1371/journal.pone.0087500

Introduction

Mycoplasmas are a wide group of microorganisms characterized by the absence of cell wall and are closely related to Gram-positive bacteria. These microorganisms possessing small streamlined genomes and a low number of metabolic pathways (Pollack et al., 1997) probably evolved as a consequence of their parasitic lifestyle. Many mycoplasmas are pathogens of humans and a wide range of animals, and most of them adhere to host cells in the first stages of infection (Rottem, 2003, Krause et al., 1982), being this step essential for further colonization (Razin and Jacobs, 1992). Some of these adherent mycoplasmas have developed highly complex polar structures assisting cells in the attachment to target tissues (Burgos et al., 2006, Mernaugh et al., 1993). These specialized structures also propel the cells when they glide across solid surfaces (Hasselbring and Krause, 2007a, Miyata, 2010) and have a pivotal role on virulence (Jordan et al., 2007, Krunkosky et al., 2007).

Mycoplasma genitalium is a human pathogen that is the causative agent of non-chlamydial and non-gonococcal urethritis (Horner et al., 1993). Besides constituting an appealing model for minimal cell and synthetic biology studies, this microorganism is also an excellent subject to investigate the adhesion mechanisms both at molecular (Burgos et al., 2006) and clinical level (Ma et al., 2010, McGowin et al., 2010, Ma et al., 2012). A collection of *M. genitalium* mutants showing attachment deficiencies is now available (Pich et al., 2008, Burgos et al., 2006) and the accurate measurement of hemadsorption (HA) activity is essential to obtain data about the function of the different proteins involved in cell adhesion. In addition, measuring the HA of the growing number of clinical isolates (Hamasuna et al., 2007, Jensen et al., 1996) may provide important clues about the infective mechanisms of this microorganism. A standardized assay to quantify HA would also benefit the growing number of studies in many other related mycoplasmas with special relevance of those involved either in human or animal health. Furthermore, the use of a standardized assay in clinical practice would help in the prognosis of mycoplasma infections, which is especially relevant in infections by outbreak strains occurring worldwide (Arnal et al., 2013, Hewicker-Trautwein et al., 2002, Spergser et al., 2013).

Different methods are currently available to quantify the HA of mycoplasmas (Miyata et al., 2000, Pich et al., 2008, Willby and Krause, 2002). However, they are very expensive, time consuming or not reproducible enough to be used in standardized clinical assays. Given these limitations, measuring HA by an approach based in flow cytometry (FC) could be interesting in terms of accuracy, reproducibility and speed. However, there are relatively few works dealing with FC and mycoplasmas, probably because of the small size of mycoplasma cells that may discourage, at first glance, their analysis by FC. Despite this, there is an increasing number of works showing that FC is an accurate method to detect and quantify mycoplasma cells in broth medium (Assuncao et al., 2006b, Assuncao et al., 2006c) or in natural samples (Assuncao et al., 2007). FC has been used also to quantify the

effect of several antibacterial agents (Assuncao et al., 2006a, Soehnlén et al., 2011) and to detect hemotropic mycoplasmas on red blood cells (RBCs) samples (Sanchez-Perez et al., 2013). Here we show that FC could be used to measure rapidly and accurately the HA activity of mycoplasmas in the presence of SYBR Green I, a vital fluorochrome that stains nucleic acids, allowing to resolve RBCs and mycoplasma cells by their different size and fluorescence. This method also permits the kinetic analysis of the obtained data, allowing a precise HA quantification based on standard parameters such as the dissociation constant K_d . An additional advantage of the kinetic analysis is the provision of a reproducible method to compare the HA activity of strains from different mycoplasma species.

Results

Cell Titration and Biomass Estimation

Once stained with SYBR Green and analyzed by FC, events from mycoplasma cells were very heterogeneous and are enclosed in a wide zone (R1, Fig. 3.2A) of FC events. Most of mycoplasma cells raised events of low SSC-H and SYBR Green fluorescence values but there were also a variable number of cell aggregates generating events with increased values for both parameters. On the other hand, and in agreement with their large size, RBCs appear in a discrete region of events (R2, Fig. 3.2A) with high SSC-H values but a low SYBR Green fluorescence due to their low content of nucleic acids. To test that mycoplasma cells were efficiently stained with SYBR Green I, a sample of stained mycoplasmas was examined by phase contrast and epifluorescence microscopy showing that virtually all mycoplasma cells were stained with this dye (Fig. 3.3).

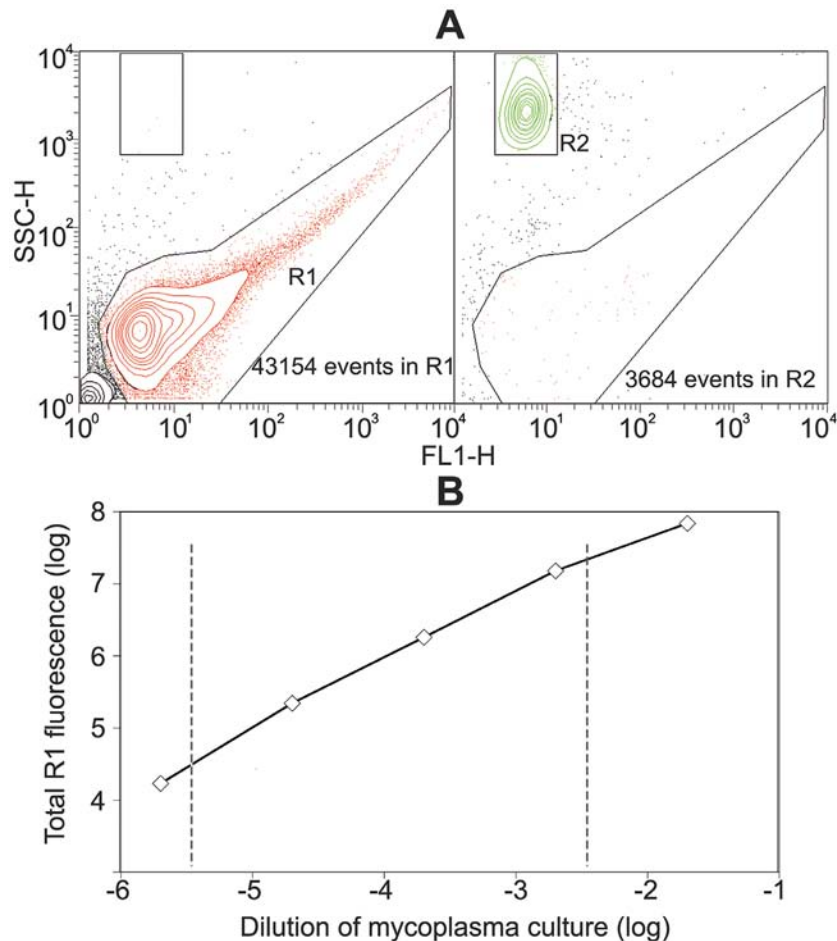
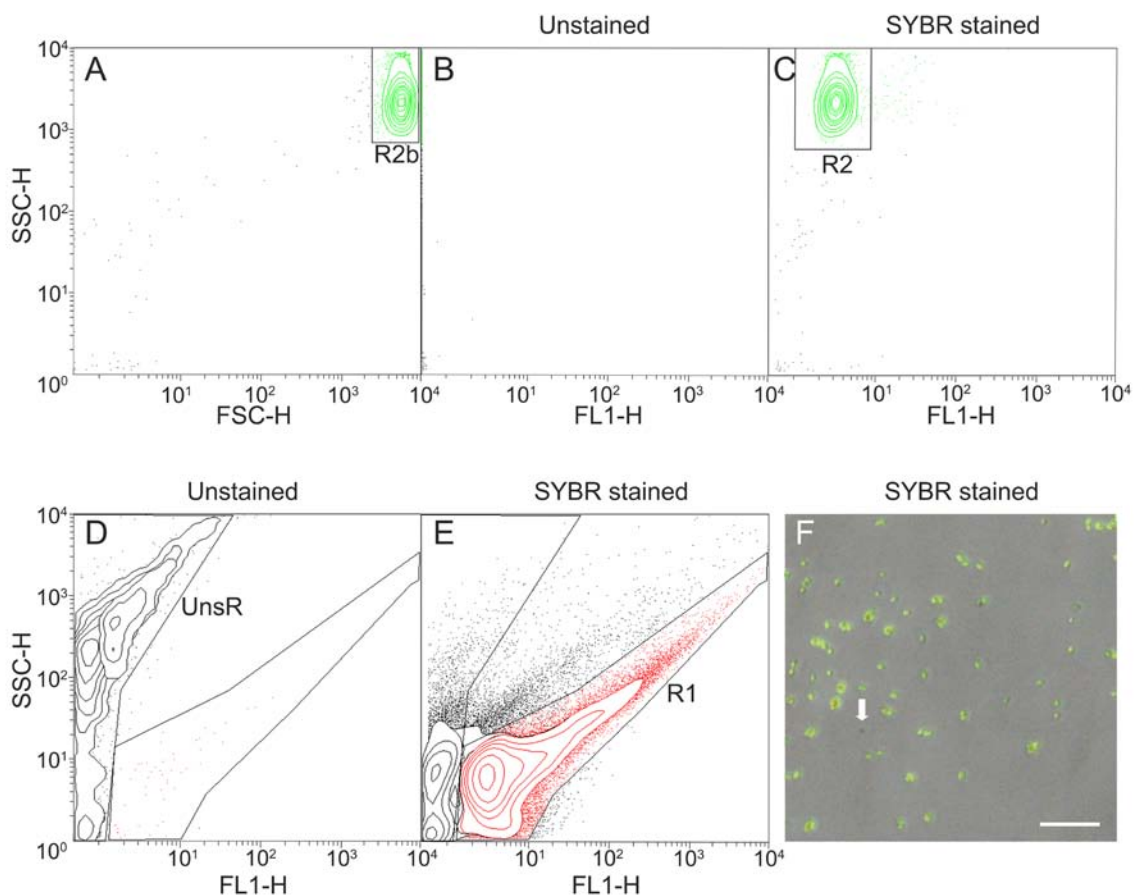


Fig. 3.2. Titration of mycoplasma cells and RBCs by flow cytometry. (A) Dual parameter dot plot of SSC-H (Side-angle-scatter) versus FL1 (SYBR Green fluorescence) showing events from a *M. genitalium* G37 population (R1 region containing $4 \cdot 10^4$ events and $8 \cdot 10^5$ arbitrary units of total fluorescence) and RBCs (R2 region containing $3.6 \cdot 10^3$ events). (B) Total fluorescence of the events in R1 region from serial dilutions of a *M. genitalium* culture showing a lineal distribution over a three log dilution range, which is indicated by dashed lines. Total fluorescence units of FL1-H were calculated by multiplying the FL1-H mean value by the total number of events in the analysed region.



<i>M. genitalium</i> sample	events in UR	events in R1
Unstained	1528 (96.6%)	54 (3.4%)
SYBR Green I stained	12253 (23%)	40958 (77%)

Fig. 3.3. RBCs and mycoplasma cells are consistently stained by SYBR Green I. (A) RBCs analyzed in the SSC-H vs. FSC-H plot. Events were counted using the light scattering properties of RBCs. (B) Unstained RBCs in SSC-H vs. FL1-H plot. Autofluorescence of unstained RBCs is extremely low and most events were found piled up in the y-axis and giving irreproducible counts. (C) SYBR Green I stained RBCs in SSC-H vs. FL1-H plot. RBCs, with a very small amount of nucleic acids, were weakly but consistently stained by SYBR Green I. When comparing values from A and C plots, 99% of events in R2 were detected after staining with SYBR Green I. (D) Unstained mycoplasma cells in SSC-H vs. FL1-H plot. Unstained mycoplasmas were slightly autofluorescent and could be enclosed in the region UR. (E) SYBR Green I stained mycoplasmas in SSC-H vs. FL1-H plot. Stained mycoplasmas were enclosed in the R1 region, which includes a very heterogeneous population of events ranging from single cells to big aggregates. A higher amount of events were detected in the stained mycoplasma sample, being the number of events in R1 consistent with the number of CFUs detected after plating the mycoplasma suspension in SP4 agar. SYBR Green I staining also allowed to discriminate mycoplasma cells from the debris using a threshold on FL1. (F) SYBR Green I stained mycoplasma sample observed by phase contrast and epifluorescence microscopy. From 400 single cells and aggregates counted, only 3 cells (0.75%) showed no fluorescence, indicating that most of mycoplasma cells, and not only cell aggregates, are consistently stained by this procedure. Bar is 10 μ m.

RBCs stock was tittered by counting the events showing high SSC-H values but a low fluorescence when stained with SYBR Green (Theron et al., 2010). However, tested mycoplasma cells were very prone to form cell aggregates and therefore the counting of the number of FC events is not a good method for assessing the biomass of these cells. We found that the total SYBR Green fluorescence of the mycoplasma population provides a better estimation of cell biomass since SYBR Green fluorescence is directly correlated with the amount of nucleic acids in the analyzed sample. Total SYBR Green fluorescence also shows a linear response spanning about three logs when examining different dilutions of *M. genitalium* cultures (Fig. 3.2B). All the mycoplasma samples used in the HA assay had a total SYBR Green fluorescence values among the limits of the linear region in Fig 3.2B.

FC Analysis of Mycoplasma HA

After incubating RBCs and mycoplasma cells, it was noticeable a decrease in the total fluorescence of the mycoplasma region R1 and a shift to higher fluorescence values of the events in the RBC region R2 (Fig. 3.4A) consistent with the attachment of mycoplasmas to RBCs. However, it was also evident a new population of events from particles generated while the FC samples were incubated with mild shaking. These particles were also apparent even in the absence of mycoplasmas and RBCs (Fig. 3.4E) suggesting that these particles were derived from the mycoplasma culture medium added to the HA reaction. The size and the total fluorescence of this new population was very variable among different experiments, with events overlapping R1 and R2 regions (Fig. 3.4A) and precluding the accurate measurement of the fluorescence in these regions. Fortunately, events of this new population had an intrinsically high red autofluorescence (Fig. 3.4B) providing a way to discriminate them from events of mycoplasma cells, which remained grouped in a new R3 region. Double gating of R1 and R3 regions allowed to construct new region MR containing only the events from mycoplasma cells (Fig. 3.4C) endowing a simple method to quantify in a reproducible way the total fluorescence of free mycoplasmas remaining after the HA reaction. Furthermore, we investigated the presence of WBCs in the RBCs stock and if these nucleated cells may interfere with the mycoplasma quantification in the HA assay. We detected a very small amount of WBCs in the preparation of RBCs, with no events overlapping the MR region of mycoplasma cells (Fig. 3.5) indicating that WBCs were not interfering the HA assay. In addition, some mycoplasma samples were also examined using a double staining by adding propidium iodide to quantify the frequency of dead cells. Only 4% of mycoplasma cells were stained with propidium iodide (Fig. 3.6), indicating that most of cells remained viable at least for two hours in the settings used to perform the HA reaction.

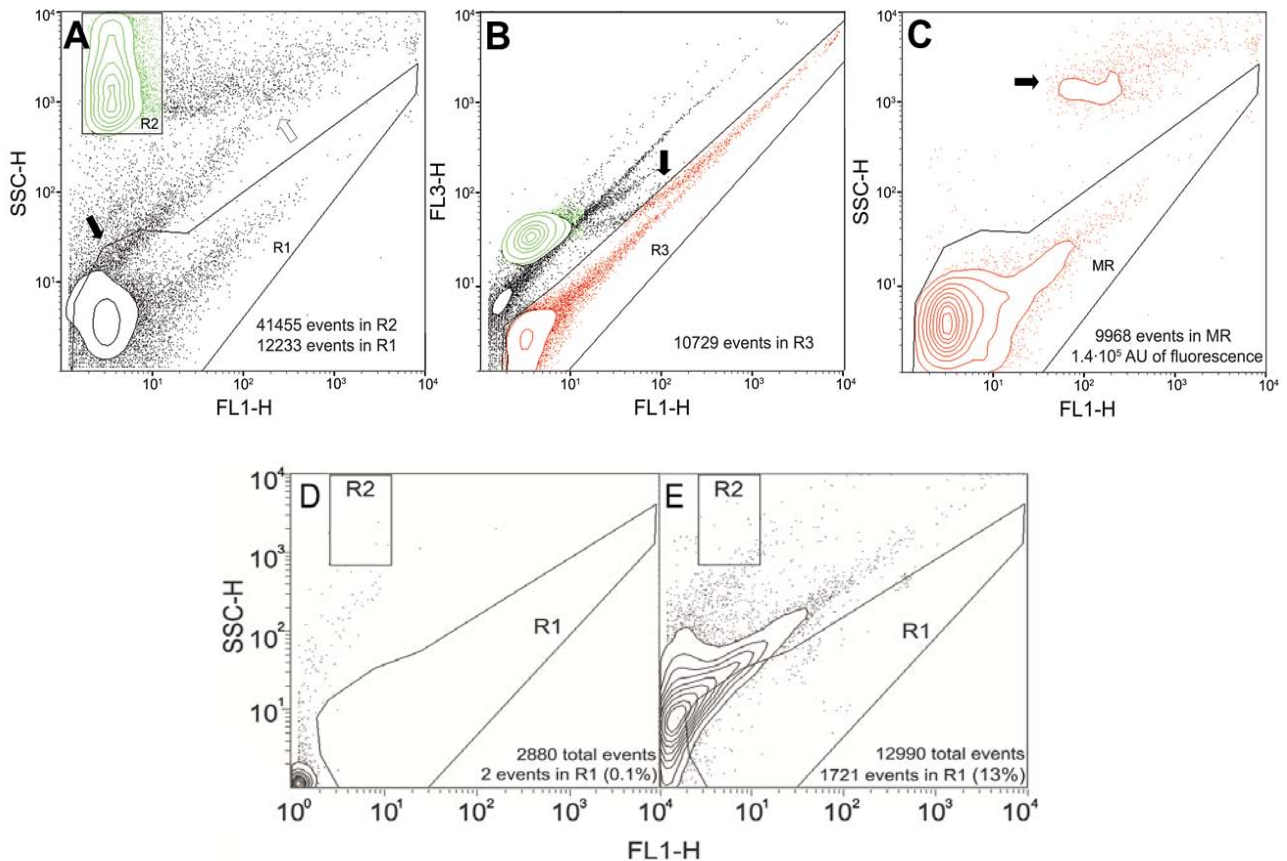


Fig. 3.4. Resolution of cell populations after the HA reaction containing RBCs, RBCs with attached mycoplasmas and free mycoplasmas. (A) Overview of the cell mixture in a dual plot of SSC-H vs. FL1-H fluorescence. R2 region includes RBCs and R1 region contains the free mycoplasmas after the HA reaction. The solid arrow points to an area where the debris from the culture medium is overlapping with mycoplasmas in the R1 region and the empty arrow indicates an area with debris overlapping the R2 region. (B) Dual plot of FL3-H vs. FL1-H fluorescence allowing the separation of the free mycoplasmas from debris due to the intrinsically high autofluorescence of these particles. Note that R3 region includes the free mycoplasmas after the HA reaction but also contains a significant fraction of RBCs with attached mycoplasmas. The arrow points to these RBCs with attached mycoplasmas invading the R3 region. (C) A new dual parameter plot of SSC-H vs. FL1-H showing only the events in R3 region finally resolves the free mycoplasmas (MR region) from the RBCs with attached mycoplasmas, pointed with an arrow. Total fluorescence of free mycoplasmas in the MR region can now be precisely quantified and used in the subsequent calculation of the HA parameters K_d and B_{max} . (D) Sample of 50 μ L of SP4 medium diluted in 1 mL of PBSCM and stained with SYBR Green I. (E) Same sample as in (D), but incubated 40 min at 37°C and end-over-end mixing before staining with SYBR Green I. This sample shows that the number of fluorescent particles increases dramatically upon incubation of SP4 medium with a significant percentage of events (13%) overlapping the mycoplasma region R1. The double gating strategy reduces drastically the number of events from medium particles overlapping with the mycoplasma region MR to 1%.

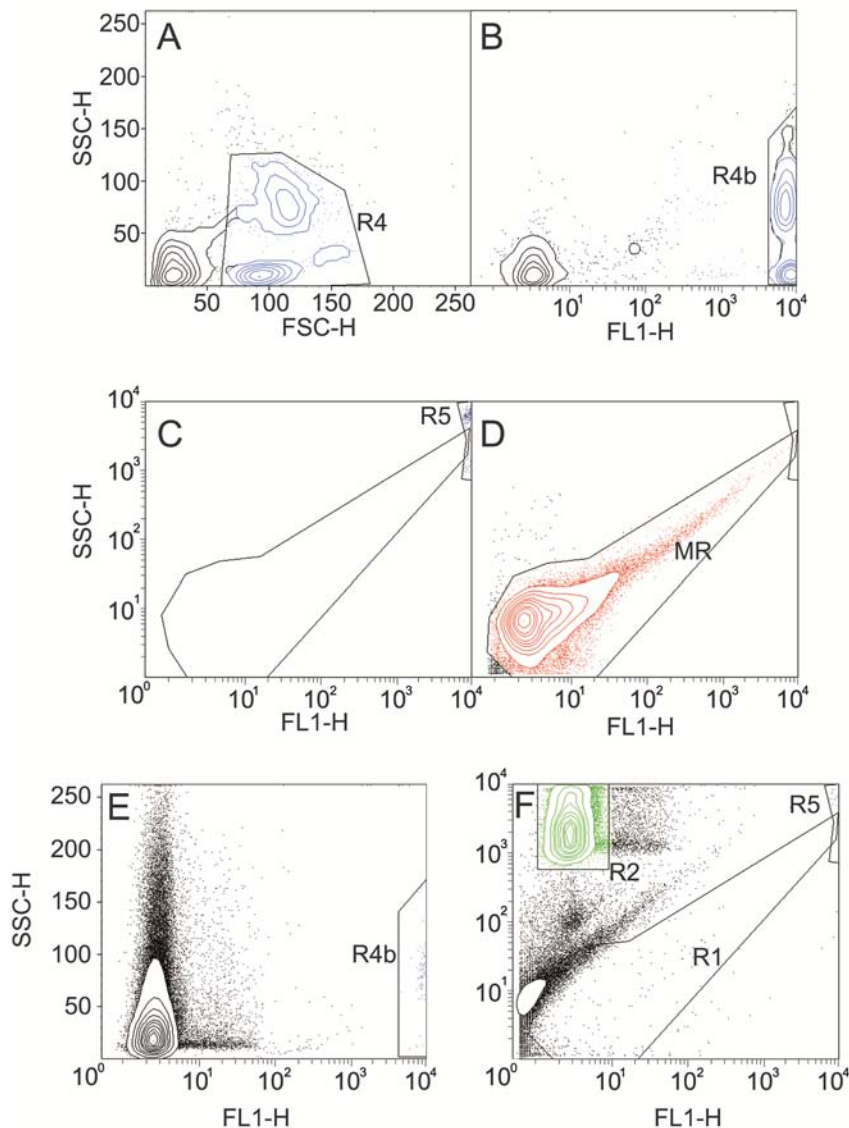


Fig. 3.5. Flow cytometry analysis of white blood cells (WBCs). Leukocytes from a 200 μ L blood sample were purified by standard procedures using ACK buffer (Bossuyt et al., 1997) and resuspended in 0.5 mL of PBSCM. This stock was diluted 1:10 in PBSCM, stained with SYBR Green I and analyzed by flow cytometry (Panels A–C). In panel A, SSC and FSC laser settings were optimized for the counting of WBCs (E00 for FSC, 400 for SSC and lineal amplification). As expected, discrete populations of leukocytes were obtained in region R4 and a total of 1091 WBCs were enumerated. In panel B, the settings for SSC were also optimized for the counting of WBCs (400 for SSC) and FL1 settings were those used for mycoplasma detection (383 for FL1). A total of 1170 WBCs were detected in the region R4b and they exhibited very high FL1-H values according to their high DNA content. In panel C, the WBCs sample was analyzed using the SSC and FL1 settings optimized for mycoplasma detection (487 for SSC, 383 for FL1 and logarithmic amplification). Only 173 events of WBCs were detected with these settings in region R5, which represent 15% of the total WBCs. From these events, 4 were detected into the region of mycoplasmas MR, representing a negligible fraction of WBCs population. Cell debris from the lysis step were removed in a FSC-H versus SSC-H plot (data not shown). To compare with the previous data, a mycoplasma sample was analyzed using the same settings (Panel D). To find out the number of WBCs in the RBCs samples used to quantify the HA activity (Panels E and F), a RBCs sample was analyzed in Panel E using the same settings as in Panel B. Only 78 events of WBCs were detected in region R4b, which is a very small number when compared with the 1170 events in the WBCs preparation. When using the settings optimized for mycoplasma detection (Panel F), the number of events from WBCs in R5 was even smaller. None of these events fell into the R1 mycoplasma region. These results indicate that the small number of WBCs remaining in the RBCs preparation has no effect when quantifying the mycoplasma cell biomass after the hemadsorption reaction.

Region	Cell type	Number of events (% of cell type)
Flow cytometry analysis of white blood cells (WBCs). Panels A, B and C.		
R4	WBCs	1091 (93%)
R4b	WBCs	1170 (100%)
R5	WBCs	173 (15%)
R5 and MR	WBCs	4 (0.3%)
Flow cytometry analysis <i>M. genitalium</i> . Panel D.		
MR	<i>M. genitalium</i> G37	41991 (100%)
R5 and MR	<i>M. genitalium</i> G37	1 (0.002%)
Flow cytometry analysis of RBCs with SP4 medium. Panels E, F.		
R4b	WBCs	78 (100%)
R5	WBCs	16 (20%)
R5 and R1	WBCs	0 (0%)
R2	RBCs	141845 (100%)
R1	SP4 Debris	350

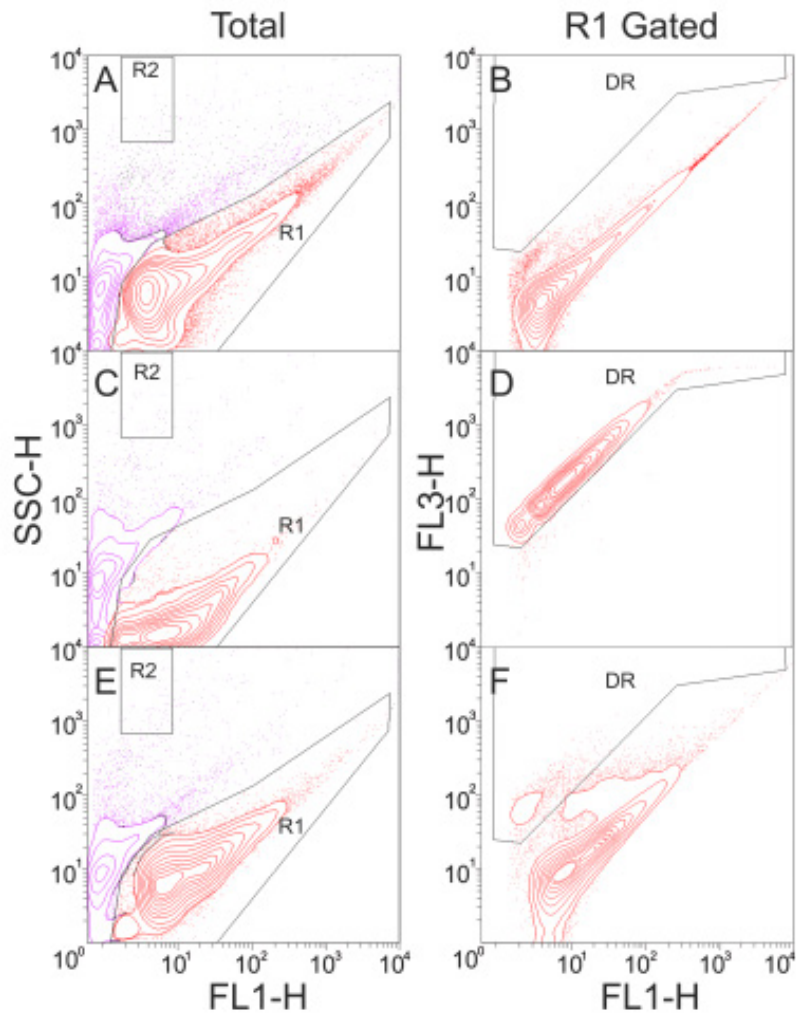


Fig. 3.6. Flow cytometry (FC) analyses of *Mycoplasma* non-viable cells. Three *Mycoplasma genitalium* cell samples were prepared at a $3 \cdot 10^6$ FL1 fluorescence units mL^{-1} (the usual working dilution for FC analyses). These samples were incubated 40 min at 37°C with end-over-end mixing and stained 20 min with SYBR Green I. To detect the presence of non-viable cells, some of the samples were also stained with $2 \mu\text{g mL}^{-1}$ propidium iodide (PI) for 5 min before being analysed by FC using SSC-H vs. FL1-H plots (panels A, C and E) and FL3-H vs. FL1-H plots (panels B, D and F). Since PI staining increases dramatically the FL3-H fluorescence of dead mycoplasma cells, the double gating strategy to reduce the number of events from medium particles overlapping with the mycoplasma region R1 could not be used. Alternatively, the mycoplasma population region R1 was delimited in SSC-H vs. FL1-H plots and this region was then gated in FL3-H vs. FL1-H plots. Panels A-B: control sample containing mycoplasma cells non-stained with PI. Panels C-D: positive control containing PI-stained cells permeabilized with 0.015% Triton X-100 to demonstrate that non-viable cells are strongly stained with PI and exhibit a concomitant increase in FL3-H fluorescence. PI-stained cells could be enclosed in a region DR. Panels E-F: unpermeabilized mycoplasma cells stained with PI. FC analyses showed a slight increase in FL3-H fluorescence and only a small fraction of the events (4.3%) fell into the DR region, suggesting that most of the mycoplasma cells remain viable in the conditions used to perform the HA assay.

The first experiments to quantify the HA reaction were conducted using a fixed amount of RBCs, increasing amounts of mycoplasma cells and measuring the shift to higher fluorescence values of the events in the RBC region. However, this approach has two severe drawbacks. By one hand, when using increasing amounts of mycoplasma cells, regions R1 and R2 were gradually closer and became eventually overlapped. On the other hand, events from the particulate material of the culture medium are very prone to overlap with R2 region as indicated above and this problem was exacerbated at the highest concentrations of mycoplasma cells (Fig. 3.7).

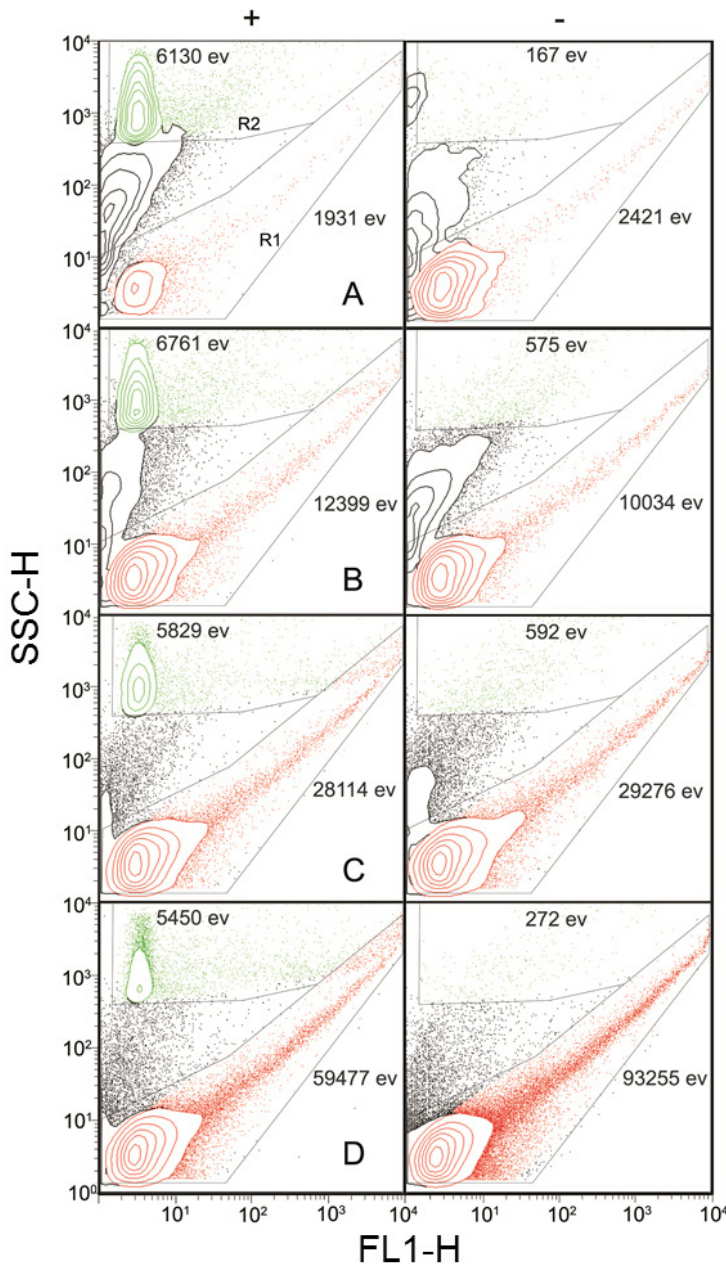


Fig. 3.7. HA assay using a fixed amount of RBCs and increasing amounts of mycoplasma cells. (+) column contains the dot plots of the mixtures of RBCs and increasing amounts of mycoplasmas. In (-) column are the dot plots of the same mycoplasma samples in the absence of RBCs, respectively. (A–D) When increasing the mycoplasma concentration from A to D in the hemadsorption reaction, the fluorescence in the RBC R2 region shifts to higher FL1-H fluorescence values as a consequence of the attachment of mycoplasmas. Despite the fact that the data could be modeled to a Langmuir plot, medium debris invade the R2 region as seen in the (-) column and, as a result, R2 FL1-H total fluorescence measures are not reliable. Furthermore, when using the highest amounts of mycoplasma cells (C–D) cell aggregates overlap to the R2 region and RBCs containing attached mycoplasma invades the R1 region, making difficult to obtain reproducible measures of RBCs in R2 region.

In consequence, we designed a new HA assay using a fixed amount of mycoplasma cells, increasing amounts of RBCs and measuring the free mycoplasmas remaining after the HA reaction. Using these conditions, the amount of free mycoplasmas decreased when increasing the amount of RBCs and the obtained results were very reproducible among different experiments (Fig. 3.8 and 3.9). The binding of mycoplasma cells to RBCs was also confirmed by examining some FC samples by phase contrast and epifluorescence microscopy (Fig. 3.9C). Since adhesion of cells from HA positive mycoplasma strains is also dependent on the RBC concentration as described previously (Baseman et al., 1982a), the binding reaction between both cells also follows a first order Langmuir isothermal kinetics (Langmuir, 1918) and the amount of free mycoplasmas found at any given RBC concentration can be modeled using the equation:

$$M_f = 1 - \frac{B_{\max} [RBC]}{K_d + [RBC]}$$

that results in an inverse Langmuir plot, where M_f is the fraction of free mycoplasma cells, $[RBC]$ is the number of FC events in R2 region per μL , B_{\max} the maximum fraction of mycoplasma cells bound to RBCs and K_d is the dissociation constant of the binding reaction. Similar to other kinetic analyses performed on binding reactions involving a ligand and a receptor, the lower K_d and the higher B_{\max} are indicative of the stronger HA activity of the tested cells.

HA Properties of Different Mycoplasma Strains

Using this method, the HA parameters of *M. genitalium* G37 WT strain and several isogenic *M. genitalium* strains as well as two additional mycoplasma species were determined (Fig. 3.8). Obtained values from three or more biological replicates for each strain were highly reproducible. Consistent with previous works (Pich et al., 2008) G37 WT strain exhibited the lower K_d while isogenic strains mg218^- and mg317^- , with an intermediate HA phenotype, showed higher K_d values, being the mg317^- strain K_d slightly higher than that of the WT strain. Interestingly, B_{\max} values were very similar for WT and mg218^- strains and lower for mg317^- strain. These results suggest that the nature of the intermediate HA phenotype of strains mg218^- and mg317^- might have a different origin at the molecular level. As expected, when testing the HA negative strain mg191^- , the number of free mycoplasmas was very high, independently of the RBC concentration and showed a non-detectable decrease even at the highest RBC concentration tested. In the absence of binding, data from strain mg191^- could not be modeled using the inverse Langmuir plot (Fig. 3.8A). We also determined the HA parameters of different mycoplasma species (Fig. 3B). Cells from *M. penetrans*, a HA positive mycoplasma, exhibited a K_d value higher than *M. genitalium* cells and a B_{\max} value not significantly lower than these cells. In contrast, cells from *M.*

hyopneumoniae, a HA negative mycoplasma, showed no detectable adhesion to RBCs and binding parameters could not be determined, similarly to the non-adherent *M. genitalium* mg191⁻ strain.

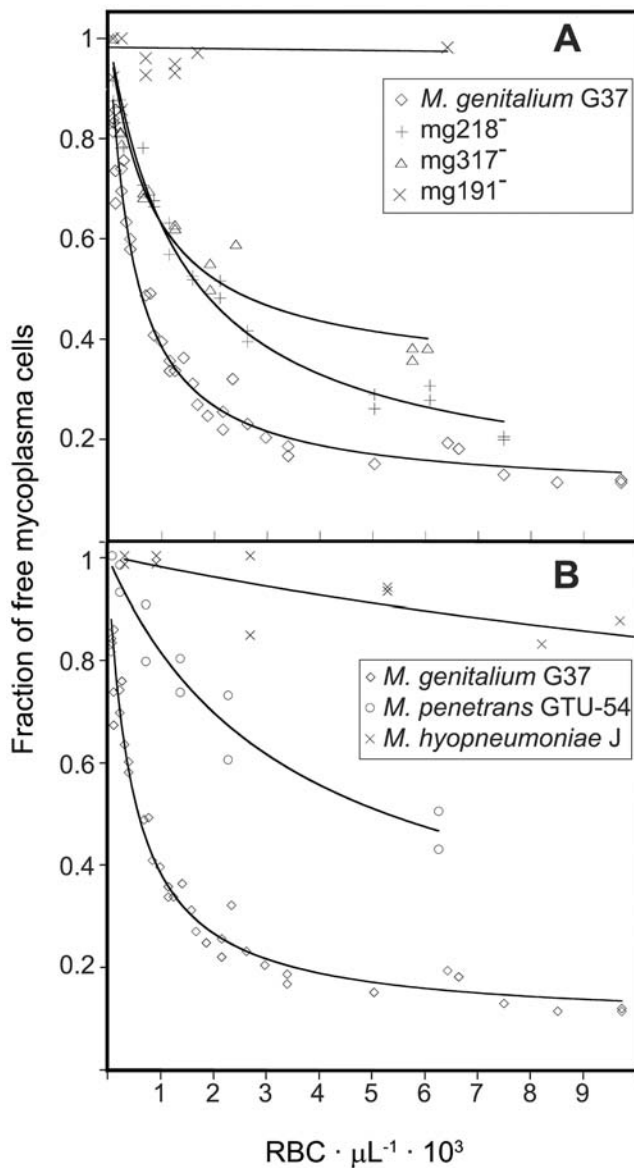


Fig. 3.8. Inverse Langmuir plots of HA assays containing a fixed amount of mycoplasma cells and increasing amounts of RBCs. The fraction of free mycoplasma cells was calculated from the total FL1-H fluorescence values in the MR region (Fig. 3.4) of each HA reaction taking as reference the total FL1-H fluorescence in a mycoplasma sample without RBCs. (A) Plots from HA assays containing *M. genitalium* G37 strain and its isogenic mutant strains mg218⁻, mg317⁻ and mg191⁻. (B) Plots from HA assays performed with different mycoplasma species.

Strain	Qualitative HA ^a	$B_{\max} \pm SE^b$	$K_d (\text{RBC} \cdot \mu\text{L}^{-1}) \pm SE^b$
<i>M. genitalium</i> G37	+	0.91 ± 0.01	474.8 ± 31.5
<i>M. genitalium</i> mg218 ⁻	+	0.91 ± 0.03	1442.5 ± 155.6
<i>M. genitalium</i> mg317 ⁻	+	0.68 ± 0.04	840.8 ± 149.4
<i>M. genitalium</i> mg191 ⁻	-	NA	NA
<i>M. penetrans</i> GTU-54	+	0.83 ± 0.13	3489.4 ± 1079.3
<i>M. hyopneumoniae</i> J	-	NA	NA

^a References: *M. genitalium* G37 (Tully et al., 1983b), *M. genitalium* mg218⁻ and mg317⁻ (Pich et al., 2008), *M. genitalium* mg191⁻ (Burgos et al., 2006), *M. penetrans* GTU-54 (Lo et al., 1992), *M. hyopneumoniae* J (Young et al., 1989).

^b SE, standard error

When analyzing the dot plots corresponding to different HA reactions, it was observed that mycoplasma cell aggregates with the highest SSC-H values and the strongest SYBR Green fluorescence bind to RBCs at a higher rate than single mycoplasma cells when increasing the concentration of RBCs. In addition, the presence of mycoplasma cell aggregates on RBCs was also observed in the epifluorescence images (Fig. 3.9C). These findings were further investigated by dividing the different dot plots into four separate quartiles (Q1 to Q4, Fig. 3.9A) and constructing inverse Langmuir plots using the fluorescence data of mycoplasma cells in each quartile. Once K_d and B_{max} were determined for data grouped into quartiles (Fig. 3.9B), there was a good correlation between the HA and the size of mycoplasma cell aggregates, being the larger aggregates those that exhibited the strongest HA and providing evidence that the binding of mycoplasma to RBCs probably follows a cooperative behavior.

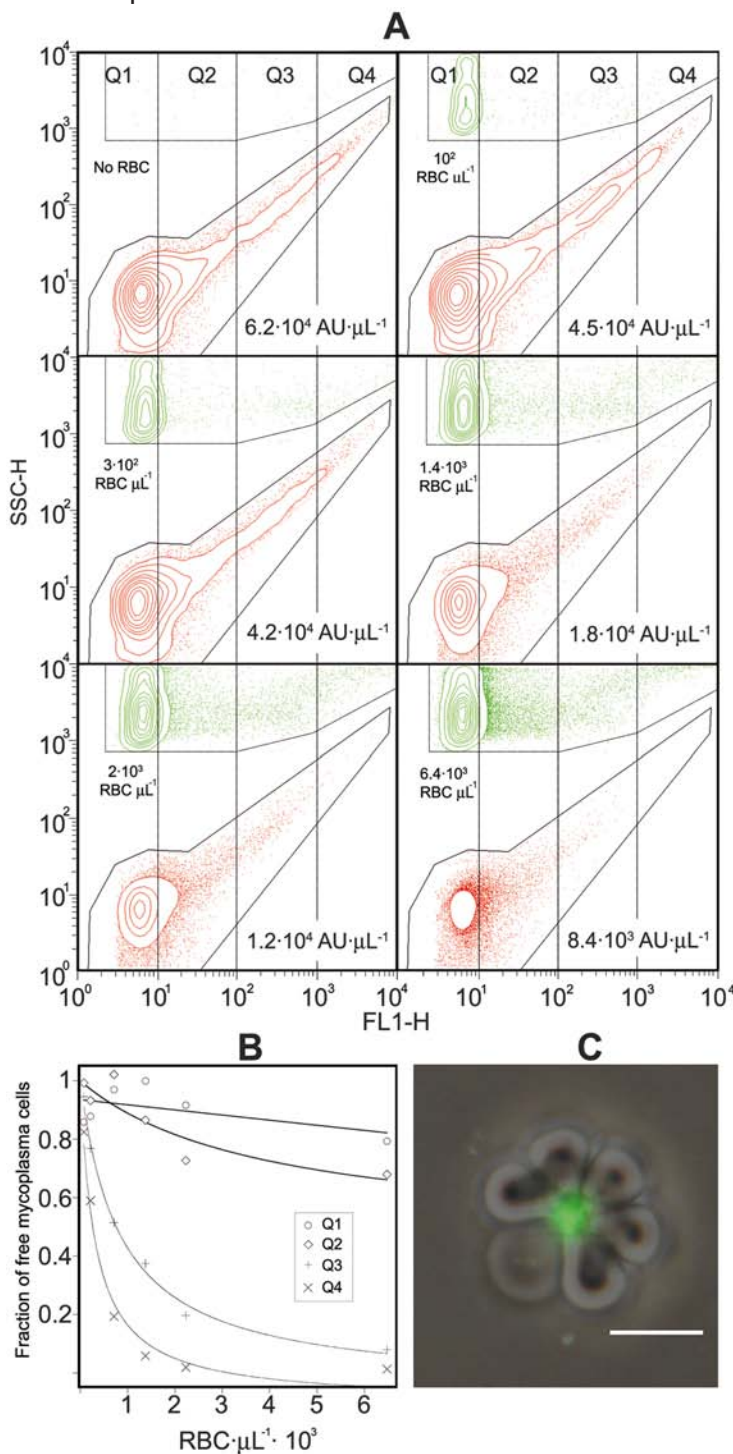


Fig. 3.9. Differential binding properties of mycoplasma cell aggregates and single mycoplasma cells. (A) Dual parameter dot plots of SSC-H vs. FL1-H fluorescence from several HA reactions showing the events in MR and R2 regions. MR region was defined as described in Fig. 3.4. R2 region contains the events from free RBCs and RBCs containing attached mycoplasmas. These plots contain a fixed amount of *M. genitalium* cells and increasing amounts of RBCs. Each dot plot was divided into four separate quartiles (Q1 to Q4) and the total fluorescence in MR region of each quartile was used to construct the respective inverse Langmuir plots in panel B. (C) Representative micrograph showing RBCs and mycoplasmas after the assay. The phase contrast picture is merged with the SYBR Green I epifluorescence picture, which is false colored to green. Bar is 10 μm . Note that most of SYBR green stained mycoplasmas are in big particles much larger than single cells, usually measuring 0.5–0.8 μm .

Discussion

Surface-attached mycoplasmas display unique polar structures of unprecedented complexity in the bacterial world that are involved in diverse aspects of the biology of these microorganisms and play a key role as virulence factors. In addition to diverse molecular methods, attachment of mycoplasma cells has been traditionally studied by determining their HA ability to RBCs and it is a distinctive trait widely investigated when characterizing the different mycoplasma species. Despite the fact that methods to qualitatively determine the HA or hemagglutination of mycoplasmas are straightforward and inexpensive, the same is not true when investigating HA at the quantitative level (Pich et al., 2008, Willby and Krause, 2002, Miyata et al., 2000, Burgos et al., 2007). Current methods to quantify mycoplasma HA rely on centrifuging RBCs after the incubation with bacterial cells. As mycoplasma cells have a very small size, only those attached to RBCs are expected to be found in the sediment (Pich et al., 2008, Willby and Krause, 2002). However, mycoplasma cells are very prone to form large cell aggregates and some of these aggregates may sediment even at very low g values, introducing a bias in the results. Therefore, we choose to explore FC to quantify the HA reaction, taking advantage that this technology could resolve RBCs and mycoplasma populations in a consistent way without the need of centrifugation. Since FC separates cell populations using their light dispersion properties and fluorescence, it provides a higher resolution than centrifugation. In addition, FC quantification of SYBR Green labeled mycoplasmas is a straightforward procedure and avoids the need of introducing a previous radioactive label or determining their ATP content by expensive enzymatic methods.

As showed before, FC data are easily modeled using a kinetic approach, which allows that the HA activity of a particular mycoplasma strain could be described by standard quantitative parameters like K_d and B_{max} . Each one of these parameters provide different information about the HA properties of tested cells. A high K_d value suggest that mycoplasma cells have a low affinity for RBCs but they are still able to adhere on their surface, especially at the highest concentrations of these cells. Likewise, a high K_d value could be expected when analyzing the HA properties of mycoplasma strains with a decreased amount of adhesins. This is in close agreement with previous reports showing that isogenic strains $mg218^-$ and $mg317^-$ have diminished amounts of the main adhesins P140 and P110 (Pich et al., 2008). Alternatively, mycoplasma strains either with an improper adhesin distribution on the cell surface or bearing adhesins not properly folded are also expected to exhibit higher K_d values. On the other hand, B_{max} values much smaller than one are suggesting that the cell population tested is heterogeneous and a significant amount of cells are non-adherent at all, even at the highest concentration of RBCs. This may be the case of the $mg317^-$ strain with a B_{max} value of 0.68, which indicates that 32% of cells are non-adherent and suggests that cells from this strain are heterogeneous regarding to the main adhesin content. Fortunately, this point is fully testable and work is currently in progress to assess it.

We have shown that mycoplasma aggregates bind preferentially to RBCs, suggesting a cooperative behavior when attaching to the surface of these cells. From this view, cell aggregation might be considered as a positive trait favoring the colonization of the target tissue/s. However, it is not clear whether cell aggregates are binding preferentially to the target tissues in the initial stages of an in vivo infection. It has been recently reported that mycoplasmas have a broad affinity for sialylated oligosaccharides (Roberts et al., 1989, Nagai and Miyata, 2006) but they show strong preferences for specific sialylated compounds, being this specificity a prominent factor to explain the marked tissue tropism that exhibit these microorganisms (Kasai et al., 2013). Bearing this in mind, the preferential attachment of cell aggregates may be simply an indication that RBC oligosaccharides promoting the binding of mycoplasmas are not as effective as those on the target tissue of a particular mycoplasma species. In this scenario, cell aggregation could be merely considered as a mechanism favoring attachment by maximizing the ratio and/or the density of adhesins on the surface of these aggregates. In addition, the preferences for particular sialylated compounds exhibited by different mycoplasma species, thus providing an explanation to the dissimilar K_d values obtained when testing the HA activity of several mycoplasma species (Fig. 3.8).

In conclusion, staining mycoplasma cells with the SYBR Green vital fluorochrome combined with the FC analysis after adsorption to RBCs is an inexpensive and reliable method to accurately quantify the HA activity of mycoplasmas. This method could be easily implemented in a standardized assay to test the growing number of clinical isolates and mutant strains of different mycoplasma species, providing valuable data about the virulence of these microorganisms.

A new model for *Mycoplasma genitalium* gliding motility

In this work we have provided solid evidence demonstrating that the rod element of the mycoplasma cytoskeleton is not essential for movement generation in motile mycoplasma cells. One of the consequences of these experimental findings is that the current inchworm model is no longer a proper model and/or mechanism to explain the motile properties of mycoplasma cells. Consequently, a new model integrating all the current knowledge about the molecular biology of mycoplasmas is needed to replace the current gliding paradigm and to provide new hypothesis for future research. This new model should integrate the following experimental data:

I. The rod component of the terminal organelle shows both bent and extended conformations when observed by ECT (Henderson and Jensen, 2006, Seybert et al., 2006, González-González, Unpublished).

II. The rod component is not involved in the generation of the gliding motility, but stabilizes the adhesins and prevents the formation of cell filaments (chapter 1).

III. P32 stabilizes the main adhesin complexes and improve the motility properties of the mutant strains deficient for the rod component (chapter 1). However, P32 protein itself is not essential for gliding motility in *M. genitalium* (González-González, unpublished).

IV. Proteins MG386, MG200, MG491 and MG219 located in the wheel-like component are essential for a proper cell motility (chapter 2) (Calisto et al., 2012, Pich et al., 2006a, González-González, Unpublished) and are found at almost WT levels in motile strains lacking of the rod component (chapters 1 and 2).

V. A new cytoskeletal structure was observed in mutant strains lacking the rod component of the terminal organelle. This new structure is able to cluster and localize the adhesins and also contains a minimized version of the motile machinery propelling *M. genitalium* cells (chapter 1).

VI. Terminal button proteins are implicated in the anchoring of the electron-dense core and in the curvature of the terminal organelle (Burgos et al., 2008, Pich et al., 2008).

We have provided evidence supporting that the gliding motility in *M. genitalium* is initiated at the terminal organelle by a rod-independent mechanism. The fact that P32 stabilizes P110 and P140 complexes and that the amount of these proteins is well-correlated with the motile

properties of rod-deficient strains. This suggests that these proteins are important elements of the molecular motor that propel cells. The thrust originated in the molecular motor pushes the terminal organelle forward and produces a change in the rod component, which adopts a straight conformation. The recovery of the bended conformation may promote the movement transmission to the main cell body. In this way, we propose that bending of the rod component is not in the origin of the cell movement but it is a consequence of such movement. In motile strains lacking the rod component, the movement is not properly transmitted to the cell body. Since the terminal organelle is still generating movement, the cells become elongated and, upon continuous extension, this process results in the formation of long filaments. Eventually, terminal organelle may detach from the cell body, thus generating the motile particles visualized in the rod-deficient mutants.

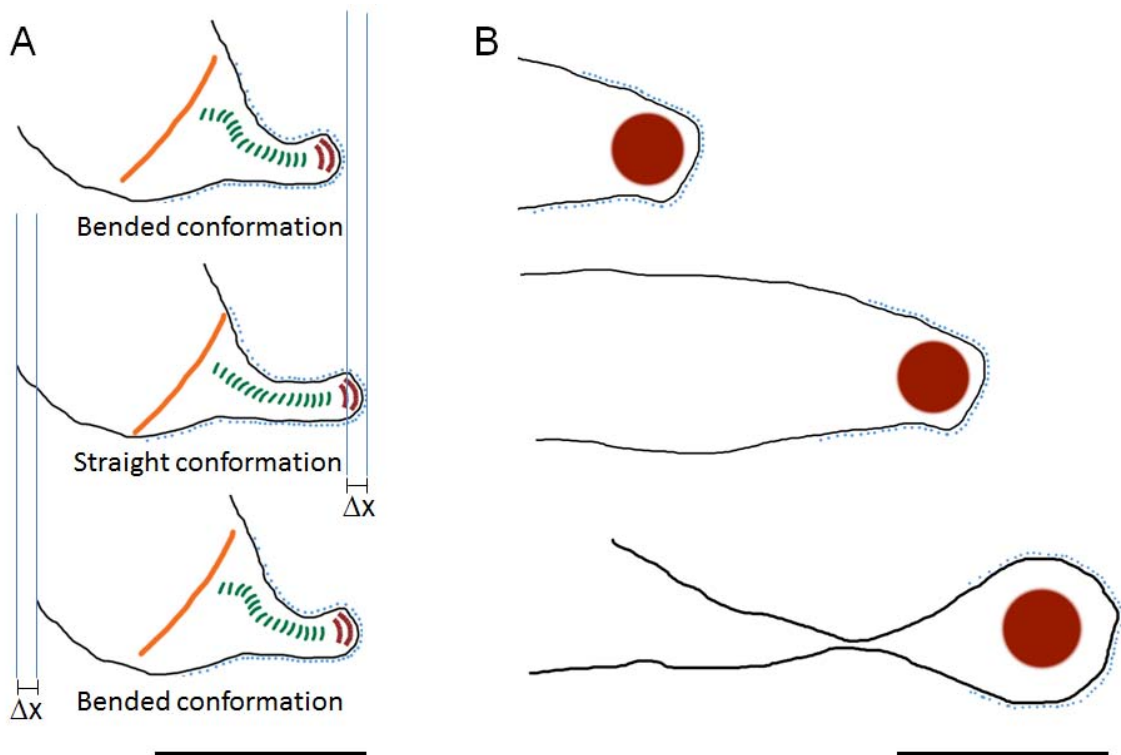


Fig. D.1. Schematic representation of a new model for *M. genitalium* gliding motility. (A) Motility of G37 WT cells. Adhesins clustered in the naps (blue dots) extend the terminal organelle and the rod (in green) adopts a straight conformation. Then the rod recovers the bended conformation and moves the cell body. (B) Motility of filamentous $\Delta mg218-P32Ch$ cells. The new cytoskeleton (in red) is able to cluster the nap structures (blue dots), which extend the filament because of the lack of a rod structure. Even, some motile parts may detach from the cell body. Bars are 0.3 μm .

The wheel-like complex has also an active role in gliding motility. Mutant strains lacking MG200, MG386 or MG219 show severe gliding deficiencies (González-González, unpublished, Pich et al., 2006a). MG200 protein, as well as its orthologue TopJ protein in *M. pneumoniae* (Cloward and Krause, 2011), has an important role in the clustering and trafficking of the adhesins (Broto, unpublished). Since the adhesins have a pivotal role in the generation of movement in our proposed model, the function of MG200 protein is essential for motility, and this explains the gliding deficiencies in the MG200 null mutant strain (Broto, unpublished, Calisto et al., 2012, Pich et al., 2006a). In this way, it is noteworthy that the

wheel-like complex proteins are at normal levels in the motile and rod-deficient mutant strains.

MG491 plays a complex role in gliding motility. This protein stabilizes MG218 and the rod component of the terminal organelle of *M. genitalium* cells, but we have shown that neither MG218 nor MG491 are essential for movement generation. However, MG491 is important for the assembly of the minimized cytoskeleton containing the motile machinery when the rod is missing. MG491 protein also forms quaternary complexes and mutations precluding the arrangement of these complexes are well-correlated with the presence of gliding deficiencies in *M. genitalium* cells. In addition, MG491 may be a phosphorylated protein similar to its *M. pneumoniae* ortholog P41 (Schmidl et al. 2010). The possibility that MG491 function might be regulated both by phosphorylation and by formation of intermolecular disulfide bonds suggests a role of MG491 in the regulation of cell motility.

Our results suggest that the nap structure plays a fundamental role in the motility of *M. genitalium* cells, either by initiating the movement, e.g. being the molecular motor, or by attaching the molecular motor to solid surfaces while cells are moving. The rod component of the terminal organelle is necessary for the transmission of the movement to the cell body and the wheel-like complex anchors the terminal organelle and regulates the movement. As previously described, the terminal button anchors the cytoskeleton at the cell membrane and directs the cells by modulating the curvature of the terminal organelle (Burgos et al., 2008). In contrast with the two previous models, we provide a specific role in gliding motility for each of the components of the terminal organelle.

Further investigation in *M. genitalium* gliding motility should be focused on the molecular motor, on the role of the adhesins in the movement generation and on the energy resources needed for this movement. But most importantly, this model also requires further research about the bending mechanism of the rod.

We can easily extend this new model to other motile mycoplasmas as *M. pneumoniae* and *M. mobile*. Proteins involved in gliding motility share a high homology in *M. genitalium* and *M. pneumoniae*. Also, the structure of the terminal organelle is nearly identical in both species. So, a common mechanism for gliding movement is suggested in these two species (Hatchel and Balish, 2008). No orthologs for terminal organelle proteins have been identified in *M. mobile*. However, it is reported that the adhesin/leg protein Gly349, is connected to a jellyfish-like internal cytoskeleton. It has been discussed that this cytoskeleton might have a role in the localization of the adhesins and/or be a scaffold to support the force generated by the gliding machinery (Nakane and Miyata, 2007). These functions are similar to that discussed below for *M. genitalium* wheel-like complex and rod, respectively. These surprising similarities between motility mechanisms of two phylogenetically distant mycoplasmas and the differences in the proteins involved in gliding motility might be a new case of convergent evolution.

Conclusions

Chapter 1: Gliding motility in electron-dense deficient mutants of *Mycoplasma genitalium*

1. A null mutant strain of *M. genitalium* deficient for MG_491 gene has very reduced levels of adhesins and adherence accessory proteins and shows filaments that extend from the cell bodies.
2. The phenotype of Δ mg491 cells was previously observed in MG_218 null mutant strain.
3. An extra copy of MG_318 gene partially restores the amount of adhesins and gliding properties in Δ mg491 and Δ mg218 strains.
4. The rod component of the terminal organelle is not essential for cell motility.
5. Cytoskeletal proteins MG200, MG219, MG386, P32, P110 and P140 are a minimized set of proteins needed for cell motility.
6. The nap structure of mycoplasmas is not only a passive element involved in cell adhesion but also plays an active role in gliding motility.
7. A new working model highlighting the role of the nap structure in motility has been proposed to explain the gliding mechanics of mycoplasmas.

Chapter 2: *Mycoplasma genitalium* strains with relevant mutations in the structure and function of MG491 protein

8. MG491 C-ter peptide_1 interacts with the EAGR box in MG200 and is required for the anchoring of the terminal organelle to the cell body.
9. Phe157 and Phe158 residues of MG491 protein, located at the loop L2, are also involved in the anchoring of the terminal organelles to the main cell body.
10. MG491 is involved in gliding motility in *M. genitalium*. The loop L2 and the Cys87 residue are required for this function.
11. The N-ter domain of MG491 is essential for the stability of the adhesins and adherence accessory proteins.

Chapter 3: Quantitative Hemadsorption Assay for Mycoplasma Species using Flow Cytometry

12. SYBR Green I stained mycoplasmas can be analyzed by flow cytometry to quantify their cell mass in a four log range.
13. Flow cytometry analysis of SYBR Green I stained mycoplasmas and red blood cells provide a simple and reproducible method to quantify the hemadsorption activity of mycoplasma cells.
14. Adhesion of mycoplasmas to red blood cells follows Langmuir isotherm curves, which allows the kinetic analysis of the hemadsorption activity of these microorganisms.
15. Kinetic parameters of the mycoplasma hemadsorption activity allow to characterize the adhesion deficiencies of mycoplasma strains.

Experimental Procedures

1. Biologic material

1.1. Bacterial strains

<i>Escherichia coli</i>	
XL1-Blue	<i>supE44 hsdR17 recA1 endA1 gyrA46 thi relA1 lac</i> F-[<i>proAB⁺ laqI^q</i> <i>lacZΔM15 Tn10(tet^r)</i>] Strain used for cloning manipulations.
<i>Mycoplasma genitalium</i>	
G37	WT Used as a WT strain in this study. Origin: ATCC 33530
mg218 ⁻	G37 MG_218::MT <i>tetM438</i> G37 with an insertion of a mini-transposon in MG_218 locus. Origin: Pich et al. 2008
mg317 ⁻	G37 MG_317::MT <i>tetM438</i> G37 with an insertion of a mini-transposon in MG_317 locus. Origin: Pich et al. 2008
mg191 ⁻	G37 ΔMG_191:: <i>tetM438</i> G37 with a deletion of MG_191 locus by gene replacement. Origin: Burgos et al. 2006
Δmg218	G37 ΔMG_218:: <i>tetM438</i> G37 with a deletion of MG_218 locus by gene replacement. Origin: Pich et al. 2008
Δmg491	G37 ΔMG_491:: <i>tetM438</i> G37 with a deletion of MG_491 locus by gene replacement. Origin: this study
Δmg491-mg491cat	ΔMG_491 MG_370::MT <i>ncatM438</i> MG_491 Δmg491 with a mini-transposon containing MG_491 wt allele. Origin: this study
Δmg218-P32Ch	ΔMG_218 MTn <i>Gm</i> MG_318:mCherry Δmg218 with a mini-transposon containing MG_438:mCherry fusion. Origin: this study

	Δ MG_491 MG_370::MTn <i>Gm</i> MG_318:mCherry
Δ mg491-P32Ch	Δ mg491 with a mini-transposon containing MG_438:mCherry fusion. Origin: this study
	G37 MG_491 Δ (T298-P322) Ω (266044pb:: <i>catM438</i>)
mg491- Δ p1	G37 with a deletion of MG_491 peptide_1 coding sequence by gene replacement. Origin: this study
	mg491- Δ p1 MTn <i>Gm</i> MG_491
mg491- Δ p1TC6	mg491- Δ p1 with a mini-transposon containing MG_491 wt allele. Origin: this study
	Δ MG_491 MG_414::MTn <i>catM438</i> MG_491C87S
mg491-C87S	Δ mg491 with a mini-transposon containing MG_491-C87S mutated allele. Origin: this study
	Δ MG_491 MG_032::MTn <i>catM438</i> MG_491-F157A-F158A
mg491-F157A-F158A	Δ mg491 with a mini-transposon containing MG_491-F157A-F158A mutated allele. Origin: this study
	Δ MG_491 MG_460::MTn <i>catM438</i> MG_491 Δ loopL2
mg491- Δ loopL2	Δ mg491 with a mini-transposon containing MG_491- Δ loopL2 mutated allele. Origin: this study
	Δ MG_491 MG_414::MTn <i>catM438</i> MG_491 Δ Nt
mg491- Δ Nt	Δ mg491 with a mini-transposon containing MG_491- Δ Nt mutated allele. Origin: this study
<i>Mycoplasma penetrans</i>	
	WT
GTU-54	Used as a WT strain in this study. Origin: ATCC 55252
<i>Mycoplasma hyopneumoniae</i>	
	WT
J	Used as a WT strain in this study. Origin: ATCC 25934

1.2. Vectors

pBluescript II SK ⁺	Phagemid used as a backbone for cloning. A DNA insertion in the MCS produces a disruption of the <i>lacZ'</i> gene. Also pBSK II ⁺ . Origin: Agilent
pMTnGm	pBSK II ⁺ containing the sequence coding for a mini-transposon modified from Tn4001. This transposon contains the sequence coding for gentamycin resistance <i>aac(6')-aph(2'')</i> gene. Origin: Pich et al. 2006
pMTnTetM438	pMTnGm with a substitution of the gentamycin resistance gene for a tetracycline resistance gene under the control of MG_438 promoter (<i>tetM438</i>). Origin: Pich et al. 2006
pMTnCat	pMTnGm with a substitution of the gentamycin resistance gene for a chloramphenicol resistance gene under the control of MG_438 promoter (<i>catM438</i>). Origin: Calisto et al. 2012
pΔmg491	pBSK II ⁺ derived plasmid used to produce a deletion of MG_491 gene in <i>M. genitalium</i> . Contains the <i>tetM438</i> tetracycline resistance gene. Origin: this study
pMTnCatmg491	pMTn <i>cat</i> derived plasmid containing the MG_491 locus under the control of MG_438 promoter into the mini-transposon sequence. Origin: this study
pMTnGmmg491	pMTnGm derived plasmid containing the MG_491 locus under the control of MG_438 promoter into the mini-transposon sequence. Origin: this study
Cherry-LacRep	Plasmid used to amplify the mCherry coding sequence. Origin: Dundr et al, 2007
pMTnGmmg318:mcherry	pMTnGm derived plasmid containing a fusion between MG_318 locus and mCherry under the control of MG_318 own promoter into the mini-transposon sequence. Origin: this study
pΔp1 <i>cat</i>	pBSK II ⁺ derived plasmid used to produce a deletion of MG_491 Ct peptide_1 in <i>M. genitalium</i> . Contains the <i>catM438</i> tetracycline resistance gene. Origin: this study
pMTn <i>cat</i> C87S	pMTn <i>Catmg491</i> derived plasmid with a point mutation that produces a substitution of MG491 Cys87 for Serine. Origin: this study
pMTn <i>cat</i> F157A-F158A	pMTn <i>Catmg491</i> derived plasmid with point mutations that produce the substitution of MG491 Phe157 and Phe158 for Alanine. Origin: this study
pMTn <i>cat</i> ΔloopL2	pMTn <i>Catmg491</i> derived plasmid with a deletion of MG491 residues Asn155-Lys160. Origin: this study
pMTn <i>cat</i> ΔNt	pMTn <i>Catmg491</i> derived plasmid with a deletion of MG491 residues Met1-Gln61. Origin: this study

1.3. List of oligonucleotides used in this work

Used for sequencing DNA insertions in plasmids	
Fup-17	5'-GTAAAACGACGGCCAGT
Rup-17	5'-GGAAACAGCTATGACCATG
To determine transposon insertion points	
CmDown	5'- ATGAATTACAACAGTACTG
GmDown	5'-AAAAATGAAAAATAATAAAGGAAG
To find recombination events inactivating MgPa operon by PCR	
R1	5'- GGTAAGTTCCAGTAGAAGTAG
R4	5'- AATACTAGTTTCTTCTTTTAGACC
R5	5'-AGTAAGAATGTTACTGCTTACA
R6	5'-AGTTATAGTTTAAACCTAACGCAT
Used in cloning	
LHmg491/5	5'-ACTGA <u>AAGCTT</u> TATGAATACTTTAGAAAGATGCGTG
LHmg491/3	5'-TATCGA <u>ATTCTT</u> TATTTACTTGCTGCTTTTTGG
RHmg491/5	5'-TACT <u>GGATCC</u> GTTAGTCAACCTGAAGTTGAAG
RHmg491/3	5'-TATC <u>ICTAGATT</u> GAGCTATGATGACAGTTGATC
5P32	5'-TAAGGTTA <u>GTCGACT</u> GGGGCTTGATTAATTAGCAGC
3P32	5'-GGGTTTTAAACCGCCTTTTGG
5Cherry	5'-AGCTATA <u>ACGTAAGCAAGG</u> GCGAGGAGG
3Cherry	5'-TATGGA <u>ATTCTT</u> ACTTGTACAGCTCGTCCATGC
MG491pr438/5	5'-GGGG <u>TGAC</u> TAGTATTTAGAATTAATAAAGTATGGTTAATAATGAATATCAA- CAAC
MG491/3	5'-ATTG <u>GCTCGAGT</u> TATTCATTATGGGTATTTTTTTCAAG
mg491/5	5'-GAAGAT <u>CTAGAAT</u> GGTTAATAATGAATATCAACAAC

mg491Δp1N	5'-CTATGTCATCCTTACTTAGTTTCGGAGGTTTGAGATCAACTTGGGGTTGGA
mg491Δp1C	5'-TCCAACCCCAAGTTGATCTCAAACCTCCGAAACTAAGTAAGGATGACATAG
mg219/3	5'-GAAGACTCGAGTTAAGATCTGGTTTTTTTATTGC
cat/5	5'-GAACTCTCGAGCAATTGTAGTATTTAGAATTAATAAAGTATG
cat/3	5'-GAAGACTCGAGTTACGCCCGCCCTGCCACTC
HRC/5	5'-AATATCTCGAGTCTGGTTTTTTTAGTGTTAACAAC
HRC/3	5'-AATATGGGCCCACTAGCTAGATATTGTTTCATATTG
P-C87SMG491/5	5'-P-ACTGGAACGCAGTTCGTTGGTTG
C87SMG491/3	5'-AAAAGAAAACCACGTTTTTGCTTG
FFAAMG491/5	5'-AACTCGGCTGCTAACAAGCTTTTAAGTGATC
P-loop/3	5'-P-TAAGACAGGGGTATATTCACTAC
loop/5	5'-CTTTTAAGTGATCCTGATCCAATC
MG491pr438ct/5	5'-TTTGGGCCCTAGTATTTAGAATTAATAAAGTATGCAATCCAGTTTCCATAAC

Restriction sites are underlined.
MG_438 promoter is in italics.
P- indicates 5' phosphorylation

1.4. Culture conditions

1.4.1. Culture of *E. coli* strains

Liquid LB medium was used for growing *E. coli* strains: bactotryptone 1% (Sharlab), yeast extract 0.5% (Sharlab) and NaCl 1%. This media is autoclaved 15 min at 120°C. *E. coli* strains were cultured in 3-15 mL of LB medium overnight (O/N) at 37°C and 250 rpm and recovered by centrifugation.

Solid LB medium was prepared by adding Bacteriological agar 1.5% (Sharlab) to liquid LB before autoclaving. Before cooling, this mixture was dispensed on 90 mm petri dishes and stored at 4°C. Colonies of *E. coli* were isolated by seeding on solid LB medium dishes and growing O/N at 37°C.

Liquid and solid LB medium was supplemented with ampicillin (Roche) 100 µg mL⁻¹ for the selection and maintenance of transformant clones with plasmids containing the *bla* gene, conferring resistance to this antibiotic.

Solid LB medium was supplemented with X-Gal (Sigma-Aldrich) $50 \mu\text{g mL}^{-1}$ for the selection of transformants with pBluescript plasmids containing a DNA insertion in the multiple cloning site. *E. coli* strains were stored at -80°C in LB supplemented with 10% of sterile glycerol.

1.4.2. Culture of *M. genitalium* strains

Liquid SP-4 medium was used for growing *M. genitalium* strains. The base for 0.5 L of this medium is prepared by mixing 1.75 g of PPLO (Becton-Dickinson), 5 g of tryptone (Becton-Dickinson), 2.65 g of bactopectone (Becton-Dickinson) and 2.5 g of glucose (Sigma-Aldrich) in 312 mL of MilliQ water (distilled water filtered through a $0.22 \mu\text{m}$ Millipore filter). This base is adjusted to pH 7.8 and autoclaved 15 min at 120°C .

After cooling the base, the following supplements were added: 50 mL of autoclaved 2% yeastolate (Becton-Dickinson), 7 mL of autoclaved phenol red 0.1% pH 7 (Sigma-Aldrich), 17.5 mL of fresh yeast extract 25%, 25 mL of CMRL 10x (Life technologies), 85 mL of Foetal Bovine Serum (FBS, Life technologies), 1.71 mL of glutamine 29.2 mg mL^{-1} (Sigma-Aldrich), 0.25 mL of ampicillin 100 mg mL^{-1} (Roche) and NaOH until reach pH 7.8.

To prepare the yeast extract for SP-4 medium, 250 g of fresh yeast were diluted in 1L of MilliQ water and autoclaved 10 min at 115°C . After cooling, the yeast is centrifuged 10 min at 400 g and the supernatant is autoclaved again. This yeast extract is aliquoted and stored at -20°C . To inactivate the complement system in the FBS, it should be heated 30 min at 56°C .

M. genitalium strains were grown in 5, 15 or 30 mL of SP-4 medium at 37°C and 5% CO_2 for 3-7 days until reaching the mid-log phase of growth in tissue culture flasks of 25 cm^2 , 75 cm^2 or 150 cm^2 , respectively (TPP). Cells were then scrapped off the flask and recovered by centrifugation 20 min at 20 000 g.

Solid SP-4 medium was used to isolated transformant colonies of *M. genitalium*. Solid SP-4 medium was prepared by adding agar 0.8% (Becton-Dickinson) to liquid SP-4 before autoclaving. Before cooling, this mixture was dispensed on 50 mm petri dishes and stored at 4°C . Colonies of *M. genitalium* were isolated by seeding on solid SP-4 medium dishes and growing 2 weeks at 37°C and 5% CO_2 .

Liquid and solid SP-4 medium was supplemented with tetracycline (Roche) $2 \mu\text{g mL}^{-1}$, gentamycin (Sigma-Aldrich) $100 \mu\text{g mL}^{-1}$ or chloramphenicol (Roche) $34 \mu\text{g mL}^{-1}$ for the selection and maintenance of transformant clones containing the *tetM438*, *aac(6')-aph(2'')* or *catM438* genes, respectively, conferring resistance to these antibiotics. *M. genitalium* strains were stored at -80°C in fresh SP-4 medium.

1.4.3. Culture of *M. penetrans* strains

M. penetrans was grown in 15 mL of liquid SP-4 medium for three days as described for *M. genitalium* strains.

1.4.4. Culture of *M. hyopneumoniae* strains

M. hyopneumoniae was grown in 15 mL of liquid Friis medium in 50 mL centrifuge tubes (TPP) at 37°C for three days. The composition of Friis medium is: irradiated horse serum 20%, yeast extract 2.4%, phenol red 0.1%, Hanks' Balanced Salt Solution 0.4% (Life technologies), Heart Infusion Broth 0.058% (Becton-Dickinson), 0.054% PPLO (Becton-Dickinson) and ampicillin 100 µg ml⁻¹, and was prepared according to the instructions in (Kobisch and Friis, 1996).

2. DNA manipulations

2.1. Genomic DNA extraction from *M. genitalium* strains

1. 15 mL culture of *M. genitalium* strains were grown in a 75 cm² culture flask until mid-late exponential phase.

2. Cells were cleaned twice in PBS (Sigma-Aldrich) and recovered in 0.5 mL of Solution I (Tris-HCl 0.1 M pH 8, NaCl 0.5 M, EDTA 10 mM). Cells from adherent strains were cleaned in the same flask and recovered by scrapping off. Cells from non-adherent strains were cleaned and recovered by centrifugate 20 min 20 000 g.

3. 20 µL of SDS 20% was added and mixed gently to promote cell lysis.

4. 1 volume of phenol-chloroform-isoamyl alcohol mix (25:24:1) was added and mixed thoroughly. Phases were separated by centrifuging 5 min at 16 000 g and the aqueous phase was recovered in a new 1.5 mL tube. This step was repeated twice.

5. 2 volumes of absolute ethanol were added and mixed carefully. Precipitated DNA was pelleted by centrifuging 5 min at 16 000 g. The supernatant was removed and the pellet cleaned twice with 1 mL of ethanol 70%.

6. The DNA pellet was dried in a vacuum desiccator for 10 min and resuspended in 100 µL of TE (Tris-HCl 10 mM pH 8, EDTA 1 mM) supplemented with 15 µg mL⁻¹ of RNase at 4°C O/N. Genomic DNA was then stored at -20 °C. For the preparation of genomic DNA for sequencing, TE buffer was diluted five times.

2.2. DNA quantification

Concentration of DNA in solution was determined using a *NanoDrop 1000 Spectrophotometer* (Thermo Scientific) and following the instructions from the manufacturer.

2.3. Agarose gel electrophoresis

Agarose gels were used to separate DNA fragments of different sizes and were carried out following standard procedures (Sambrook and Russell, 2001). Agarose (SeaKem® LE Agarose) was prepared to the desired concentration (0.8-1.2%) depending on the predicted sizes of the DNA fragments in TAE (Tris-acetate 40 mM pH 8, EDTA 1 mM). DNA samples were diluted in DNA loading buffer (Tris-acetate 40 mM pH 8, EDTA 1 mM Bromophenol blue 0.25 mg mL⁻¹, xylene cyanol 0.25 mg mL⁻¹, glycerol 30%) and introduced into gel wells. Electrophoresis were run at 70V for approximately 90 min. Finally, gels were soaked into an ethidium bromide 0.5 µg mL⁻¹ solution in TAE for 20 min and visualized using UV light in a *Gel doc™ XR* (BioRad) transilluminator. To estimate fragment sizes, a *1kb plus DNA ladder* (LifeTechnologies) was used. For band recovery, bands were excised from the agarose gel and purified using the *EZNA® gel extraction kit* (Omega Bio-tek).

2.4. DNA amplification

DNA fragments were amplified from genomic and plasmidic DNA preparations by PCR using *Phusion® DNA Polymerase* (FINNZYMES) in an *MJ Mini™ thermocycler* (BioRad). The general setup used for PCRs was:

- 3 ng of DNA template
- 1 µM of each primer
- 0.6 Units of *Phusion® DNA polymerase*
- 200 µM dNTPs
- 10 µL HF buffer 5x
- Sterile MQ water to 50 µL

Before the PCR cycle, the DNA was heated 2 min at 95°C. The PCR cycles were:

1. Denaturalization: 20 sec at 95°C
2. Annealing: 30 sec at (T_m+3)°C. T_m is the melting temperature of the primers used.
3. Extension: 30 sec/kb at 72°C

The PCR cycle was repeated 35 times. A final extension of the PCR products was performed by keeping the samples at 72 °C 5 min.

2.5. Two-step recombinant PCR or overlap extension

Recombinant PCR is a technique used to fusion DNA sequences. Briefly, two sequences are amplified separately. The 3' primer used to amplify the upstream DNA segment and the 5' primer used to amplify the downstream DNA segment are reverse and complementary, and contain at their 5' tails the complementary sequence corresponding to the other segment. The PCR products are then mixed together and are employed as primers in a second PCR. The primers 5' of the upstream segment and 3' of the downstream segment are also added to the second PCR in order to amplify the final fused product.

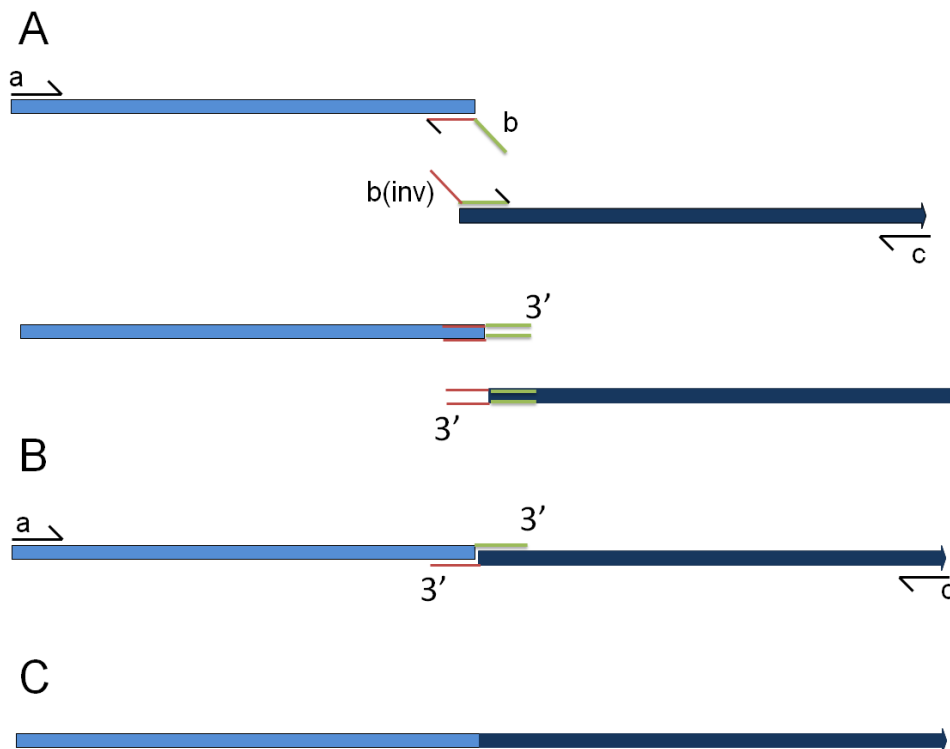


Fig. M.1. Schematic of the overlap extension strategy. (A) Two independent PCRs amplify the two sequences to be fused. Primers b and b(inv) are reverse and complementary. Green fragment correspond to the 5' end of the downstream fragment incorporated in the upstream amplicon as a tail in primer b. Red fragment correspond to the sequence of the upstream fragment that is incorporated in the downstream fragment as a tail in b(inv). (B) The second round of PCR uses the 3' end of both red and green fragments as a primer to extend the upstream and downstream segments. (C) Primers a and c amplifies the resulting fusion of the fragments.

2.6. Exsite mutagenesis

This PCR-based technique allows the mutagenesis in fragments of DNA cloned in a small plasmid. The whole plasmid is amplified with two primers oriented in opposite directions. One of the two primers contains the mutation and it is required that one of the two primers has its 5' end phosphorylated. After the mutagenic PCR, the amplicon can be circularized by ligation of its ends thanks to this phosphorylation, recovering the initial plasmid but with

the intended mutation. The use of a polymerase that does not include additional adenines at the 3', as *Phusion® DNA polymerase*, is essential. To generate deletions, the opposite primers have to be separated by the sequence corresponding to the desired deletion.

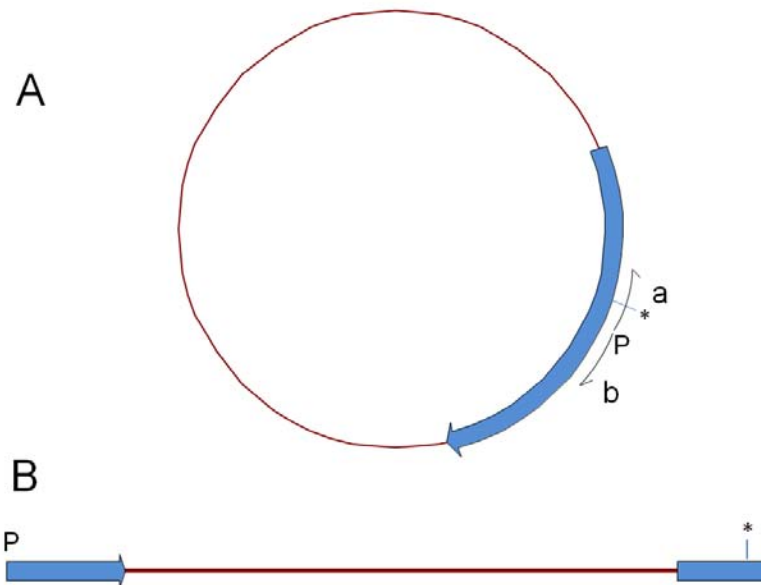


Fig. M.2. Schematic of the Exsite strategy. (A) Two primers are used to amplify by PCR the whole plasmid. Primer “a” include the mutation (*) and primer “b” is phosphorylated at its 5' end. (B) The lineal amplicon containing the mutation can be circularized with T4 DNA ligase.

2.7. Restriction of DNA

Restriction enzymes (Roche or Fermentas) were used to cleave DNA fragments at specific restriction sites following the manufacturers' instructions. DNA fragments were analysed and/or purified by agarose gel electrophoresis.

2.8. Dephosphorylation of plasmidic DNA

Before ligation, cleaved plasmids showing blunt ends were treated with alkaline phosphatase (Roche) according to the instructions of the manufacturer to reduce the recircularization of the vector during the ligation.

2.9. Ligation of DNA fragments

The ligation of DNA fragments into plasmids was performed using T4 DNA ligase (Roche) enzyme, following the guidelines of the manufacturer.

2.10. DNA transformation in *E.coli* XL1-Blue strain

Competence of cells from *E. coli* XL1-Blue strain was achieved using the standard Inoue method (Sambrook and Russell, 2001). Aliquots of 0.1 mL of competent cells were cooled in liquid nitrogen and stored at -80°C. Plasmids were transformed into XL1-Blue competent cells by using an standard heat shock protocol (Sambrook and Russell, 2001).

2.11. Plasmidic DNA extraction

2.11.1. Minipreparations

Minipreparations of plasmidic DNA were performed from 2 mL of *E. coli* XL1-Blue O/N cultures using the commercial kit *FastPlasmid™ Miniprep* (5prime) following the supplied guidelines. This DNA was stored at -20°C and used for screening purposes.

2.11.2. Midipreparations

Midipreparations of plasmidic DNA were carried out from 15 mL of *E. coli* O/N cultures using a standard alkalyne lysis protocol (Sambrook and Russell, 2001) with some modifications. Briefly, cells were harvested and cleaned with 1 mL Solution I (Tris-HCl 0.25 mM pH 8, EDTA 10 mM, Glucose 50 mM). After pelleting the cells by centrifuging 1 min at 16 000 g, cell were resuspended in 200 µL of Solution I supplemented with RNase (0.3 mg mL⁻¹) and were lysed with 400 µL of Solution II (NaOH 0.2M, SDS 1%). Cell debris was precipitated by addition of 300 µL of Solution III (Potassium acetate 3M, Acetic acid 11.5%) and separated by centrifuging 5 min at 16 000 g. The supernatant was then cleaned in a column of the *EZNA® gel extraction kit* (Omega Bio-tek) following the supplied instructions. For cloning applications, the DNA was eluted in 40 µL of elution buffer (supplied in the kit) and stored at -20°C. To electroporate *M. genitalium* cells with this plasmidic preparation, DNA was eluted in 40 µL of electroporation buffer and stored at -20°C.

2.12. Transformation of *M. genitalium* strains

The current protocol for *M. genitalium* transformation of suicide plasmids is adapted from (Reddy et al., 1996). Briefly:

1. A 15 mL culture of the *M. genitalium* strain is grown in SP-4 until mid-log phase.
2. 10 mL of SP-4 were removed and the cells were scrapped off the flask in the other 5 mL of SP-4. These 5 mL were passed through a 0.45 µm low protein binding filter (Millipore) and were used to seed 30 mL of fresh SP-4 medium, and grown O/N. This step was not

done when transforming non-adherent strains.

3. SP-4 medium was removed and cells were washed three times with electroporation buffer (HEPES 8 mM pH 7.4, sucrose 272 mM). Then, cells were recovered in 1 mL of electroporation buffer by scrapping off. Non-adherent strains are recovered and washed by centrifugation 20 min 20 000xg. Then, they were passed 10 times through a 25 gauge syringe to break the aggregates.

4. 0.1 mL of cells were mixed with 10 µg of plasmidic DNA (for transposon mutagenesis) or 30 µg of plasmidic DNA (for gene replacement mutagenesis) in an electroporation cuvette with 2 mm of separation between electrodes.

5. The mixture was cooled in ice for 15 min and then introduced into the electroporator (ECM 630 BTX). The electric shock was programmed to 2.5 kV, 250 Ω and 25 mF.

6. Cells were kept in ice 15 min and then 0.9 mL of SP-4 was added to the mixture and incubated 2h at 37°C.

7. The cells were dispensed in SP-4 agar plates supplemented with the appropriate antibiotic. Non-electroporated cells were also seeded on SP-4 supplemented with antibiotic agar plates as negative control. Electroporated cells were seeded on SP-4 agar plates to assess viability after electroporation.

8. Plates were incubated two weeks as previously described and the colonies were recovered in 5 mL of liquid SP-4. After two weeks, approximately, SP-4 medium was removed and the cells were recovered in 0.5 mL of fresh SP-4 and stored at -80°C.

Cell stocks recovered from this protocol were designated as master or passage 1 (P1) and were grown in 15 mL (P2) as previously described. These P2 cells were used for the further analyses.

2.13. Southern blot

Southern blot analysis is a technique that allows the detection of a DNA fragment within a genome using a labelled probe. In this work, a Southern blot was performed to detect the presence of double recombinants when isolating *M. genitalium* Δmg491 clones. For this purpose, genomic DNA from G37 WT strain and transformants were cleaved with *Bgl*III restriction enzyme (Roche) and the mutation was detected using a probe corresponding in sequence to the LHR DNA fragment. The Southern blot was performed using the following guidelines:

2.13.1. Non-radioactive probe labelling

DNA fragments used as a probe for Southern blotting were labelled with digoxigenin-11-dUTP (Roche). The labelling was performed using the *DIG DNA Labelling & Detection Nonradioactive Kit* (Roche) and following the guidelines from the manufacturer. The ratio between digoxigenin-11-dUTP and dTTP was set at 1:2.

2.13.2. Alkaline transference

Alkaline transference was performed using standard procedures (Sambrook and Russell, 2001). 1 µg of genomic DNA from *M. genitalium* G37 WT and mutant strains were cleaved with restriction enzymes not presenting star activity. The digestion samples were separated in a 0.8% agarose gel electrophoresis run at 30V with a molecular weight marker and stained with ethidium bromide as previously described. This electrophoresis was visualized and the image was used to estimate the length of the bands detected in the Southern Blot. Ethidium bromide was removed and the DNA denatured by soaking the gel in TTA buffer (NaOH 0.4M, NaCl 1M). The DNA was then transferred by capilarity 1h to a nylon membrane in TTA buffer. After this step, the membrane was soaked in neutralization buffer (Tris-HCl 0.5M pH 7.2, NaCl 1M).

2.13.3. Hybridization with the probe

The membrane with the transferred genomic DNA was treated with hybridization buffer (SSC 5x (Roche), formamide 50%, N-laurylsarcosine 0.1%, SDS 0.02%, blocking reagent 5% (Roche)) during 1h at 42°C and mild agitation in an hybridization oven (Amersham Pharmacia Biotech). The labelled probe was then denatured by heating at 98°C 10 min. 15 µL of this probe were diluted in 8 mL of hybridization buffer, added to the membrane and incubated O/N at 42°C.

2.13.4. Detection of the probe

The membrane was then washed with low restrictivity (SSC 2x, SDS 0.1%), high restrictivity (SSC 0.1x, SDS 0.1%) and washing (maleic acid 0.1M pH7.5, NaCl 0.15M, Tween 20 0.3%) buffers and incubated 30 min with blocking solution (maleic acid 0.1M pH7.5, NaCl 0.15M, blocking reagent 1%). Then, the membrane was incubated 20 min with anti-Dig conjugated with alkaline phosphatase diluted 1:10 000 in blocking reagent. Finally, the membrane was washed with washing buffer, equilibrated with detection buffer (Tris-HCl 0.1M pH 9.5, NaCl 0.1M, MgCl₂ 0.05M) and revealed in this buffer containing the NBT/BCIP mix (Roche) until apparition of the bands.

2.14. DNA sequencing

DNA fragments cloned in pBluescript SK II vectors were sequenced with Fup-17 and Rup-17 primers. The determination of the insertion point of the transposons in the transformant strains analyzed in this work was assessed by sequencing the genomic DNA of these strains with CmDown and GmDown primers. Sequencing reactions were performed with *Big Dye™ 3.0 Terminator Kit* (Applied Biosystems) and analyzed in a *ABI 3100 Genetic Analyzer* (Applied Biosystems) at the Servei de Genòmica i Bioinformàtica from UAB.

2.15. Construction of plasmids

2.15.1. pΔmg491

When designing the intended deletion in MG_491 locus, a 220 bp region from 3' end of the MG_491 gene was preserved to avoid undesired effects in the transcriptional and translational status of the downstream flanking genes (Fig. 1.1A). A 1 kb fragment encompassing the upstream region of MG_491 gene (LHR) was amplified by PCR using the primers LHmg491/5 and LHmg491/3 containing respectively *Hind*III and *Eco*RI restriction sites at their 5' ends. Another 1 kb fragment corresponding to the downstream region of MG_491 gene (RHR) was amplified with the primers RHmg491/5 and RHmg491/3, containing respectively the *Bam*HI and *Xba*I restriction sites at their 5' ends. Both homology regions were cleaved to generate cohesive ends and mixed with the *tet*M438 gene marker which was previously excised from pMTn*Tet*M438 plasmid by digestion with *Eco*RI and *Bam*HI. Finally, these fragments were ligated to a *Hind*III and *Xba*I digested pBSK II and transformed into *E. coli* XL1-Blue cells.

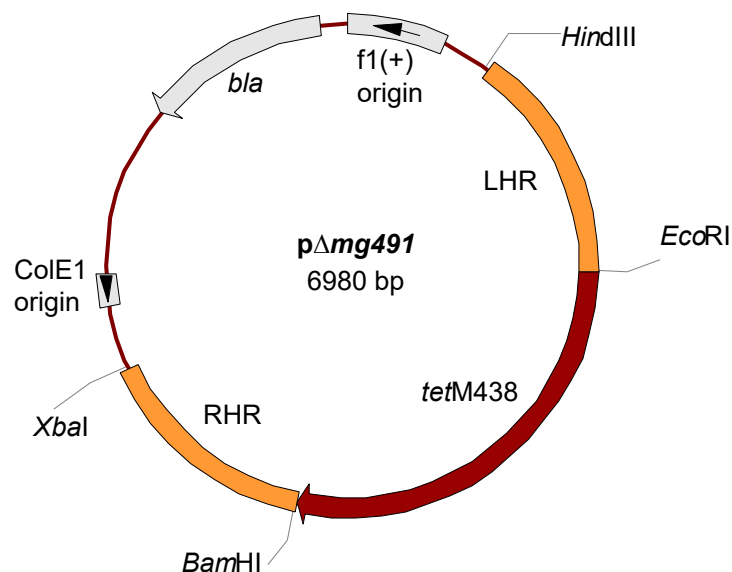


Fig. M.3. pΔmg491 suicide plasmid used to delete the MG_491 gene from *M. genitalium* genome. Restriction sites used for its construction are marked. LHR and RHR are homologous regions to *M. genitalium* genome. *tet*M438 confers resistance to tetracycline. *bla* confers resistance to ampicillin. ColE1 and f1(+) are origins for replication in *E. coli*.

2.15.2. pMTnGmmg318:mcherry

A 1584 bp DNA fragment encompassing the MG_318 gene coding for P32 protein and 744 bp of the upstream region containing regulatory sequences (Waldo et al., 1999) was amplified from G37 genomic DNA using primers 5P32 (containing a *Sal*I site at its 5' end) and 3P32. Another 840 bp DNA fragment containing the coding sequence for mCherry protein was amplified from Cherry-LacRep plasmid (Dundr et al., 2007) using primers 5Cherry and 3Cherry, containing respectively the *Sna*BI and *Eco*RI restriction sites at their 5' ends. Then, the pMTnGm plasmid was linearized with *Sal*I and *Eco*RI, ligated with the PCR fragments cleaved with the corresponding restriction enzymes and transformed into *E. coli* XL1-Blue cells.

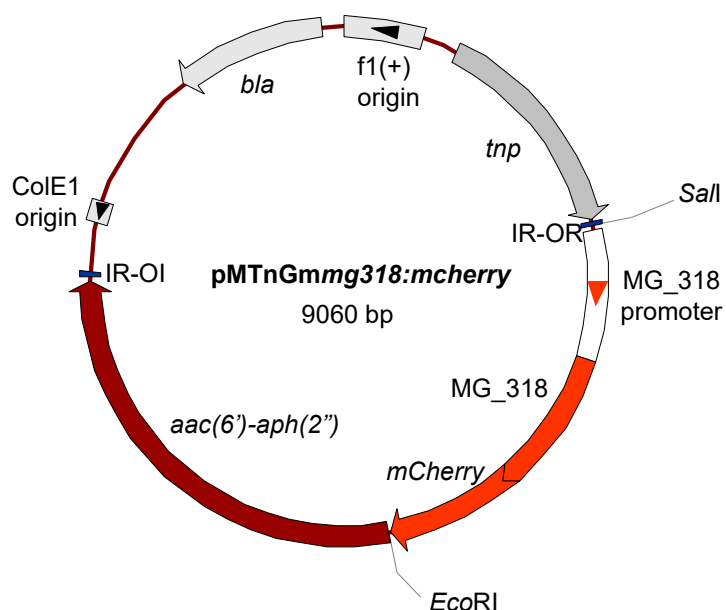


Fig. M.4. pMTnGmmg318:mcherry suicide plasmid containing a mini-transposon used to insert a copy of MG_438 gene fused with mCherry gene into the genome of *M. genitalium* and under the control of its own promoter. Restriction sites used for its construction are marked. *tnp* encodes for the transposase that inserts the sequence between IR-OI and IR-OR. *aac(6')-aph(2'')* is a resistance gene to gentamycin.

2.15.3. pMTncatmg491 and pMTnGmmg491

The coding sequence of MG_491 gene was amplified from *M. genitalium* genome using the primers MG491pr438/5 and MG491/3, containing respectively the *Sal*I and *Xho*I sites at their 5' ends. Primer MG491pr438/5 included also the promoter region of MG_438 gene. The excised PCR fragment was ligated into a pMTncat and into a pMTnGm excised with *Xho*I and dephosphorylated as previously described, and finally transformed into *E. coli* XL1-Blue cells.

2.15.4. p Δ p1*cat*

A two-step recombinant PCR was used to construct a fragment of DNA encompassing MG_491 and MG_219 and excluding the sequence from nucleotides 895 to 969 of MG_491, encoding for the MG491 Ct_peptide 1. Firstly, 5' MG_491 was amplified using primers mg491/5 and mg491 Δ p1N, while a fragment including MG_219 and the 3' end of MG_491 was amplified using primers mg491 Δ p1C and mg219/3. Secondly, the two previously obtained fragments were fused using the complementary ends included in primers mg491 Δ p1N and mg491 Δ p1C and the fusion product was amplified using primers mg491/5 and mg219/3, which include respectively *Xba*I and *Xho*I restriction sites. Finally, a second PCR fragment encompassing a 1 kb region downstream to MG_219 was amplified using primers HRC/5 and HRC/3 which include respectively *Xho*I and *Apa*I restriction sites. Both PCR products were cleaved to generate cohesive ends, ligated to a pBSK II plasmid digested with *Xba*I and *Apa*I and transformed in *E. coli* XL1-Blue cells. The resulting p Δ p1 plasmid was then cleaved with *Xho*I and ligated to a PCR fragment containing the *cat* gene under the control of the MG_438 promoter. This PCR fragment was amplified from the pMT*ncat* plasmid using primers cat/5 and cat/3, both including a *Xho*I restriction site. p Δ p1*cat* plasmid was transformed into *E. coli* XL1-Blue cells.

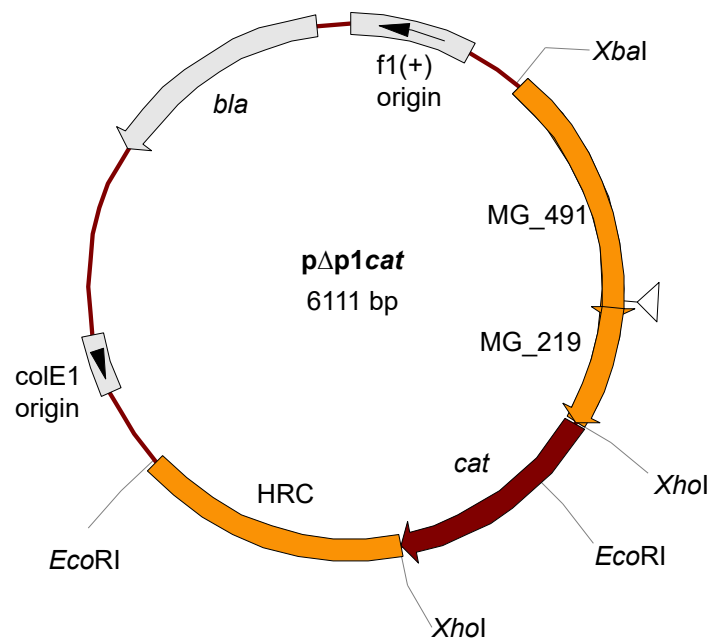
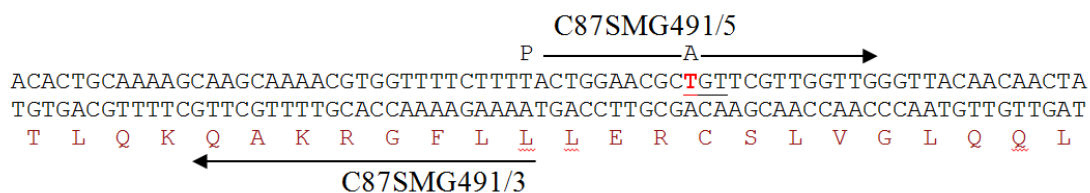


Fig. M.5. p Δ p1*cat* suicide plasmid used to delete 75 pb (marked with an empty triangle) from the Ct region of MG_491 gene from the *M. genitalium* genome. Restriction sites used for its construction are marked. *cat* gene confers resistance to chloramphenicol.

2.15.5. pMT*ncat*C87S

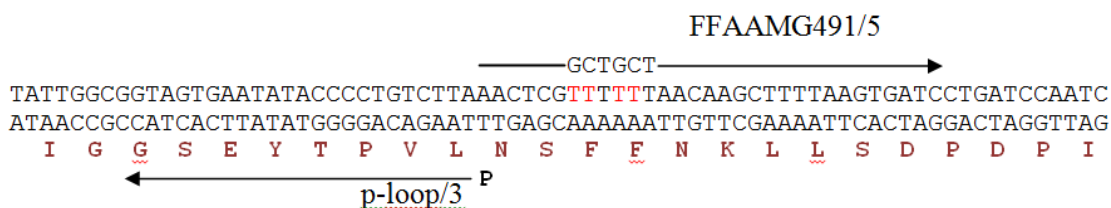
An *exsite* strategy was used to substitute the TGT codon coding for Cys87 to an AGT codon coding for Serine. The whole pMT*ncat*mg491 plasmid was amplified using the phosphorylated oligonucleotide P-C87SMG491/5, which incorporates the substitution, and

the primer C87SMG491/3. The resulting lineal fragment was religated and transformed in *E. coli* XL1-Blue.



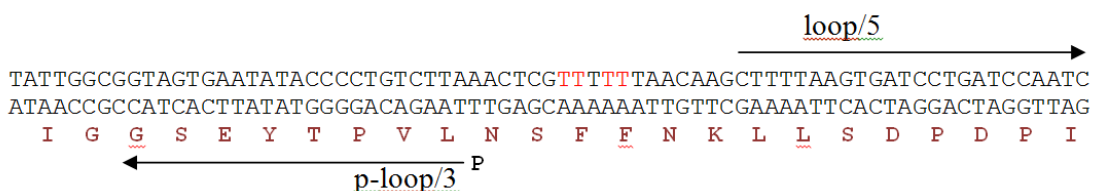
2.15.6. pMTncatF157A-F158A

A similar *exsite* strategy was used to generate a mutant allele of MG_491 with the substitution of the Phe157 and Phe158 codons for alanine codons. The pMTncatMG491 plasmid was amplified using the oligonucleotide FFAAMG491/5, which incorporates the intended mutations, and the phosphorylated oligonucleotide P-loop/3. The resulting lineal fragment was religated with T4 DNA ligase and transformed in *E. coli* XL1-Blue.



2.15.7. pMTncatΔloopL2

The *exsite* PCR was also used to generate an MG_491 allele lacking the coding sequence for residues N155-K160 in MG491 protein. The pMTncatMG491 plasmid was amplified using the oligonucleotide loop/5 and the phosphorylated oligonucleotide P-loop/3. This amplicon do not include the sequence coding for N155-K160 residues. The resulting lineal fragment was religated with T4 DNA ligase and transformed in *E. coli* XL1-Blue.



2.15.8. pMTncatΔNt

The 855 bp 3' coding sequence of MG_491 was amplified by PCR using primers MG491pr438ct/5 and MG491/3. Oligonucleotide MG491pr438ct/5 incorporates the sequence of the MG_438 promoter. The PCR fragment was excised with *Apal* and *XhoI*

restriction enzymes and was ligated into a pMTncaT plasmid also cleaved with *Apal* and *XhoI*. The resulting pMTncaT Δ Nt plasmid was then transformed into *E. coli* XL1-Blue strain.

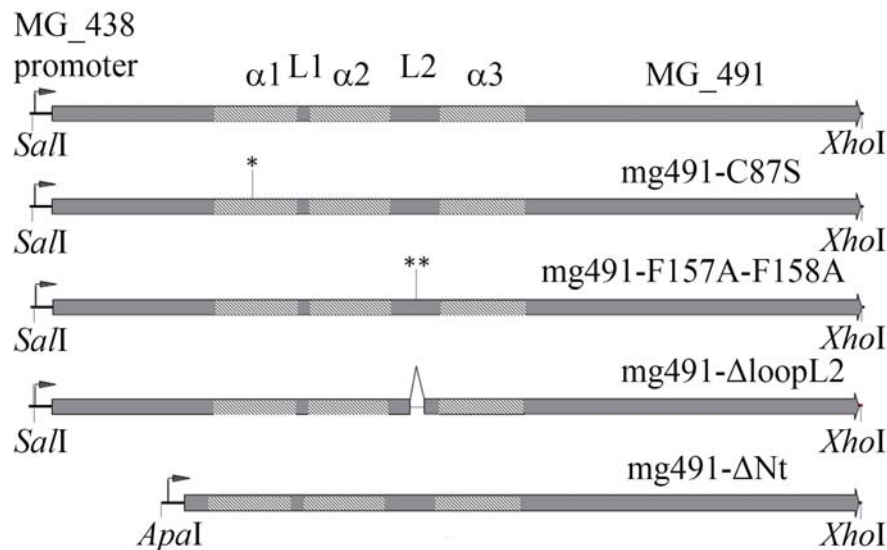


Fig. M.6. Schematic of the MG_491 alleles introduced in Δ mg491 cells in a mini-transposon. Coding sequences for helices $\alpha 1$, $\alpha 2$ and $\alpha 3$ and loops L1 and L2 are indicated. The C87S mutation is labelled with an asterisk (*) in the MG_491C87S allele. A double asterisk (**) is pointing to the F157A and F158A mutations in the MG491-F157A-F158A allele. Deletion of the 463-480 bp region from MG_491 coding for Asn155 to Lys160 is labelled with lines in the MG491-loopL2 allele.

3. Protein analysis

3.1. Protein extraction from *M. genitalium*

Samples of total protein from the *M. genitalium* strains used in this work were prepared using standard protocols (Sambrook and Russell, 2001). Briefly, these strains were grown in 15 mL of SP-4 until reaching mid-log phase of growth. Then, cells were scrapped off the flask and centrifuged at 20 000 g 20 min. SP-4 medium was removed and the cells were washed three times in PBS (Sigma-Aldrich). Finally, they were resuspended in 150 μ L of PBS and lysed by adding 50 μ L of reducing protein loading buffer 4x (Tris-HCl 0.25M pH 6.8, SDS 8%, Glycerol 40%, Bromophenol blue 0.2%, β -mercaptoethanol 20%).

3.2. SDS- polyacrylamide gel electrophoresis (SDS-PAGE)

Protein profiles from the *M. genitalium* strains were analyzed in 7.5-15% acrylamide/ bisacrylamide gels (Sigma-Aldrich). The preparation of the gels were performed using standard procedures (Sambrook and Russell, 2001). Protein samples were run at 20mA until the bromophenol blue colorant reach the bottom of the gel. Then, proteins were visualized by staining with Coomassie Brilliant Blue R-250 (Sigma-Aldrich) and analyzed in a GS-800TM Calibrated Densitometer (BioRad). *BenchmarkTM Protein Ladder* (Life Technologies) was used to determine the molecular weight of the visualized bands.

3.3. Western blot

The detection of a protein in the *M. genitalium* strains was assessed by detection with specific antibodies. To this purpose, total protein samples from these strains were separated by SDS-PAGE and transferred to a PVDF membrane (Millipore). *Precision Plus Protein™ Dual Xtra Standards* (BioRad) was added in a lane to determine the molecular weight of the visualized bands. For the electrotransference of the proteins, SDS-PAGE gel and PVDF membrane were introduced in a *Mini Trans-Blot® electrophoretic transfer cell* (BioRad) following standard procedures (Sambrook and Russell, 2001) and submerged in cooled transference buffer (Tris 25 mM-glycine 192 mM pH 8.3, methanol 20%). 100V were applied during 1 hour for the electrotransference.

The PVDF membrane was cleaned with PBS supplemented with Tween 20 0.05% (Sigma-Aldrich) and incubated 1h with blocking solution (PBS supplemented with Tween 20 0.05% and BSA 1%). Then, the membrane was incubated with an appropriate dilution of the specific antibody in blocking solution, which was then detected with a secondary antibody (anti-Rabbit or anti-Mouse) conjugated with peroxidase HRP (Life Technologies). Visualization was performed in a *Molecular Imager® VersaDoc™* after adding the *Luminata™ Forte Western HRP substrate*.

Table M.1. Primary antibodies used in this work

Antibody	Antigen	Nature	Secondary	Dilution	Origin
Anti-P140**	P140	Monoclonal	Anti-mouse	1:1 000	(Morrison-Plummer et al., 1987)
Anti-P110**	P110	Polyclonal	Anti-rabbit	1:1 000	(Dhandayuthapani et al., 1999)
Anti-HMW1*	MG312	Polyclonal	Anti-rabbit	1:8 000	(Stevens and Krause, 1992)
Anti-HMW3*	MG317	Polyclonal	Anti-rabbit	1:5 000	(Stevens and Krause, 1992)
Anti-MG218	MG218	Polyclonal	Anti-mouse	1:1 000	(Pich et al., 2008)
Anti-MG218c	MG218Ct	Monoclonal	Anti-mouse	1:2 000	(Pich et al., 2008)
Anti-P41*	MG491	Polyclonal	Anti-rabbit	1:1 000	(Krause et al., 1997)
Anti-MG217	MG217	Polyclonal	Anti-mouse	1:1 000	(Burgos et al., 2008)
Anti-MG219	MG219	Polyclonal	Anti-mouse	1:1 000	González-González, Unpublished
Anti-P32C	P32Ct	Polyclonal	Anti-mouse	1:2 000	González-González, Unpublished

* provided by Dr. Duncan Krause (UGA) and prepared against *M. pneumoniae* ortholog.

** provided by Dr. Joel Baseman (UTHSCSA)

4. Quantification of the hemadsorption of mycoplasma strains

4.1. Purification of human erythrocytes

Samples of 0.250 mL of peripheral blood were extracted from a human healthy donor using *Ames Minilet™ Lancets* (Bayer). The red blood cells (RBCs) were washed three times with 10 mL of Dulbecco's phosphate buffered saline containing 0.9 mM CaCl_2 and 0.49 mM MgCl_2 (PBSCM, Sigma-Aldrich Corp.) and resuspended in 25 mL of the same buffer. Special care was taken to remove the upper layer of white blood cells (WBCs) in the RBCs pellet. The stock of RBCs obtained by this method was stored on ice and used in the interval of four hours in the HA assay. Written informed consent was obtained from the blood donor. All the procedures were under the guidelines established by the Human and Animal Experimentation Ethics Committee (CEEAH) of UAB and approved by this committee. Human RBCs prepared following this instructions were used in qualitative and quantitative hemadsorption of mycoplasma assays.

4.2. Qualitative hemadsorption assay

The capacity of a mycoplasma strain to bind erythrocytes have been investigated by qualitative and quantitative methods. For the qualitative hemadsorption assay, cells of the mycoplasma strain were diluted to 10^{-5} - 10^{-7} and seeded on SP-4 agar plates as previously described. After two weeks, 2 mL of a 1:100 suspension of human erythrocytes in PBS was added to the plates and incubated 1h at 37°C. Then, unattached erythrocytes were removed by washing the plates three times with PBS. Finally, the colonies of mycoplasmas were visualized and photographed in a LeicaMZFLIII stereomicroscope.

4.3. Quantitative hemadsorption assay

In this work, we have developed a new method to quantify the hemadsorption of mycoplasma strains by flow cytometry. Fluorophore SYBR Green I (Life technologies) binds to nucleic acids and was selected for this method due to the different content of nucleic acids between mycoplasma cells and erythrocytes. After this staining, populations of mycoplasma cells, mycoplasma aggregates, RBCs and RBCs with attached mycoplasmas can be separated and measured. A detailed protocol is provided here.

4.3.1. Preparation of the mycoplasma stock

Mycoplasma strains were grown as previously described. Both adherent mycoplasma cells scrapped off the tissue culture flasks and cells growing in suspension were recovered by centrifugation 20 minutes at 20 000 g and resuspended in 0.5 mL of culture medium.

Mycoplasma cells were passed ten times through a syringe with a 25G needle and stored on ice.

4.3.2. Titration of the mycoplasma and RBCs stock

The different mycoplasma samples were first diluted 1:200 in culture medium. Then, 20 μL of these suspensions were diluted again in 0.5 mL of PBSCM and stained with SYBR Green I at a 1:10 000 (v/v) dilution from the commercial stock for 20 min protected from light. At the same time, a sample of 0.5 mL of PBSCM containing 20 μL of SP4 medium was stained by the same procedure and was used as negative control. Similarly, the stock of RBCs was diluted 1:150 in PBSCM and stained also with SYBR Green at a 1:10 000 dilution.

Samples were titrated by FC using a FACSCalibur (Becton Dickinson) equipped with an air-cooled 488 nm argon laser and a 633 nm red diode laser. Side-angle-scatter (SSC-H), green fluorescence (FL1-H detector, 530/30 filter) and red autofluorescence (FL3-H detector, 670LP filter) were used to quantify the different cell types used. FC data was acquired in four-decade logarithmic scale and the samples were measured during 90 seconds at the lowest flow rate ($12 \mu\text{L min}^{-1}$) to increase the resolution of readings. The primary threshold was set at 11 units of SSC-H and the secondary threshold at 27 units of FL1-H. FC data were analyzed with the CellQuest-Pro software (Becton Dickinson) and contour plots were made using FACSDiva software (Becton Dickinson).

To identify and titrate mycoplasma cells and RBCs, several dilutions of the fresh mycoplasma stock containing the same amount of SP-4 medium and several dilutions of RBCs stock were used. Total fluorescence units of FL1-H were calculated by multiplying the FL1-H mean value by the total number of events in the analyzed region. The total fluorescence is a measure the mycoplasma cell mass once subtracted the total fluorescence of this region in the negative control sample. Events in R2 region indicates the RBCs concentration when subtracted the number of events in the corresponding region of the negative control.

The viability of mycoplasma cells was assessed in a sample of SYBR Green I stained mycoplasmas by adding propidium iodide (PI) to the mixture at a final concentration of $2 \mu\text{g mL}^{-1}$. Non viable cells were expected to show increased FL3-H fluorescence values when analyzed by FC. To define the region containing non-viable mycoplasmas, a mycoplasma sample containing SYBR Green I and propidium iodide was permeabilized with 0.015% Triton X-100 (Fluka) just before submitting the sample to FC analysis.

4.3.3. Hemadsorption reaction

A fixed amount of mycoplasma cells (about $3 \cdot 10^7$ FL1-H fluorescence units) was incubated

with increasing amounts of RBCs (from 0 to 10^7 FC events) in 1 mL of PBSCM. It was found essential for reproducible results that mycoplasma culture medium in the hemadsorption reaction was at least 5% (v/v). We used the following bank of conditions:

Table M.1. Bank of conditions.

Tube	PBSCM (μL)	RBC (μL)	Medium (μL)	Mycoplasma (μL)
1	947	3	20	30
2	940	10	20	30
3	920	30	20	30
4	890	60	20	30
5	850	100	20	30
6	750	200	20	30
7	650	300	20	30
0	950	0	20	30

The RBCs stock was diluted to $2 \cdot 10^7$ events $\cdot \text{mL}^{-1}$ in PBSCM and the mycoplasma stock was diluted to $1 \cdot 10^9$ units of total FL1-H fluorescence. The 0 sample was used to calculate the actual number of mycoplasma cells in the experiment

The same bank, but without mycoplasma cells, was used to subtract the background in R1 and to enumerate the actual RBCs in each dilution. Samples were gently mixed end-over-end for 40 min at 37 °C and then SYBR Green was added at a 1:10 000 dilution and stained for 20 min protected from light. The fraction of free mycoplasma cells remaining after the HA reaction was quantified by FC as described above and plotted versus the amount of RBCs. Plots and data fitting to inverse Langmuir isotherm curves were performed by using the KaleidaGraph software (Synergy).

After FC analyses, some of the samples of RBCs mixed with mycoplasmas were examined by phase contrast and epifluorescence using a Nikon Eclipse TE2000e microscope. Pictures obtained with a Digital Sight-SMC Nikon camera were processed using the NIS-Elements BR software.

5. Techniques in microscopy

5.1. Localization of P32:mCherry by epifluorescence microscopy

Samples of G37 WT, Δmg491 , Δmg218 , G37-P32Ch, $\Delta\text{mg491-P32ch}$ and $\Delta\text{mg218-P32ch}$ strains were grown in 0.2 mL of SP-4 O/N in 8-well μ -slides ibiTreat (Ibidi). Then, SP-4 medium was removed and slides were washed three times in Buffer A (phosphate buffer 10 mM pH 7.2, sodium chloride 150 mM). Cells were observed by phase contrast and epifluorescence in a Nikon Eclipse TE 2000-E inverted microscope in the presence of Buffer A supplemented with Hoechst 33342 0.01 mg mL^{-1} . Phase contrast images and DAPI (excitation 387/11 nm, emission 447/60 nm) and Texas Red (excitation 560/20 nm, emission 593/40 nm) epifluorescence images were captured with a Digital Sight DS-SMC Nikon camera controlled by NIS-Elements BR software.

5.2. Time-lapse microcinematography

Gliding properties of G37 WT and mutant strains were analyzed by time-lapse microcinematography. For this purpose, *M. genitalium* samples from mid-log phase cultures were diluted 1:200 and grown in 0.2 mL of SP-4 O/N on 8-well μ -slides ibiTreat (Ibidi). Δ mg491 and Δ mg218 strains were only diluted 1:4. Prior observation, medium was replaced with fresh SP-4 medium prewarmed at 37 °C and cell movement was examined at 37°C and 5% CO₂ using a Nikon Eclipse TE 2000-E inverted microscope. Images were captured at 2 sec intervals for a total of 2 min for G37, Δ mg491, Δ mg491-mg491cat, mg491- Δ p1, Δ p1TC6, mg491-C87S, mg491-F157A-F158A, mg491- Δ loopL2 strains and mg491- Δ Nt; at 5 min intervals for a total of 30 minutes for Δ mg491-P32ch and Δ mg218-P32ch strains; and every 30 minutes for a total of 16 hours for Δ mg491 and Δ mg218 strains. Analysis of the gliding properties was performed using the ImageJ 1.48v software with the MTrack2 plugin (<http://imagej.nih.gov/ij>). The frequency of motile cells as well as the frequency of resting periods (cell stoppings of more than 5 sec) was determined by examining 200 isolated cells. The mean velocity was measured from at least 25 motile, isolated cells. The diameter of the tracks drawn by G37, mg491- Δ p1 and Δ p1TC6 was measured from 100 motile, isolated cells. The mean velocity of the filament extension was determined by measuring the position at 5 min intervals of the extending tips in 10 isolated filaments.

5.3. Scanning electron microscopy

M. genitalium G37 WT and mutant strains were grown until mid-log phase over glass coverslips. These samples were washed three times with PBS, fixed with glutaraldehyde 1% in PBS 1 hour and dehydrated by soaking the coverslips 10 min in increasing concentrations of ethanol (30%, 50%, 70%, 90% and 100%). The coverslips were then critical point dried in a *K850 Critical point dryer* (Quorum technologies) and sputter coated with gold. Sample preparation and examination in a *Merlin scanning electron microscope* (Zeiss) was performed at Servei de microscòpia of the UAB.

5.4. Cryo-EM imaging

M. genitalium G37 WT and mutant strains were grown in SP-4 medium over holey carbon-coated grids O/N at 37°C. Each grid was washed with PBSCM, blotted to remove the liquid excess and immediately plunged into liquid ethane in the *Leica EM CPC cryoworkstation* (Leica Microsystems). The grids were transferred to liquid nitrogen and then to a *626 Gatan cryoholder* (Gatan) and maintained at -179°C during imaging. The grids were examined on a *JEOL 2011 transmission electron microscope* operating at an accelerating voltage of 200 kV. Micrographs were recorded on a *Gatan USC1000* (Gatan) camera under low electron dose conditions to minimize the damage by the electron beam radiation. A moderate underfocus (between -30 and -15 μ m) was used to increase contrast of the samples.

References

- Adan-Kubo, J., Uenoyama, A., Arata, T., Miyata, M., 2006. Morphology of isolated Gli349, a leg protein responsible for *Mycoplasma mobile* gliding via glass binding, revealed by rotary shadowing electron microscopy. *J Bacteriol* 188, 2821-2828.
- Algire, M.A., Lartigue, C., Thomas, D.W., Assad-Garcia, N., Glass, J.I., Merryman, C., 2009. New selectable marker for manipulating the simple genomes of *Mycoplasma* species. *Antimicrob Agents Chemother* 53, 4429-4432.
- Anagrius, C., Lore, B., Jensen, J.S., 2005. *Mycoplasma genitalium*: prevalence, clinical significance, and transmission. *Sex Transm Infect* 81, 458-462.
- Anagrius, C., Lore, B., Jensen, J.S., 2013. Treatment of *Mycoplasma genitalium*. Observations from a Swedish STD Clinic. *PLoS One* 8.
- Antelmann, H., Helmann, J.D., 2011. Thiol-based redox switches and gene regulation. *Antioxidants & redox signaling* 14, 1049-1063.
- Anttila, T., Saikku, P., Koskela, P., Bloigu, A., Dillner, J., Ikaheimo, I., Jellum, E., Lehtinen, M., Lenner, P., Hakulinen, T., Narvanen, A., Pukkala, E., Thoresen, S., Youngman, L., Paavonen, J., 2001. Serotypes of *Chlamydia trachomatis* and risk for development of cervical squamous cell carcinoma. *JAMA* 285, 47-51.
- Arnal, M., Herrero, J., de la Fe, C., Revilla, M., Prada, C., Martinez-Duran, D., Gomez-Martin, A., Fernandez-Arberas, O., Amores, J., Contreras, A., Garcia-Serrano, A., de Luco, D.F., 2013. Dynamics of an infectious keratoconjunctivitis outbreak by *Mycoplasma conjunctivae* on *Pyrenean Chamois Rupicapra p. pyrenaica*. *PLoS One* 8, e61887.
- Assuncao, P., Antunes, N.T., Rosales, R.S., Poveda, C., Poveda, J.B., Davey, H.M., 2006a. Flow cytometric determination of the effects of antibacterial agents on *Mycoplasma agalactiae*, *Mycoplasma putrefaciens*, *Mycoplasma capricolum subsp. capricolum*, and *Mycoplasma mycoides subsp. mycoides* large colony type. *Antimicrob Agents Chemother* 50, 2845-2849.
- Assuncao, P., Davey, H.M., Rosales, R.S., Antunes, N.T., de la Fe, C., Ramirez, A.S., de Galarreta, C.M., Poveda, J.B., 2007. Detection of mycoplasmas in goat milk by flow cytometry. *Cytometry. Part A : the journal of the International Society for Analytical Cytology* 71, 1034-1038.
- Assuncao, P., de la Fe, C., Antunes, N.T., Rosales, R.S., Ruiz de Galarreta, C.M., Poveda, J.B., 2006b. Use of flow cytometry for enumeration of *Mycoplasma mycoides subsp. mycoides* large-colony type in broth medium. *Journal of applied microbiology* 100, 878-884.
- Assuncao, P., Rosales, R.S., Rifatbegovic, M., Antunes, N.T., de la Fe, C., Ruiz de Galarreta, C.M., Poveda, J.B., 2006c. Quantification of mycoplasmas in broth medium with sybr green-I and flow cytometry. *Frontiers in bioscience : a journal and virtual library* 11, 492-

497.

- Atkinson, T.P., Balish, M.F., Waites, K.B., 2008. Epidemiology, clinical manifestations, pathogenesis and laboratory detection of *Mycoplasma pneumoniae* infections. *FEMS Microbiol Rev* 32, 956-973.
- Baczynska, A., Funch, P., Fedder, J., Knudsen, H.J., Birkelund, S., Christiansen, G., 2007. Morphology of human Fallopian tubes after infection with *Mycoplasma genitalium* and *Mycoplasma hominis*--in vitro organ culture study. *Hum Reprod* 22, 968-979.
- Balish, M.F., 2006. Subcellular structures of mycoplasmas. *Frontiers in bioscience : a journal and virtual library* 11, 2017-2027.
- Balish, M.F., Hahn, T.W., Popham, P.L., Krause, D.C., 2001. Stability of *Mycoplasma pneumoniae* cytoadherence-accessory protein HMW1 correlates with its association with the triton shell. *J Bacteriol* 183, 3680-3688.
- Balish, M.F., Krause, D.C., 2006. Mycoplasmas: a distinct cytoskeleton for wall-less bacteria. *Journal of molecular microbiology and biotechnology* 11, 244-255.
- Balish, M.F., Santurri, R.T., Ricci, A.M., Lee, K.K., Krause, D.C., 2003. Localization of *Mycoplasma pneumoniae* cytoadherence-associated protein HMW2 by fusion with green fluorescent protein: implications for attachment organelle structure. *Molecular microbiology* 47, 49-60.
- Barre, A., de Daruvar, A., Blanchard, A., 2004. MolliGen, a database dedicated to the comparative genomics of Mollicutes. *Nucleic Acids Res* 32, D307-310.
- Baseman, J.B., 1993. The cytoadhesins of *Mycoplasma pneumoniae* and *M. genitalium*. *Subcellular biochemistry* 20, 243-259.
- Baseman, J.B., Banai, M., Kahane, I., 1982a. Sialic acid residues mediate *Mycoplasma pneumoniae* attachment to human and sheep erythrocytes. *Infect Immun* 38, 389-391.
- Baseman, J.B., Cole, R.M., Krause, D.C., Leith, D.K., 1982b. Molecular basis for cytoadsorption of *Mycoplasma pneumoniae*. *J Bacteriol* 151, 1514-1522.
- Baseman, J.B., Dallo, S.F., Tully, J.G., Rose, D.L., 1988. Isolation and characterization of *Mycoplasma genitalium* strains from the human respiratory tract. *J Clin Microbiol* 26, 2266-2269.
- Baseman, J.B., Lange, M., Criscimagna, N.L., Giron, J.A., Thomas, C.A., 1995. Interplay between Mycoplasmas and Host Target-Cells. *Microb Pathogenesis* 19, 105-116.
- Bergemann, A.D., Whitley, J.C., Finch, L.R., 1989. Homology of mycoplasma plasmid pADB201 and staphylococcal plasmid pE194. *J Bacteriol* 171, 593-595.
- Bhugra, B., Voelker, L.L., Zou, N., Yu, H., Dybvig, K., 1995. Mechanism of antigenic variation in *Mycoplasma pulmonis*: interwoven, site-specific DNA inversions. *Molecular*

- microbiology 18, 703-714.
- Biberfeld, G., Biberfeld, P., 1970. Ultrastructural features of *Mycoplasma pneumoniae*. J Bacteriol 102, 855-861.
- Blaylock, M.W., Musatovova, O., Baseman, J.G., Baseman, J.B., 2004. Determination of infectious load of *Mycoplasma genitalium* in clinical samples of human vaginal cells. J Clin Microbiol 42, 746-752.
- Boonmee, A., Ruppert, T., Herrmann, R., 2009. The gene mpn310 (hmw2) from *Mycoplasma pneumoniae* encodes two proteins, HMW2 and HMW2-s, which differ in size but use the same reading frame. FEMS microbiology letters 290, 174-181.
- Bose, S., Segovia, J.A., Somarajan, S.R., Chang, T.H., Kannan, T.R., Baseman, J.B., 2014. ADP-ribosylation of NLRP3 by *Mycoplasma pneumoniae* CARDS toxin regulates inflammasome activity. mBio 5.
- Bose, S.R., Balish, M.F., Krause, D.C., 2009. *Mycoplasma pneumoniae* cytoskeletal protein HMW2 and the architecture of the terminal organelle. J Bacteriol 191, 6741-6748.
- Bowie, W.R., Wang, S.P., Alexander, E.R., Floyd, J., Forsyth, P.S., Pollock, H.M., Lin, J.S., Buchanan, T.M., Holmes, K.K., 1977. Etiology of nongonococcal urethritis. Evidence for *Chlamydia trachomatis* and *Ureaplasma urealyticum*. J Clin Invest 59, 735-742.
- Bradshaw, C.S., Fairley, C.K., Lister, N.A., Chen, S.J., Garland, S.M., Tabrizi, S.N., 2009. *Mycoplasma genitalium* in men who have sex with men at male-only saunas. Sex Transm Infect 85, 432-435.
- Bredt, W., 1968. Motility and multiplication of *Mycoplasma pneumoniae*. A phase contrast study. Pathologia et microbiologia 32, 321-326.
- Bredt, W., Kist, M., Jacobs, E., 1981. Phagocytosis and complement action. Isr J Med Sci 17, 637-640.
- Burgos, R., Pich, O.Q., Ferrer-Navarro, M., Baseman, J.B., Querol, E., Pinol, J., 2006. *Mycoplasma genitalium* P140 and P110 cytoadhesins are reciprocally stabilized and required for cell adhesion and terminal-organelle development. J Bacteriol 188, 8627-8637.
- Burgos, R., Pich, O.Q., Querol, E., Pinol, J., 2007. Functional analysis of the *Mycoplasma genitalium* MG312 protein reveals a specific requirement of the MG312 N-terminal domain for gliding motility. J Bacteriol 189, 7014-7023.
- Burgos, R., Pich, O.Q., Querol, E., Pinol, J., 2008. Deletion of the *Mycoplasma genitalium* MG_217 gene modifies cell gliding behaviour by altering terminal organelle curvature. Mol Microbiol 69, 1029-1040.
- Calisto, B.M., Broto, A., Martinelli, L., Querol, E., Pinol, J., Fita, I., 2012. The EAGR box structure: a motif involved in mycoplasma motility. Molecular microbiology 86, 382-393.

- Cao, J., Kapke, P.A., Minion, F.C., 1994. Transformation of *Mycoplasma gallisepticum* with Tn916, Tn4001, and integrative plasmid vectors. *J Bacteriol* 176, 4459-4462.
- Casin, I., Vexiau-Robert, D., De La Salmoniere, P., Eche, A., Grandry, B., Janier, M., 2002. High prevalence of *Mycoplasma genitalium* in the lower genitourinary tract of women attending a sexually transmitted disease clinic in Paris, France. *Sex Transm Dis* 29, 353-359.
- Chan, P.J., Seraj, I.M., Kalugdan, T.H., King, A., 1996. Prevalence of mycoplasma conserved DNA in malignant ovarian cancer detected using sensitive PCR-ELISA. *Gynecol Oncol* 63, 258-260.
- Chopra-Dewasthaly, R., Marendra, M., Rosengarten, R., Jechlinger, W., Citti, C., 2005a. Construction of the first shuttle vectors for gene cloning and homologous recombination in *Mycoplasma agalactiae*. *FEMS microbiology letters* 253, 89-94.
- Chopra-Dewasthaly, R., Zimmermann, M., Rosengarten, R., Citti, C., 2005b. First steps towards the genetic manipulation of *Mycoplasma agalactiae* and *Mycoplasma bovis* using the transposon Tn4001mod. *International journal of medical microbiology : IJMM* 294, 447-453.
- Chrisment, D., Charron, A., Cazanave, C., Pereyre, S., Bebear, C., 2012. Detection of macrolide resistance in *Mycoplasma genitalium* in France. *J Antimicrob Chemother* 67, 2598-2601.
- Citti, C., Marechal-Drouard, L., Saillard, C., Weil, J.H., Bove, J.M., 1992. *Spiroplasma citri* UGG and UGA tryptophan codons: sequence of the two tryptophanyl-tRNAs and organization of the corresponding genes. *J Bacteriol* 174, 6471-6478.
- Citti, C., Nouvel, L.X., Baranowski, E., 2010. Phase and antigenic variation in mycoplasmas. *Future microbiology* 5, 1073-1085.
- Citti, C., Wise, K.S., 1995. *Mycoplasma hyorhinis* vlp gene transcription: critical role in phase variation and expression of surface lipoproteins. *Molecular microbiology* 18, 649-660.
- Clausen, H.F., Fedder, J., Drasbek, M., Nielsen, P.K., Toft, B., Ingerslev, H.J., Birkelund, S., Christiansen, G., 2001. Serological investigation of *Mycoplasma genitalium* in infertile women. *Hum Reprod* 16, 1866-1874.
- Cloward, J.M., Krause, D.C., 2009. *Mycoplasma pneumoniae* J-domain protein required for terminal organelle function. *Molecular microbiology* 71, 1296-1307.
- Cloward, J.M., Krause, D.C., 2010. Functional domain analysis of the *Mycoplasma pneumoniae* co-chaperone TopJ. *Molecular microbiology* 77, 158-169.
- Cloward, J.M., Krause, D.C., 2011. Loss of co-chaperone TopJ impacts adhesin P1 presentation and terminal organelle maturation in *Mycoplasma pneumoniae*. *Molecular*

microbiology 81, 528-539.

- Cohen, C.R., Manhart, L.E., Bukusi, E.A., Astete, S., Brunham, R.C., Holmes, K.K., Sinei, S.K., Bwayo, J.J., Totten, P.A., 2002. Association between *Mycoplasma genitalium* and acute endometritis. *Lancet* 359, 765-766.
- Cohen, C.R., Mugo, N.R., Astete, S.G., Odondo, R., Manhart, L.E., Kiehlbauch, J.A., Stamm, W.E., Waiyaki, P.G., Totten, P.A., 2005. Detection of *Mycoplasma genitalium* in women with laparoscopically diagnosed acute salpingitis. *Sex Transm Infect* 81, 463-466.
- Cohen, C.R., Nosek, M., Meier, A., Astete, S.G., Iverson-Cabral, S., Mugo, N.R., Totten, P.A., 2007. *Mycoplasma genitalium* infection and persistence in a cohort of female sex workers in Nairobi, Kenya. *Sex Transm Dis* 34, 274-279.
- Cohen, M.S., 1998. Sexually transmitted diseases enhance HIV transmission: no longer a hypothesis. *Lancet* 351 Suppl 3, 5-7.
- Collier, A.M., Carson, J.L., Hu, P.C., Hu, S.S., Huang, C.H., Barile, M.F., 1990. Attachment of *Mycoplasma genitalium* to the Ciliated Epithelium of Human Fallopian-Tubes. *Zbl Bakt S* 20, 730-732.
- Collier, A.M., Clyde, W.A., 1971. Relationships Between *Mycoplasma pneumoniae* and Human Respiratory Epithelium. *Infect Immun* 3, 694-701.
- Cordova, C.M., Lartigue, C., Sirand-Pugnet, P., Renaudin, J., Cunha, R.A., Blanchard, A., 2002. Identification of the origin of replication of the *Mycoplasma pulmonis* chromosome and its use in oriC replicative plasmids. *J Bacteriol* 184, 5426-5435.
- Couldwell, D.L., Tagg, K.A., Jeffreys, N.J., Gilbert, G.L., 2013. Failure of moxifloxacin treatment in *Mycoplasma genitalium* infections due to macrolide and fluoroquinolone resistance. *Int J STD AIDS* 24, 822-828.
- Dallo, S.F., Baseman, J.B., 2000. Intracellular DNA replication and long-term survival of pathogenic mycoplasmas. *Microb Pathogenesis* 29, 301-309.
- Dallo, S.F., Chavoya, A., Su, C.J., Baseman, J.B., 1989a. DNA and protein sequence homologies between the adhesins of *Mycoplasma genitalium* and *Mycoplasma pneumoniae*. *Infect Immun* 57, 1059-1065.
- Dallo, S.F., Horton, J.R., Su, C.J., Baseman, J.B., 1989b. Homologous regions shared by adhesin genes of *Mycoplasma pneumoniae* and *Mycoplasma genitalium*. *Microb Pathog* 6, 69-73.
- Dallo, S.F., Lazzell, A.L., Chavoya, A., Reddy, S.P., Baseman, J.B., 1996. Biofunctional domains of the *Mycoplasma pneumoniae* P30 adhesin. *Infect Immun* 64, 2595-2601.
- Das, K., De la Garza, G., Maffi, S., Saikolappan, S., Dhandayuthapani, S., 2012. Methionine sulfoxide reductase A (MsrA) deficient *Mycoplasma genitalium* shows decreased interactions with host cells. *PLoS One* 7, e36247.

- Das, K., De la Garza, G., Siwak, E.B., Scofield, V.L., Dhandayuthapani, S., 2014. *Mycoplasma genitalium* promotes epithelial crossing and peripheral blood mononuclear cell infection by HIV-1. *Int J Infect Dis* 23, 31-38.
- Datcu, R., Gesink, D., Mulvad, G., Montgomery-Andersen, R., Rink, E., Koch, A., Ahrens, P., Jensen, J.S., 2013. Vaginal microbiome in women from Greenland assessed by microscopy and quantitative PCR. *BMC Infect Dis* 13, 480.
- de Barbeyrac, B., Bernet-Poggi, C., Febrer, F., Renaudin, H., Dupon, M., Bebear, C., 1993. Detection of *Mycoplasma pneumoniae* and *Mycoplasma genitalium* in clinical samples by polymerase chain reaction. *Clin Infect Dis* 17 Suppl 1, S83-89.
- Deguchi, T., Maeda, S., 2002. *Mycoplasma genitalium*: another important pathogen of nongonococcal urethritis. *J Urol* 167, 1210-1217.
- Deguchi, T., Yasuda, M., Yokoi, S., Nakano, M., Ito, S., Ohkusu, K., Ezaki, T., Hoshina, S., 2009. Failure to detect *Mycoplasma genitalium* in the pharynges of female sex workers in Japan. *J Infect Chemother* 15, 410-413.
- Dehon, P.M., McGowin, C.L., 2014. *Mycoplasma genitalium* Infection Is Associated with Microscopic Signs of Cervical Inflammation in Liquid Cytology Specimens. *J Clin Microbiol* 52, 2398-2405.
- Dhandayuthapani, S., Blaylock, M.W., Bebear, C.M., Rasmussen, W.G., Baseman, J.B., 2001. Peptide methionine sulfoxide reductase (MsrA) is a virulence determinant in *Mycoplasma genitalium*. *J Bacteriol* 183, 5645-5650.
- Dhandayuthapani, S., Rasmussen, W.G., Baseman, J.B., 1999. Disruption of gene mg218 of *Mycoplasma genitalium* through homologous recombination leads to an adherence-deficient phenotype. *Proc Natl Acad Sci U S A* 96, 5227-5232.
- Dhandayuthapani, S., Rasmussen, W.G., Baseman, J.B., 2002. Stability of cytoadherence-related proteins P140/P110 in *Mycoplasma genitalium* requires MG218 and unidentified factors. *Archives of medical research* 33, 1-5.
- dos Santos, G., Kutuzov, M.A., Ridge, K.M., 2012. The inflammasome in lung diseases. *American journal of physiology. Lung cellular and molecular physiology* 303, L627-633.
- Dundr, M., Ospina, J.K., Sung, M.H., John, S., Upender, M., Ried, T., Hager, G.L., Matera, A.G., 2007. Actin-dependent intranuclear repositioning of an active gene locus in vivo. *The Journal of cell biology* 179, 1095-1103.
- Dybvig, K., Cassell, G.H., 1987. Transposition of gram-positive transposon Tn916 in *Acholeplasma laidlawii* and *Mycoplasma pulmonis*. *Science* 235, 1392-1394.
- Dybvig, K., Sitaraman, R., French, C.T., 1998. A family of phase-variable restriction enzymes with differing specificities generated by high-frequency gene rearrangements. *Proc Natl Acad Sci U S A* 95, 13923-13928.

- Edwards, R.K., Ferguson, R.J., Reyes, L., Brown, M., Theriaque, D.W., Duff, P., 2006. Assessing the relationship between preterm delivery and various microorganisms recovered from the lower genital tract. *J Matern Fetal Neonatal Med* 19, 357-363.
- Embree, J., 1988. *Mycoplasma-Hominis* in Maternal and Fetal Infections. *Ann Ny Acad Sci* 549, 56-64.
- Fahey, R.C., 2013. Glutathione analogs in prokaryotes. *Biochimica et biophysica acta* 1830, 3182-3198.
- Falk, L., Fredlund, H., Jensen, J.S., 2003. Tetracycline treatment does not eradicate *Mycoplasma genitalium*. *Sex Transm Infect* 79, 318-319.
- Falk, L., Fredlund, H., Jensen, J.S., 2004. Symptomatic urethritis is more prevalent in men infected with *Mycoplasma genitalium* than with *Chlamydia trachomatis*. *Sex Transm Infect* 80, 289-293.
- Falk, L., Fredlund, H., Jensen, J.S., 2005. Signs and symptoms of urethritis and cervicitis among women with or without *Mycoplasma genitalium* or *Chlamydia trachomatis* infection. *Sex Transm Infect* 81, 73-78.
- Feldner, J., Gobel, U., Bredt, W., 1982. *Mycoplasma pneumoniae* adhesin localized to tip structure by monoclonal antibody. *Nature* 298, 765-767.
- Feng, S.H., Tsai, S., Rodriguez, J., Lo, S.C., 1999. Mycoplasmal infections prevent apoptosis and induce malignant transformation of interleukin-3-dependent 32D hematopoietic cells. *Mol Cell Biol* 19, 7995-8002.
- Fisseha, M., Gohlmann, H.W., Herrmann, R., Krause, D.C., 1999. Identification and complementation of frameshift mutations associated with loss of cytoadherence in *Mycoplasma pneumoniae*. *J Bacteriol* 181, 4404-4410.
- Fleming, D.T., Wasserheit, J.N., 1999. From epidemiological synergy to public health policy and practice: the contribution of other sexually transmitted diseases to sexual transmission of HIV infection. *Sex Transm Infect* 75, 3-17.
- Francis, S.C., Kent, C.K., Klausner, J.D., Rauch, L., Kohn, R., Hardick, A., Gaydos, C.A., 2008. Prevalence of rectal *Trichomonas vaginalis* and *Mycoplasma genitalium* in male patients at the San Francisco STD clinic, 2005-2006. *Sex Transm Dis* 35, 797-800.
- Fraser, C.M., Gocayne, J.D., White, O., Adams, M.D., Clayton, R.A., Fleischmann, R.D., Bult, C.J., Kerlavage, A.R., Sutton, G., Kelley, J.M., Fritchman, R.D., Weidman, J.F., Small, K.V., Sandusky, M., Fuhrmann, J., Nguyen, D., Utterback, T.R., Saudek, D.M., Phillips, C.A., Merrick, J.M., Tomb, J.F., Dougherty, B.A., Bott, K.F., Hu, P.C., Lucier, T.S., Peterson, S.N., Smith, H.O., Hutchison, C.A., 3rd, Venter, J.C., 1995. The minimal gene complement of *Mycoplasma genitalium*. *Science* 270, 397-403.
- Frydman, J., 2001. Folding of newly translated proteins in vivo: the role of molecular

- chaperones. *Annual review of biochemistry* 70, 603-647.
- Gaurivaud, P., Laigret, F., Bove, J.M., 1996. Insusceptibility of members of the class Mollicutes to rifampin: studies of the *Spiroplasma citri* RNA polymerase beta-subunit gene. *Antimicrob Agents Chemother* 40, 858-862.
- Gesink, D.C., Mulvad, G., Montgomery-Andersen, R., Poppel, U., Montgomery-Andersen, S., Binzer, A., Vernich, L., Frosst, G., Stenz, F., Rink, E., Olsen, O.R., Koch, A., Jensen, J.S., 2012. *Mycoplasma genitalium* presence, resistance and epidemiology in Greenland. *Int J Circumpolar Health* 71, 1-8.
- Gibson, D.G., Benders, G.A., Andrews-Pfannkoch, C., Denisova, E.A., Baden-Tillson, H., Zaveri, J., Stockwell, T.B., Brownley, A., Thomas, D.W., Algire, M.A., Merryman, C., Young, L., Noskov, V.N., Glass, J.I., Venter, J.C., Hutchison, C.A., 3rd, Smith, H.O., 2008a. Complete chemical synthesis, assembly, and cloning of a *Mycoplasma genitalium* genome. *Science* 319, 1215-1220.
- Gibson, D.G., Benders, G.A., Axelrod, K.C., Zaveri, J., Algire, M.A., Moodie, M., Montague, M.G., Venter, J.C., Smith, H.O., Hutchison, C.A., 3rd, 2008b. One-step assembly in yeast of 25 overlapping DNA fragments to form a complete synthetic *Mycoplasma genitalium* genome. *Proc Natl Acad Sci U S A* 105, 20404-20409.
- Gibson, D.G., Glass, J.I., Lartigue, C., Noskov, V.N., Chuang, R.Y., Algire, M.A., Benders, G.A., Montague, M.G., Ma, L., Moodie, M.M., Merryman, C., Vashee, S., Krishnakumar, R., Assad-Garcia, N., Andrews-Pfannkoch, C., Denisova, E.A., Young, L., Qi, Z.Q., Segall-Shapiro, T.H., Calvey, C.H., Parmar, P.P., Hutchison, C.A., 3rd, Smith, H.O., Venter, J.C., 2010. Creation of a bacterial cell controlled by a chemically synthesized genome. *Science* 329, 52-56.
- Giles, N.M., Watts, A.B., Giles, G.I., Fry, F.H., Littlechild, J.A., Jacob, C., 2003. Metal and redox modulation of cysteine protein function. *Chemistry & biology* 10, 677-693.
- Glass, J.I., Assad-Garcia, N., Alperovich, N., Yooseph, S., Lewis, M.R., Maruf, M., Hutchison, C.A., 3rd, Smith, H.O., Venter, J.C., 2006. Essential genes of a minimal bacterium. *Proc Natl Acad Sci U S A* 103, 425-430.
- Glass, J.I., Hutchison, C.A., 3rd, Smith, H.O., Venter, J.C., 2009. A systems biology tour de force for a near-minimal bacterium. *Molecular systems biology* 5, 330.
- Gobel, U., Speth, V., Brecht, W., 1981. Filamentous structures in adherent *Mycoplasma pneumoniae* cells treated with nonionic detergents. *The Journal of cell biology* 91, 537-543.
- Grover, R.K., Zhu, X., Nieuwma, T., Jones, T., Boero, I., MacLeod, A.S., Mark, A., Niessen, S., Kim, H.J., Kong, L., Assad-Garcia, N., Kwon, K., Chesi, M., Smider, V.V., Salomon, D.R., Jelinek, D.F., Kyle, R.A., Pyles, R.B., Glass, J.I., Ward, A.B., Wilson, I.A., Lerner, R.A., 2014. A structurally distinct human mycoplasma protein that generically blocks

- antigen-antibody union. *Science* 343, 656-661.
- Guell, M., van Noort, V., Yus, E., Chen, W.H., Leigh-Bell, J., Michalodimitrakis, K., Yamada, T., Arumugam, M., Doerks, T., Kuhner, S., Rode, M., Suyama, M., Schmidt, S., Gavin, A.C., Bork, P., Serrano, L., 2009. Transcriptome complexity in a genome-reduced bacterium. *Science* 326, 1268-1271.
- Haggerty, C.L., 2008. Evidence for a role of *Mycoplasma genitalium* in pelvic inflammatory disease. *Curr Opin Infect Dis* 21, 65-69.
- Haggerty, C.L., Taylor, B.D., 2011. *Mycoplasma genitalium*: an emerging cause of pelvic inflammatory disease. *Infect Dis Obstet Gynecol* 2011, 959816.
- Hahn, T.W., Mothershed, E.A., Waldo, R.H., 3rd, Krause, D.C., 1999. Construction and analysis of a modified Tn4001 conferring chloramphenicol resistance in *Mycoplasma pneumoniae*. *Plasmid* 41, 120-124.
- Hahn, T.W., Willby, M.J., Krause, D.C., 1998. HMW1 is required for cytoadhesin P1 trafficking to the attachment organelle in *Mycoplasma pneumoniae*. *J Bacteriol* 180, 1270-1276.
- Hamasuna, R., Imai, H., Tsukino, H., Jensen, J.S., Osada, Y., 2008. Prevalence of *Mycoplasma genitalium* among female students in vocational schools in Japan. *Sex Transm Infect* 84, 303-305.
- Hamasuna, R., Osada, Y., Jensen, J.S., 2007. Isolation of *Mycoplasma genitalium* from first-void urine specimens by coculture with Vero cells. *J Clin Microbiol* 45, 847-850.
- Hannu, T., 2011. Reactive arthritis. *Best Pract Res Clin Rheumatol* 25, 347-357.
- Hardy, R.D., Coalson, J.J., Peters, J., Chaparro, A., Techasaensiri, C., Cantwell, A.M., Kannan, T.R., Baseman, J.B., Dube, P.H., 2009. Analysis of pulmonary inflammation and function in the mouse and baboon after exposure to *Mycoplasma pneumoniae* CARDS toxin. *PLoS One* 4, e7562.
- Hartmann, M., 2009. Genital Mycoplasmas. *J Dtsch Dermatol Ges* 7, 371-377.
- Hasselbring, B.M., Jordan, J.L., Krause, D.C., 2005. Mutant analysis reveals a specific requirement for protein P30 in *Mycoplasma pneumoniae* gliding motility. *J Bacteriol* 187, 6281-6289.
- Hasselbring, B.M., Jordan, J.L., Krause, R.W., Krause, D.C., 2006a. Terminal organelle development in the cell wall-less bacterium *Mycoplasma pneumoniae*. *Proceedings of the National Academy of Sciences of the United States of America* 103, 16478-16483.
- Hasselbring, B.M., Krause, D.C., 2007a. Cytoskeletal protein P41 is required to anchor the terminal organelle of the wall-less prokaryote *Mycoplasma pneumoniae*. *Molecular microbiology* 63, 44-53.
- Hasselbring, B.M., Krause, D.C., 2007b. Proteins P24 and P41 function in the regulation

- of terminal-organelle development and gliding motility in *Mycoplasma pneumoniae*. J Bacteriol 189, 7442-7449.
- Hasselbring, B.M., Page, C.A., Sheppard, E.S., Krause, D.C., 2006b. Transposon mutagenesis identifies genes associated with *Mycoplasma pneumoniae* gliding motility. J Bacteriol 188, 6335-6345.
- Hasselbring, B.M., Sheppard, E.S., Krause, D.C., 2012. P65 truncation impacts P30 dynamics during *Mycoplasma pneumoniae* gliding. J Bacteriol 194, 3000-3007.
- Hata, A., Honda, Y., Asada, K., Sasaki, Y., Kenri, T., Hata, D., 2008. *Mycoplasma hominis* meningitis in a neonate: Case report and review. J Infection 57, 338-343.
- Hatchel, J.M., Balish, M.F., 2008. Attachment organelle ultrastructure correlates with phylogeny, not gliding motility properties, in *Mycoplasma pneumoniae* relatives. Microbiology 154, 286-295.
- Hedreyda, C.T., Krause, D.C., 1995. Identification of a possible cytoadherence regulatory locus in *Mycoplasma pneumoniae*. Infect Immun 63, 3479-3483.
- Hedreyda, C.T., Lee, K.K., Krause, D.C., 1993. Transformation of *Mycoplasma pneumoniae* with Tn4001 by electroporation. Plasmid 30, 170-175.
- Hegermann, J., Herrmann, R., Mayer, F., 2002. Cytoskeletal elements in the bacterium *Mycoplasma pneumoniae*. Die Naturwissenschaften 89, 453-458.
- Henderson, G.P., Jensen, G.J., 2006. Three-dimensional structure of *Mycoplasma pneumoniae*'s attachment organelle and a model for its role in gliding motility. Molecular microbiology 60, 376-385.
- Hendrick, J.P., Hartl, F.U., 1995. The role of molecular chaperones in protein folding. FASEB journal : official publication of the Federation of American Societies for Experimental Biology 9, 1559-1569.
- Henning, D., Eade, D., Langstone, A., Bean-Hodges, A., Marceglia, A., Azzopardi, P., 2014. Asymptomatic *Mycoplasma genitalium* infection amongst marginalised young people accessing a youth health service in Melbourne. Int J STD AIDS 25, 299-302.
- Henry, C.H., Hughes, C.V., Gerard, H.C., Hudson, A.P., Wolford, L.M., 2000. Reactive arthritis: preliminary microbiologic analysis of the human temporomandibular joint. J Oral Maxillofac Surg 58, 1137-1142; discussion 1143-1134.
- Hewicker-Trautwein, M., Feldmann, M., Kehler, W., Schmidt, R., Thiede, S., Seeliger, F., Wohlsein, P., Ball, H.J., Buchenau, I., Spergser, J., Rosengarten, R., 2002. Outbreak of pneumonia and arthritis in beef calves associated with *Mycoplasma bovis* and *Mycoplasma californicum*. The Veterinary record 151, 699-703.
- Himmelreich, R., Hilbert, H., Plagens, H., Pirkl, E., Li, B.C., Herrmann, R., 1996. Complete sequence analysis of the genome of the bacterium *Mycoplasma pneumoniae*. Nucleic

Acids Res 24, 4420-4449.

- Hitti, J., Garcia, P., Totten, P., Paul, K., Astete, S., Holmes, K.K., 2010. Correlates of cervical *Mycoplasma genitalium* and risk of preterm birth among Peruvian women. Sex Transm Dis 37, 81-85.
- Hjorth, S.V., Bjornelius, E., Lidbrink, P., Falk, L., Dohn, B., Berthelsen, L., Ma, L., Martin, D.H., Jensen, J.S., 2006. Sequence-based typing of *Mycoplasma genitalium* reveals sexual transmission. J Clin Microbiol 44, 2078-2083.
- Horner, P.J., Gilroy, C.B., Thomas, B.J., Naidoo, R.O., Taylor-Robinson, D., 1993. Association of *Mycoplasma genitalium* with acute non-gonococcal urethritis. Lancet 342, 582-585.
- Horner, P.J., Taylor-Robinson, D., 2011. Association of *Mycoplasma genitalium* with balanoposthitis in men with non-gonococcal urethritis. Sex Transm Infect 87, 38-40.
- Hu, P.C., Schaper, U., Collier, A.M., Clyde, W.A., Jr., Horikawa, M., Huang, Y.S., Barile, M.F., 1987. A *Mycoplasma genitalium* protein resembling the *Mycoplasma pneumoniae* attachment protein. Infect Immun 55, 1126-1131.
- Huang, S., Li, J.Y., Wu, J., Meng, L., Shou, C.C., 2001. Mycoplasma infections and different human carcinomas. World J Gastroenterol 7, 266-269.
- Hutchison, C.A., Peterson, S.N., Gill, S.R., Cline, R.T., White, O., Fraser, C.M., Smith, H.O., Venter, J.C., 1999. Global transposon mutagenesis and a minimal *Mycoplasma* genome. Science 286, 2165-2169.
- Idahl, A., Lundin, E., Jurstrand, M., Kumlin, U., Elgh, F., Ohlson, N., Ottander, U., 2011. *Chlamydia trachomatis* and *Mycoplasma genitalium* plasma antibodies in relation to epithelial ovarian tumors. Infect Dis Obstet Gynecol 2011, 824627.
- Inamine, J.M., Ho, K.C., Loechel, S., Hu, P.C., 1990. Evidence that UGA is read as a tryptophan codon rather than as a stop codon by *Mycoplasma pneumoniae*, *Mycoplasma genitalium*, and *Mycoplasma gallisepticum*. J Bacteriol 172, 504-506.
- Inamine, J.M., Loechel, S., Collier, A.M., Barile, M.F., Hu, P.C., 1989. Nucleotide sequence of the MgPa (mgp) operon of *Mycoplasma genitalium* and comparison to the P1 (mpp) operon of *Mycoplasma pneumoniae*. Gene 82, 259-267.
- Iverson-Cabral, S.L., Astete, S.G., Cohen, C.R., Rocha, E.P., Totten, P.A., 2006. Intrastrain heterogeneity of the mgpB gene in *Mycoplasma genitalium* is extensive in vitro and in vivo and suggests that variation is generated via recombination with repetitive chromosomal sequences. Infect Immun 74, 3715-3726.
- Iverson-Cabral, S.L., Astete, S.G., Cohen, C.R., Totten, P.A., 2007. mgpB and mgpC sequence diversity in *Mycoplasma genitalium* is generated by segmental reciprocal recombination with repetitive chromosomal sequences. Molecular microbiology 66, 55-73.

- Jacobs, E., Watter, T., Schaefer, H.E., Bredt, W., 1991. Comparison of host responses after intranasal infection of guinea-pigs with *Mycoplasma genitalium* or with *Mycoplasma pneumoniae*. *Microb Pathog* 10, 221-229.
- Janis, C., Lartigue, C., Frey, J., Wroblewski, H., Thiaucourt, F., Blanchard, A., Sirand-Pugnet, P., 2005. Versatile use of oriC plasmids for functional genomics of *Mycoplasma capricolum subsp. capricolum*. *Appl Environ Microbiol* 71, 2888-2893.
- Jarrell, K.F., McBride, M.J., 2008. The surprisingly diverse ways that prokaryotes move. *Nature reviews. Microbiology* 6, 466-476.
- Jensen, J.S., 2004. *Mycoplasma genitalium*: the aetiological agent of urethritis and other sexually transmitted diseases. *J Eur Acad Dermatol Venereol* 18, 1-11.
- Jensen, J.S., Blom, J., Lind, K., 1994. Intracellular location of *Mycoplasma genitalium* in cultured Vero cells as demonstrated by electron microscopy. *Int J Exp Pathol* 75, 91-98.
- Jensen, J.S., Hansen, H.T., Lind, K., 1996. Isolation of *Mycoplasma genitalium* strains from the male urethra. *J Clin Microbiol* 34, 286-291.
- Jordan, J.L., Berry, K.M., Balish, M.F., Krause, D.C., 2001. Stability and subcellular localization of cytoadherence-associated protein P65 in *Mycoplasma pneumoniae*. *J Bacteriol* 183, 7387-7391.
- Jordan, J.L., Chang, H.Y., Balish, M.F., Holt, L.S., Bose, S.R., Hasselbring, B.M., Waldo, R.H., 3rd, Krunkosky, T.M., Krause, D.C., 2007. Protein P200 is dispensable for *Mycoplasma pneumoniae* hemadsorption but not gliding motility or colonization of differentiated bronchial epithelium. *Infect Immun* 75, 518-522.
- Kannan, T.R., Baseman, J.B., 2000. Hemolytic and hemoxidative activities in *Mycoplasma penetrans*. *Infect Immun* 68, 6419-6422.
- Kannan, T.R., Baseman, J.B., 2006. ADP-ribosylating and vacuolating cytotoxin of *Mycoplasma pneumoniae* represents unique virulence determinant among bacterial pathogens. *Proc Natl Acad Sci U S A* 103, 6724-6729.
- Karr, J.R., Sanghvi, J.C., Macklin, D.N., Gutschow, M.V., Jacobs, J.M., Bolival, B., Jr., Assad-Garcia, N., Glass, J.I., Covert, M.W., 2012. A whole-cell computational model predicts phenotype from genotype. *Cell* 150, 389-401.
- Kasai, T., Nakane, D., Ishida, H., Ando, H., Kiso, M., Miyata, M., 2013. Role of binding in *Mycoplasma mobile* and *Mycoplasma pneumoniae* gliding analyzed through inhibition by synthesized sialylated compounds. *J Bacteriol* 195, 429-435.
- Keane, F.E., Thomas, B.J., Gilroy, C.B., Renton, A., Taylor-Robinson, D., 2000. The association of *Chlamydia trachomatis* and *Mycoplasma genitalium* with non-gonococcal urethritis: observations on heterosexual men and their female partners. *Int J STD AIDS* 11, 435-439.

- Keceli, S.A., Miles, R.J., 2002. Differential inhibition of mollicute growth: an approach to development of selective media for specific mollicutes. *Appl Environ Microbiol* 68, 5012-5016.
- Kenri, T., Seto, S., Horino, A., Sasaki, Y., Sasaki, T., Miyata, M., 2004. Use of fluorescent-protein tagging to determine the subcellular localization of *Mycoplasma pneumoniae* proteins encoded by the cytoadherence regulatory locus. *J Bacteriol* 186, 6944-6955.
- Kikuchi, M., Ito, S., Yasuda, M., Tsuchiya, T., Hatazaki, K., Takanashi, M., Ezaki, T., Deguchi, T., 2014. Remarkable increase in fluoroquinolone-resistant *Mycoplasma genitalium* in Japan. *J Antimicrob Chemother*.
- King, K.W., Dybvig, K., 1992. Nucleotide sequence of *Mycoplasma mycoides subspecies Mycoides* plasmid pKMK1. *Plasmid* 28, 86-91.
- Kobisch, M., Friis, N.F., 1996. Swine mycoplasmoses. *Revue scientifique et technique* 15, 1569-1605.
- Krause, D.C., 1996. *Mycoplasma pneumoniae* cytoadherence: unravelling the tie that binds. *Molecular microbiology* 20, 247-253.
- Krause, D.C., Balish, M.F., 2001. Structure, function, and assembly of the terminal organelle of *Mycoplasma pneumoniae*. *FEMS microbiology letters* 198, 1-7.
- Krause, D.C., Balish, M.F., 2004. Cellular engineering in a minimal microbe: structure and assembly of the terminal organelle of *Mycoplasma pneumoniae*. *Molecular microbiology* 51, 917-924.
- Krause, D.C., Baseman, J.B., 1982. *Mycoplasma pneumoniae* proteins that selectively bind to host cells. *Infect Immun* 37, 382-386.
- Krause, D.C., Baseman, J.B., 1983. Inhibition of *Mycoplasma pneumoniae* hemadsorption and adherence to respiratory epithelium by antibodies to a membrane protein. *Infect Immun* 39, 1180-1186.
- Krause, D.C., Leith, D.K., Wilson, R.M., Baseman, J.B., 1982. Identification of *Mycoplasma pneumoniae* proteins associated with hemadsorption and virulence. *Infect Immun* 35, 809-817.
- Krause, D.C., Proft, T., Hedreyda, C.T., Hilbert, H., Plagens, H., Herrmann, R., 1997. Transposon mutagenesis reinforces the correlation between *Mycoplasma pneumoniae* cytoskeletal protein HMW2 and cytoadherence. *J Bacteriol* 179, 2668-2677.
- Krieg, N.R., Staley, J.T., Brown, D.R., Hedlund, B.P., Paster, B.J., Ward, N.L., Ludwig, W., Whitman, W.B., 2011. *Bergey's manual of systematic bacteriology*. Vol 4., 2nd ed. Springer, New York.
- Krieger, J.N., Riley, D.E., Roberts, M.C., Berger, R.E., 1996. Prokaryotic DNA sequences in patients with chronic idiopathic prostatitis. *J Clin Microbiol* 34, 3120-3128.

- Krishnakumar, R., Assad-Garcia, N., Benders, G.A., Phan, Q., Montague, M.G., Glass, J.I., 2010. Targeted chromosomal knockouts in *Mycoplasma pneumoniae*. *Appl Environ Microbiol* 76, 5297-5299.
- Krunkosky, T.M., Jordan, J.L., Chambers, E., Krause, D.C., 2007. *Mycoplasma pneumoniae* host-pathogen studies in an air-liquid culture of differentiated human airway epithelial cells. *Microb Pathog* 42, 98-103.
- Kuhner, S., van Noort, V., Betts, M.J., Leo-Macias, A., Batische, C., Rode, M., Yamada, T., Maier, T., Bader, S., Beltran-Alvarez, P., Castano-Diez, D., Chen, W.H., Devos, D., Guell, M., Norambuena, T., Racke, I., Rybin, V., Schmidt, A., Yus, E., Aebersold, R., Herrmann, R., Bottcher, B., Frangakis, A.S., Russell, R.B., Serrano, L., Bork, P., Gavin, A.C., 2009. Proteome organization in a genome-reduced bacterium. *Science* 326, 1235-1240.
- Langmuir, 1918. The Adsorption of Gases on Plane Surfaces of Glass, Mica and Platinum. *Journal of the American Chemical Society* 40, 1361–1403.
- Lartigue, C., Glass, J.I., Alperovich, N., Pieper, R., Parmar, P.P., Hutchison, C.A., 3rd, Smith, H.O., Venter, J.C., 2007. Genome transplantation in bacteria: changing one species to another. *Science* 317, 632-638.
- Lartigue, C., Vashee, S., Algire, M.A., Chuang, R.Y., Benders, G.A., Ma, L., Noskov, V.N., Denisova, E.A., Gibson, D.G., Assad-Garcia, N., Alperovich, N., Thomas, D.W., Merryman, C., Hutchison, C.A., 3rd, Smith, H.O., Venter, J.C., Glass, J.I., 2009. Creating bacterial strains from genomes that have been cloned and engineered in yeast. *Science* 325, 1693-1696.
- Layh-Schmitt, G., Hilbert, H., Pirkl, E., 1995. A spontaneous hemadsorption-negative mutant of *Mycoplasma pneumoniae* exhibits a truncated adhesin-related 30-kilodalton protein and lacks the cytoadherence-accessory protein HMW1. *J Bacteriol* 177, 843-846.
- Leichert, L.I., Jakob, U., 2004. Protein thiol modifications visualized in vivo. *PLoS biology* 2, e333.
- Lesoil, C., Nonaka, T., Sekiguchi, H., Osada, T., Miyata, M., Afrin, R., Ikai, A., 2010. Molecular shape and binding force of *Mycoplasma mobile*'s leg protein Gli349 revealed by an AFM study. *Biochemical and biophysical research communications* 391, 1312-1317.
- Lipton, S.A., Choi, Y.B., Takahashi, H., Zhang, D., Li, W., Godzik, A., Bankston, L.A., 2002. Cysteine regulation of protein function--as exemplified by NMDA-receptor modulation. *Trends in neurosciences* 25, 474-480.
- Lluch-Senar, M., Luong, K., Llorens-Rico, V., Delgado, J., Fang, G., Spittle, K., Clark, T.A., Schadt, E., Turner, S.W., Korlach, J., Serrano, L., 2013. Comprehensive methylome characterization of *Mycoplasma genitalium* and *Mycoplasma pneumoniae* at single-base resolution. *PLoS genetics* 9, e1003191.
- Lluch-Senar, M., Querol, E., Pinol, J., 2010. Cell division in a minimal bacterium in the

- absence of *ftsZ*. *Molecular microbiology* 78, 278-289.
- Lluch-Senar, M., Vallmitjana, M., Querol, E., Pinol, J., 2007. A new promoterless reporter vector reveals antisense transcription in *Mycoplasma genitalium*. *Microbiology* 153, 2743-2752.
- Lo, S.C., Hayes, M.M., Tully, J.G., Wang, R.Y., Kotani, H., Pierce, P.F., Rose, D.L., Shih, J.W., 1992. *Mycoplasma penetrans* sp. nov., from the urogenital tract of patients with AIDS. *Int J Syst Bacteriol* 42, 357-364.
- Loi, V.V., Rossius, M., Antelmann, H., 2015. Redox regulation by reversible protein S-thiolation in bacteria. *Frontiers in microbiology* 6, 187.
- Lyon, B.R., May, J.W., Skurray, R.A., 1984. Tn4001: a gentamicin and kanamycin resistance transposon in *Staphylococcus aureus*. *Molecular & general genetics : MGG* 193, 554-556.
- Ma, L., Jensen, J.S., Mancuso, M., Hamasuna, R., Jia, Q., McGowin, C.L., Martin, D.H., 2010. Genetic variation in the complete MgPa operon and its repetitive chromosomal elements in clinical strains of *Mycoplasma genitalium*. *PLoS One* 5, e15660.
- Ma, L., Jensen, J.S., Mancuso, M., Hamasuna, R., Jia, Q., McGowin, C.L., Martin, D.H., 2012. Variability of trinucleotide tandem repeats in the MgPa operon and its repetitive chromosomal elements in *Mycoplasma genitalium*. *J Med Microbiol* 61, 191-197.
- Ma, L., Jensen, J.S., Myers, L., Burnett, J., Welch, M., Jia, Q., Martin, D.H., 2007. *Mycoplasma genitalium*: an efficient strategy to generate genetic variation from a minimal genome. *Molecular microbiology* 66, 220-236.
- Ma, L., Taylor, S., Jensen, J.S., Myers, L., Lillis, R., Martin, D.H., 2008. Short tandem repeat sequences in the *Mycoplasma genitalium* genome and their use in a multilocus genotyping system. *BMC Microbiol* 8, 130.
- Mahairas, G.G., Minion, F.C., 1989. Random insertion of the gentamicin resistance transposon Tn4001 in *Mycoplasma pulmonis*. *Plasmid* 21, 43-47.
- Maier, T., Marcos, J., Wodke, J.A., Paetzold, B., Liebeke, M., Gutierrez-Gallego, R., Serrano, L., 2013. Large-scale metabolome analysis and quantitative integration with genomics and proteomics data in *Mycoplasma pneumoniae*. *Molecular bioSystems* 9, 1743-1755.
- Maier, T., Schmidt, A., Guell, M., Kuhner, S., Gavin, A.C., Aebersold, R., Serrano, L., 2011. Quantification of mRNA and protein and integration with protein turnover in a bacterium. *Molecular systems biology* 7, 511.
- Mandar, R., Raukas, E., Turk, S., Korrovits, P., Punab, M., 2005. Mycoplasmas in semen of chronic prostatitis patients. *Scand J Urol Nephrol* 39, 479-482.
- Manhart, L.E., 2013. *Mycoplasma genitalium*: An emergent sexually transmitted disease? *Infect Dis Clin North Am* 27, 779-792.

- Manhart, L.E., Critchlow, C.W., Holmes, K.K., Dutro, S.M., Eschenbach, D.A., Stevens, C.E., Totten, P.A., 2003. Mucopurulent cervicitis and *Mycoplasma genitalium*. *J Infect Dis* 187, 650-657.
- Manhart, L.E., Holmes, K.K., Hughes, J.P., Houston, L.S., Totten, P.A., 2007. *Mycoplasma genitalium* among young adults in the United States: an emerging sexually transmitted infection. *Am J Public Health* 97, 1118-1125.
- Manhart, L.E., Kay, N., 2010. *Mycoplasma genitalium*: Is It a Sexually Transmitted Pathogen? *Curr Infect Dis Rep* 12, 306-313.
- Manhart, L.E., Mostad, S.B., Baeten, J.M., Astete, S.G., Mandaliya, K., Totten, P.A., 2008. High *Mycoplasma genitalium* organism burden is associated with shedding of HIV-1 DNA from the cervix. *J Infect Dis* 197, 733-736.
- Manolukas, J.T., Barile, M.F., Chandler, D.K., Pollack, J.D., 1988. Presence of anaplerotic reactions and transamination, and the absence of the tricarboxylic acid cycle in mollicutes. *J Gen Microbiol* 134, 791-800.
- Mardh, P.A., 1983. Mycoplasmal Pids - a Review of Natural and Experimental Infections. *Yale J Biol Med* 56, 529-536.
- Mavedzenge, S.N., Van Der Pol, B., Weiss, H.A., Kwok, C., Mambo, F., Chipato, T., Van der Straten, A., Salata, R., Morrison, C., 2012. The association between *Mycoplasma genitalium* and HIV-1 acquisition in African women. *AIDS* 26, 617-624.
- McBride, M.J., 2001. Bacterial gliding motility: multiple mechanisms for cell movement over surfaces. *Annual review of microbiology* 55, 49-75.
- McGowin, C.L., Anderson-Smits, C., 2011. *Mycoplasma genitalium*: an emerging cause of sexually transmitted disease in women. *PLoS Pathog* 7, e1001324.
- McGowin, C.L., Popov, V.L., Pyles, R.B., 2009. Intracellular *Mycoplasma genitalium* infection of human vaginal and cervical epithelial cells elicits distinct patterns of inflammatory cytokine secretion and provides a possible survival niche against macrophage-mediated killing. *BMC Microbiol* 9, 139.
- McGowin, C.L., Spagnuolo, R.A., Pyles, R.B., 2010. *Mycoplasma genitalium* rapidly disseminates to the upper reproductive tracts and knees of female mice following vaginal inoculation. *Infect Immun* 78, 726-736.
- Medina, J.L., Coalson, J.J., Brooks, E.G., Winter, V.T., Chaparro, A., Principe, M.F., Kannan, T.R., Baseman, J.B., Dube, P.H., 2012. *Mycoplasma pneumoniae* CARDS toxin induces pulmonary eosinophilic and lymphocytic inflammation. *American journal of respiratory cell and molecular biology* 46, 815-822.
- Meloni, G.A., Bertoloni, G., Busolo, F., Conventi, L., 1980. Colony morphology, ultrastructure and morphogenesis in *Mycoplasma hominis*, *Acholeplasma laidlawii* and *Ureaplasma*

- urealyticum*. J Gen Microbiol 116, 435-443.
- Meng, K.E., Pfister, R.M., 1980. Intracellular structures of *Mycoplasma pneumoniae* revealed after membrane removal. J Bacteriol 144, 390-399.
- Mernaugh, G.R., Dallo, S.F., Holt, S.C., Baseman, J.B., 1993. Properties of adhering and nonadhering populations of *Mycoplasma genitalium*. Clin Infect Dis 17 Suppl 1, S69-78.
- Miles, R.J., 1992. Catabolism in mollicutes. J Gen Microbiol 138, 1773-1783.
- Minion, F.C., Jarvill-Taylor, K.J., Billings, D.E., Tigges, E., 1993. Membrane-associated nuclease activities in mycoplasmas. J Bacteriol 175, 7842-7847.
- Miyata, M., 2008. Centipede and inchworm models to explain *Mycoplasma* gliding. Trends in microbiology 16, 6-12.
- Miyata, M., 2010. Unique centipede mechanism of *Mycoplasma* gliding. Annu Rev Microbiol 64, 519-537.
- Miyata, M., Petersen, J.D., 2004. Spike structure at the interface between gliding *Mycoplasma mobile* cells and glass surfaces visualized by rapid-freeze-and-fracture electron microscopy. J Bacteriol 186, 4382-4386.
- Miyata, M., Yamamoto, H., Shimizu, T., Uenoyama, A., Citti, C., Rosengarten, R., 2000. Gliding mutants of *Mycoplasma mobile*: relationships between motility and cell morphology, cell adhesion and microcolony formation. Microbiology 146 (Pt 6), 1311-1320.
- Moi, H., Reinton, N., Moghaddam, A., 2009. *Mycoplasma genitalium* in women with lower genital tract inflammation. Sex Transm Infect 85, 10-14.
- Moller, B.R., Taylor-Robinson, D., Furr, P.M., Freundt, E.A., 1985. Acute upper genital-tract disease in female monkeys provoked experimentally by *Mycoplasma genitalium*. Br J Exp Pathol 66, 417-426.
- Morrison-Plummer, J., Lazzell, A., Baseman, J.B., 1987. Shared epitopes between *Mycoplasma pneumoniae* major adhesin protein P1 and a 140-kilodalton protein of *Mycoplasma genitalium*. Infect Immun 55, 49-56.
- Moss, S.F., Blaser, M.J., 2005. Mechanisms of disease: Inflammation and the origins of cancer. Nat Clin Pract Oncol 2, 90-97; quiz 91 p following 113.
- Musatovova, O., Baseman, J.B., 2009. Analysis identifying common and distinct sequences among Texas clinical strains of *Mycoplasma genitalium*. J Clin Microbiol 47, 1469-1475.
- Musatovova, O., Dhandayuthapani, S., Baseman, J.B., 2003. Transcriptional starts for cytoadherence-related operons of *Mycoplasma genitalium*. FEMS microbiology letters 229, 73-81.

- Nagai, R., Miyata, M., 2006. Gliding motility of *Mycoplasma mobile* can occur by repeated binding to N-acetylneuraminylactose (sialyllactose) fixed on solid surfaces. *J Bacteriol* 188, 6469-6475.
- Nakane, D., Miyata, M., 2007. Cytoskeletal “jellyfish” structure of *Mycoplasma mobile*. *Proc Natl Acad Sci U S A* 104, 19518-19523.
- Nakane, D., Miyata, M., 2012. *Mycoplasma mobile* cells elongated by detergent and their pivoting movements in gliding. *J Bacteriol* 194, 122-130.
- Namiki, K., Goodison, S., Porvasnik, S., Allan, R.W., Iczkowski, K.A., Urbanek, C., Reyes, L., Sakamoto, N., Rosser, C.J., 2009. Persistent exposure to *Mycoplasma* induces malignant transformation of human prostate cells. *PLoS One* 4, e6872.
- Napierala Mavedzenge, S., Weiss, H.A., 2009. Association of *Mycoplasma genitalium* and HIV infection: a systematic review and meta-analysis. *AIDS* 23, 611-620.
- Navas-Castillo, J., Laigret, F., Tully, J.G., Bove, J.M., 1992. [Mollicute *Acholeplasma florum* possesses a gene of phosphoenolpyruvate sugar phosphotransferase system and it uses UGA as tryptophan codon]. *C R Acad Sci III* 315, 43-48.
- Neimark, H.C., 1977. Extraction of an actin-like protein from the prokaryote *Mycoplasma pneumoniae*. *Proc Natl Acad Sci U S A* 74, 4041-4045.
- Ohtani, N., Miyata, M., 2007. Identification of a novel nucleoside triphosphatase from *Mycoplasma mobile*: a prime candidate motor for gliding motility. *The Biochemical journal* 403, 71-77.
- Page, C.A., Krause, D.C., 2013. Protein kinase/phosphatase function correlates with gliding motility in *Mycoplasma pneumoniae*. *J Bacteriol* 195, 1750-1757.
- Palmer, H.M., Gilroy, C.B., Claydon, E.J., Taylor-Robinson, D., 1991. Detection of *Mycoplasma genitalium* in the genitourinary tract of women by the polymerase chain reaction. *Int J STD AIDS* 2, 261-263.
- Parraga-Nino, N., Colome-Calls, N., Canals, F., Querol, E., Ferrer-Navarro, M., 2012. A comprehensive proteome of *Mycoplasma genitalium*. *Journal of proteome research* 11, 3305-3316.
- Pepin, J., Labbe, A.C., Khonde, N., Deslandes, S., Alary, M., Dzokoto, A., Asamoah-Adu, C., Meda, H., Frost, E., 2005. *Mycoplasma genitalium*: an organism commonly associated with cervicitis among west African sex workers. *Sex Transm Infect* 81, 67-72.
- Perez, G., Skurnick, J.H., Denny, T.N., Stephens, R., Kennedy, C.A., Regivick, N., Nahmias, A., Lee, F.K., Lo, S.C., Wang, R.Y., Weiss, S.H., Luria, D.B., 1998. Herpes simplex type II and *Mycoplasma genitalium* as risk factors for heterosexual HIV transmission: report from the heterosexual HIV transmission study. *Int J Infect Dis* 3, 5-11.
- Peterson, S.N., Bailey, C.C., Jensen, J.S., Borre, M.B., King, E.S., Bott, K.F., Hutchison,

- C.A., 3rd, 1995. Characterization of repetitive DNA in the *Mycoplasma genitalium* genome: possible role in the generation of antigenic variation. Proc Natl Acad Sci U S A 92, 11829-11833.
- Pich, O.Q., Burgos, R., Ferrer-Navarro, M., Querol, E., Pinol, J., 2006a. *Mycoplasma genitalium* mg200 and mg386 genes are involved in gliding motility but not in cytodherence. Molecular microbiology 60, 1509-1519.
- Pich, O.Q., Burgos, R., Ferrer-Navarro, M., Querol, E., Pinol, J., 2008. Role of *Mycoplasma genitalium* MG218 and MG317 cytoskeletal proteins in terminal organelle organization, gliding motility and cytodherence. Microbiology 154, 3188-3198.
- Pich, O.Q., Burgos, R., Planell, R., Querol, E., Pinol, J., 2006b. Comparative analysis of antibiotic resistance gene markers in *Mycoplasma genitalium*: application to studies of the minimal gene complement. Microbiology 152, 519-527.
- Pich, O.Q., Burgos, R., Querol, E., Pinol, J., 2009. P110 and P140 cytodherence-related proteins are negative effectors of terminal organelle duplication in *Mycoplasma genitalium*. PloS one 4, e7452.
- Pillay, D.G., Hoosen, A.A., Vezi, B., Moodley, C., 1994. Diagnosis of *Trichomonas vaginalis* in male urethritis. Trop Geogr Med 46, 44-45.
- Pollack, J.D., Williams, M.V., McElhaney, R.N., 1997. The comparative metabolism of the mollicutes (Mycoplasmas): the utility for taxonomic classification and the relationship of putative gene annotation and phylogeny to enzymatic function in the smallest free-living cells. Crit Rev Microbiol 23, 269-354.
- Popham, P.L., Hahn, T.W., Krebes, K.A., Krause, D.C., 1997. Loss of HMW1 and HMW3 in noncytadhering mutants of *Mycoplasma pneumoniae* occurs post-translationally. Proc Natl Acad Sci U S A 94, 13979-13984.
- Pour-El, I., Adams, C., Minion, F.C., 2002. Construction of mini-Tn4001tet and its use in *Mycoplasma gallisepticum*. Plasmid 47, 129-137.
- Prince, O.A., Krunkosky, T.M., Krause, D.C., 2014. In vitro spatial and temporal analysis of *Mycoplasma pneumoniae* colonization of human airway epithelium. Infect Immun 82, 579-586.
- Pritchard, R.E., Balish M.F., 2015. *Mycoplasma iowae*: relationships among oxygen, virulence, and protection from oxidative stress. Vet Res. 46(1):36.
- Radestock, U., Bredt, W., 1977. Motility of *Mycoplasma pneumoniae*. J Bacteriol 129, 1495-1501.
- Razin, S., Jacobs, E., 1992. Mycoplasma adhesion. J Gen Microbiol 138, 407-422.
- Razin, S., Yogev, D., Naot, Y., 1998a. Molecular biology and pathogenicity of mycoplasmas. Microbiology and molecular biology reviews : MMBR 62, 1094-1156.

- Razin, S., Yogev, D., Naot, Y., 1998b. Molecular biology and pathogenicity of mycoplasmas. *Microbiol Mol Biol R* 62, 1094-+.
- Reddy, S.P., Rasmussen, W.G., Baseman, J.B., 1995. Molecular cloning and characterization of an adherence-related operon of *Mycoplasma genitalium*. *J Bacteriol* 177, 5943-5951.
- Reddy, S.P., Rasmussen, W.G., Baseman, J.B., 1996. Isolation and characterization of transposon Tn4001-generated, cytoadherence-deficient transformants of *Mycoplasma pneumoniae* and *Mycoplasma genitalium*. *FEMS immunology and medical microbiology* 15, 199-211.
- Regula, J.T., Boguth, G., Gorg, A., Hegermann, J., Mayer, F., Frank, R., Herrmann, R., 2001. Defining the mycoplasma 'cytoskeleton': the protein composition of the Triton X-100 insoluble fraction of the bacterium *Mycoplasma pneumoniae* determined by 2-D gel electrophoresis and mass spectrometry. *Microbiology* 147, 1045-1057.
- Relich, R.F., Balish, M.F., 2011. Insights into the function of *Mycoplasma pneumoniae* protein P30 from orthologous gene replacement. *Microbiology* 157, 2862-2870.
- Roberts, D.D., Olson, L.D., Barile, M.F., Ginsburg, V., Krivan, H.C., 1989. Sialic acid-dependent adhesion of *Mycoplasma pneumoniae* to purified glycoproteins. *J Biol Chem* 264, 9289-9293.
- Rocha, E.P., Blanchard, A., 2002. Genomic repeats, genome plasticity and the dynamics of *Mycoplasma* evolution. *Nucleic Acids Res* 30, 2031-2042.
- Romero-Arroyo, C.E., Jordan, J., Peacock, S.J., Willby, M.J., Farmer, M.A., Krause, D.C., 1999. *Mycoplasma pneumoniae* protein P30 is required for cytoadherence and associated with proper cell development. *J Bacteriol* 181, 1079-1087.
- Ross, J.D., Brown, L., Saunders, P., Alexander, S., 2009. *Mycoplasma genitalium* in asymptomatic patients: implications for screening. *Sex Transm Infect* 85, 436-437.
- Rottem, S., 2003. Interaction of mycoplasmas with host cells. *Physiol Rev* 83, 417-432.
- Ruland, K., Wenzel, R., Herrmann, R., 1990. Analysis of three different repeated DNA elements present in the P1 operon of *Mycoplasma pneumoniae*: size, number and distribution on the genome. *Nucleic Acids Res* 18, 6311-6317.
- Sakata, H., Hayashi, T., Hirano, Y., Maruyama, S., Narita, M., 1993. [Brain stem encephalitis due to *Mycoplasma genitalium*]. *Kansenshogaku Zasshi* 67, 500-504.
- Sambrook, J., Russell, D.W., 2001. *Molecular cloning : a laboratory manual*, 3rd ed. Cold Spring Harbor Laboratory Press, Cold Spring Harbor, N.Y.
- Sanchez-Perez, A., Brown, G., Malik, R., Assinder, S.J., Cantlon, K., Gotsis, C., Dunbar, S., Fraser, S.T., 2013. Rapid detection of haemotropic mycoplasma infection of feline erythrocytes using a novel flow cytometric approach. *Parasites & vectors* 6, 158.

- Schmidl, S.R., Gronau, K., Pietack, N., Hecker, M., Becher, D., Stulke, J., 2010. The phosphoproteome of the minimal bacterium *Mycoplasma pneumoniae*: analysis of the complete known Ser/Thr kinome suggests the existence of novel kinases. *Molecular & cellular proteomics* : MCP 9, 1228-1242.
- Seto, S., Kenri, T., Tomiyama, T., Miyata, M., 2005a. Involvement of P1 adhesin in gliding motility of *Mycoplasma pneumoniae* as revealed by the inhibitory effects of antibody under optimized gliding conditions. *J Bacteriol* 187, 1875-1877.
- Seto, S., Layh-Schmitt, G., Kenri, T., Miyata, M., 2001. Visualization of the attachment organelle and cytoadherence proteins of *Mycoplasma pneumoniae* by immunofluorescence microscopy. *J Bacteriol* 183, 1621-1630.
- Seto, S., Miyata, M., 2003. Attachment organelle formation represented by localization of cytoadherence proteins and formation of the electron-dense core in wild-type and mutant strains of *Mycoplasma pneumoniae*. *J Bacteriol* 185, 1082-1091.
- Seto, S., Uenoyama, A., Miyata, M., 2005b. Identification of a 521-kilodalton protein (Gli521) involved in force generation or force transmission for *Mycoplasma mobile* gliding. *J Bacteriol* 187, 3502-3510.
- Seybert, A., Herrmann, R., Frangakis, A.S., 2006. Structural analysis of *Mycoplasma pneumoniae* by cryo-electron tomography. *Journal of structural biology* 156, 342-354.
- Sharma, S., Citti, C., Sagne, E., Marendia, M.S., Markham, P.F., Browning, G.F., 2015. Development and host compatibility of plasmids for two important ruminant pathogens, *Mycoplasma bovis* and *Mycoplasma agalactiae*. *PLoS One* 10, e0119000.
- Shen, X., Gumulak, J., Yu, H., French, C.T., Zou, N., Dybvig, K., 2000. Gene rearrangements in the *vsa* locus of *Mycoplasma pulmonis*. *J Bacteriol* 182, 2900-2908.
- Simms, I., Eastick, K., Mallinson, H., Thomas, K., Gokhale, R., Hay, P., Herring, A., Rogers, P.A., 2003. Associations between *Mycoplasma genitalium*, *Chlamydia trachomatis* and pelvic inflammatory disease. *J Clin Pathol* 56, 616-618.
- Sirand-Pugnet, P., Lartigue, C., Marendia, M., Jacob, D., Barre, A., Barbe, V., Schenowitz, C., Mangenot, S., Couloux, A., Segurens, B., de Daruvar, A., Blanchard, A., Citti, C., 2007. Being pathogenic, plastic, and sexual while living with a nearly minimal bacterial genome. *PLoS genetics* 3, e75.
- Soehnen, M.K., Kunze, M.E., Karunathilake, K.E., Henwood, B.M., Kariyawasam, S., Wolfgang, D.R., Jayarao, B.M., 2011. In vitro antimicrobial inhibition of *Mycoplasma bovis* isolates submitted to the Pennsylvania Animal Diagnostic Laboratory using flow cytometry and a broth microdilution method. *Journal of veterinary diagnostic investigation: official publication of the American Association of Veterinary Laboratory Diagnosticians, Inc* 23, 547-551.
- Soni, S., Alexander, S., Verlander, N., Saunders, P., Richardson, D., Fisher, M., Ison, C.,

2010. The prevalence of urethral and rectal *Mycoplasma genitalium* and its associations in men who have sex with men attending a genitourinary medicine clinic. *Sex Transm Infect* 86, 21-24.
- Spergser, J., Macher, K., Kargl, M., Lysnyansky, I., Rosengarten, R., 2013. Emergence, re-emergence, spread and host species crossing of *Mycoplasma bovis* in the Austrian Alps caused by a single endemic strain. *Veterinary microbiology* 164, 299-306.
- Stevens, M.K., Krause, D.C., 1992. *Mycoplasma pneumoniae* cytoadherence phase-variable protein HMW3 is a component of the attachment organelle. *J Bacteriol* 174, 4265-4274.
- Su, C.J., Dallo, S.F., Chavoya, A., Baseman, J.B., 1993. Possible origin of sequence divergence in the P1 cytoadhesin gene of *Mycoplasma pneumoniae*. *Infect Immun* 61, 816-822.
- Svenstrup, H.F., Fedder, J., Abraham-Peskir, J., Birkelund, S., Christiansen, G., 2003. *Mycoplasma genitalium* attaches to human spermatozoa. *Hum Reprod* 18, 2103-2109.
- Svenstrup, H.F., Fedder, J., Kristoffersen, S.E., Trolle, B., Birkelund, S., Christiansen, G., 2008. *Mycoplasma genitalium*, *Chlamydia trachomatis*, and tubal factor infertility--a prospective study. *Fertil Steril* 90, 513-520.
- Svenstrup, H.F., Jensen, J.S., Gevaert, K., Birkelund, S., Christiansen, G., 2006. Identification and characterization of immunogenic proteins of *Mycoplasma genitalium*. *Clinical and vaccine immunology : CVI* 13, 913-922.
- Svenstrup, H.F., Nielsen, P.K., Drasbek, M., Birkelund, S., Christiansen, G., 2002. Adhesion and inhibition assay of *Mycoplasma genitalium* and *M. pneumoniae* by immunofluorescence microscopy. *J Med Microbiol* 51, 361-373.
- Tagg, K.A., Jeoffreys, N.J., Couldwell, D.L., Donald, J.A., Gilbert, G.L., 2013. Fluoroquinolone and macrolide resistance-associated mutations in *Mycoplasma genitalium*. *J Clin Microbiol* 51, 2245-2249.
- Taylor-Robinson, D., 2002. *Mycoplasma genitalium* -- an up-date. *Int J STD AIDS* 13, 145-151.
- Taylor-Robinson, D., Bebear, C., 1997. Antibiotic susceptibilities of mycoplasmas and treatment of mycoplasmal infections. *J Antimicrob Chemother* 40, 622-630.
- Taylor-Robinson, D., Furr, P.M., Tully, J.G., Barile, M.F., Moller, B.R., 1987. Animal models of *Mycoplasma genitalium* urogenital infection. *Isr J Med Sci* 23, 561-564.
- Taylor-Robinson, D., Gilroy, C.B., Horowitz, S., Horowitz, J., 1994. *Mycoplasma genitalium* in the joints of two patients with arthritis. *Eur J Clin Microbiol Infect Dis* 13, 1066-1069.
- Taylor-Robinson, D., Gilroy, C.B., Keane, F.E., 2003. Detection of several *Mycoplasma* species at various anatomical sites of homosexual men. *Eur J Clin Microbiol Infect Dis* 22, 291-293.

- Taylor-Robinson, D., Jensen, J.S., 2011. *Mycoplasma genitalium*: from Chrysalis to multicolored butterfly. Clin Microbiol Rev 24, 498-514.
- Taylor-Robinson, D., Lamont, R.F., 2011. Mycoplasmas in pregnancy. Bjog-Int J Obstet Gy 118, 164-174.
- Taylor-Robinson, D., Shirai, A., Sobeslavsky, O., Chanock, R.M., 1966. Serologic response to Mycoplasma pneumoniae infection. II. Significance of antibody measured by different techniques. American journal of epidemiology 84, 301-313.
- Terada, M., Izumi, K., Ohki, E., Yamagishi, Y., Mikamo, H., 2012. Antimicrobial efficacies of several antibiotics against uterine cervicitis caused by *Mycoplasma genitalium*. J Infect Chemother 18, 313-317.
- Theron, M., Hesketh, R.L., Subramanian, S., Rayner, J.C., 2010. An adaptable two-color flow cytometric assay to quantitate the invasion of erythrocytes by Plasmodium falciparum parasites. Cytometry. Part A : the journal of the International Society for Analytical Cytology 77, 1067-1074.
- Torres-Puig, S., Broto, A., Querol, E., Pinol, J., Pich, O.Q., 2015. A novel sigma factor reveals a unique regulon controlling cell-specific recombination in *Mycoplasma genitalium*. Nucleic Acids Res 43, 4923-4936.
- Tosh, A.K., Van Der Pol, B., Fortenberry, J.D., Williams, J.A., Katz, B.P., Batteiger, B.E., Orr, D.P., 2007. *Mycoplasma genitalium* among adolescent women and their partners. J Adolesc Health 40, 412-417.
- Totten, P.A., Schwartz, M.A., Sjostrom, K.E., Kenny, G.E., Handsfield, H.H., Weiss, J.B., Whittington, W.L., 2001. Association of *Mycoplasma genitalium* with nongonococcal urethritis in heterosexual men. J Infect Dis 183, 269-276.
- Trachtenberg, S., 2005. Mollicutes. Curr Biol 15, R483-484.
- Tsai, S., Wear, D.J., Shih, J.W., Lo, S.C., 1995. Mycoplasmas and oncogenesis: persistent infection and multistage malignant transformation. Proc Natl Acad Sci U S A 92, 10197-10201.
- Tully, J.G., Rose, D.L., Baseman, J.B., Dallo, S.F., Lazzell, A.L., Davis, C.P., 1995a. *Mycoplasma pneumoniae* and *Mycoplasma genitalium* mixture in synovial fluid isolate. J Clin Microbiol 33, 1851-1855.
- Tully, J.G., Rose, D.L., Yunker, C.E., Carle, P., Bove, J.M., Williamson, D.L., Whitcomb, R.F., 1995b. Spiroplasma ixodetis sp. nov., a new species from Ixodes pacificus ticks collected in Oregon. International Journal of Systematic Bacteriology 45, 23-28.
- Tully, J.G., Taylor-Robinson, D., Cole, R.M., Rose, D.L., 1981. A newly discovered mycoplasma in the human urogenital tract. Lancet 1, 1288-1291.
- Tully, J.G., Taylor-Robinson, D., Rose, D.L., Cole, R.M., Bove, J.M., 1983a. *Mycoplasma*

- genitalium*, a New Species from the Human Urogenital Tract Int J Syst Evol Microbiol 33, 387-396.
- Tully, J.G., Taylor-Robinson, D., Rose, D.L., Furr, P.M., Graham, C.E., Barile, M.F., 1986. Urogenital challenge of primate species with *Mycoplasma genitalium* and characteristics of infection induced in chimpanzees. J Infect Dis 153, 1046-1054.
- Tully, J.G., Taylorrobinson, D., Rose, D.L., Cole, R.M., Bove, J.M., 1983b. Mycoplasma-Genitalium, a New Species from the Human Urogenital Tract. International Journal of Systematic Bacteriology 33, 387-396.
- Tulum, I., Yabe, M., Uenoyama, A., Miyata, M., 2014. Localization of P42 and F(1)-ATPase alpha-subunit homolog of the gliding machinery in *Mycoplasma mobile* revealed by newly developed gene manipulation and fluorescent protein tagging. J Bacteriol 196, 1815-1824.
- Ueno, P.M., Timenetsky, J., Centonze, V.E., Wewer, J.J., Cagle, M., Stein, M.A., Krishnan, M., Baseman, J.B., 2008. Interaction of *Mycoplasma genitalium* with host cells: evidence for nuclear localization. Microbiology 154, 3033-3041.
- Uenoyama, A., Kusumoto, A., Miyata, M., 2004. Identification of a 349-kilodalton protein (Gli349) responsible for cytoadherence and glass binding during gliding of *Mycoplasma mobile*. J Bacteriol 186, 1537-1545.
- Uenoyama, A., Miyata, M., 2005a. Gliding ghosts of *Mycoplasma mobile*. Proc Natl Acad Sci U S A 102, 12754-12758.
- Uenoyama, A., Miyata, M., 2005b. Identification of a 123-kilodalton protein (Gli123) involved in machinery for gliding motility of *Mycoplasma mobile*. J Bacteriol 187, 5578-5584.
- Uenoyama, A., Seto, S., Nakane, D., Miyata, M., 2009. Regions on Gli349 and Gli521 protein molecules directly involved in movements of *Mycoplasma mobile* gliding machinery, suggested by use of inhibitory antibodies and mutants. J Bacteriol 191, 1982-1985.
- Uno, M., Deguchi, T., Komeda, H., Hayasaki, M., Iida, M., Nagatani, M., Kawada, Y., 1997. *Mycoplasma genitalium* in the cervixes of Japanese women. Sex Transm Dis 24, 284-286.
- van Noort, V., Seebacher, J., Bader, S., Mohammed, S., Vonkova, I., Betts, M.J., Kuhner, S., Kumar, R., Maier, T., O'Flaherty, M., Rybin, V., Schmeisky, A., Yus, E., Stulke, J., Serrano, L., Russell, R.B., Heck, A.J., Bork, P., Gavin, A.C., 2012. Cross-talk between phosphorylation and lysine acetylation in a genome-reduced bacterium. Molecular systems biology 8, 571.
- Vandepitte, J., Weiss, H.A., Bukonya, J., Kyakuwa, N., Muller, E., Buve, A., Van der Stuyft, P., Hayes, R.J., Grosskurth, H., 2014. Association between *Mycoplasma genitalium* infection and HIV acquisition among female sex workers in Uganda: evidence from a nested case-control study. Sex Transm Infect.

- Vivancos, A.P., Guell, M., Dohm, J.C., Serrano, L., Himmelbauer, H., 2010. Strand-specific deep sequencing of the transcriptome. *Genome research* 20, 989-999.
- Waites, K.B., Xiao, L., Paralanov, V., Viscardi, R.M., Glass, J.I., 2012. Molecular methods for the detection of *Mycoplasma* and *ureaplasma* infections in humans: a paper from the 2011 William Beaumont Hospital Symposium on molecular pathology. *J Mol Diagn* 14, 437-450.
- Waldo, R.H., 3rd, Popham, P.L., Romero-Arroyo, C.E., Mothershed, E.A., Lee, K.K., Krause, D.C., 1999. Transcriptional analysis of the hmw gene cluster of *Mycoplasma pneumoniae*. *J Bacteriol* 181, 4978-4985.
- Wenzel, R., Herrmann, R., 1988. Repetitive DNA sequences in *Mycoplasma pneumoniae*. *Nucleic Acids Res* 16, 8337-8350.
- Wikstrom, A., Jensen, J.S., 2006. *Mycoplasma genitalium*: a common cause of persistent urethritis among men treated with doxycycline. *Sex Transm Infect* 82, 276-279.
- Willby, M.J., Balish, M.F., Ross, S.M., Lee, K.K., Jordan, J.L., Krause, D.C., 2004. HMW1 is required for stability and localization of HMW2 to the attachment organelle of *Mycoplasma pneumoniae*. *J Bacteriol* 186, 8221-8228.
- Willby, M.J., Krause, D.C., 2002. Characterization of a *Mycoplasma pneumoniae* hmw3 mutant: implications for attachment organelle assembly. *J Bacteriol* 184, 3061-3068.
- Wilson, M.H., Collier, A.M., 1976. Ultrastructural study of *Mycoplasma pneumoniae* in organ culture. *J Bacteriol* 125, 332-339.
- Wodke, J.A., Puchalka, J., Lluch-Senar, M., Marcos, J., Yus, E., Godinho, M., Gutierrez-Gallego, R., dos Santos, V.A., Serrano, L., Klipp, E., Maier, T., 2013. Dissecting the energy metabolism in *Mycoplasma pneumoniae* through genome-scale metabolic modeling. *Molecular systems biology* 9, 653.
- Woese, C.R., Maniloff, J., Zablen, L.B., 1980. Phylogenetic analysis of the mycoplasmas. *Proc Natl Acad Sci U S A* 77, 494-498.
- Wolgemuth, C.W., Igoshin, O., Oster, G., 2003. The motility of mollicutes. *Biophysical journal* 85, 828-842.
- Xavier, J.C., Patil, K.R., Rocha, I., 2014. Systems biology perspectives on minimal and simpler cells. *Microbiology and molecular biology reviews* : MMBR 78, 487-509.
- Young, T.F., Erickson, B.Z., Ross, R.F., Wannemuehler, Y., 1989. Hemagglutination and hemagglutination inhibition of turkey red blood cells with *Mycoplasma hyopneumoniae*. *American journal of veterinary research* 50, 1052-1055.
- Yu, J.T., Tang, W.Y., Lau, K.H., Chong, L.Y., Lo, K.K., 2008. Asymptomatic urethral infection in male sexually transmitted disease clinic attendees. *Int J STD AIDS* 19, 155-158.

- Yus, E., Guell, M., Vivancos, A.P., Chen, W.H., Lluch-Senar, M., Delgado, J., Gavin, A.C., Bork, P., Serrano, L., 2012. Transcription start site associated RNAs in bacteria. *Molecular systems biology* 8, 585.
- Yus, E., Maier, T., Michalodimitrakis, K., van Noort, V., Yamada, T., Chen, W.H., Wodke, J.A., Guell, M., Martinez, S., Bourgeois, R., Kuhner, S., Raineri, E., Letunic, I., Kalinina, O.V., Rode, M., Herrmann, R., Gutierrez-Gallego, R., Russell, R.B., Gavin, A.C., Bork, P., Serrano, L., 2009. Impact of genome reduction on bacterial metabolism and its regulation. *Science* 326, 1263-1268.
- Zhang, Q., Wise, K.S., 1996. Molecular basis of size and antigenic variation of a *Mycoplasma hominis* adhesin encoded by divergent vaa genes. *Infect Immun* 64, 2737-2744.
- Zhang, W., Baseman, J.B., 2014. Functional characterization of osmotically inducible protein C (MG_427) from *Mycoplasma genitalium*. *J Bacteriol* 196(5):1012-1019.

Acknowledgments / Agraïments

Aquest apartat l'escric clar i català.

Vull agrair el suport a tothom qui m'ha acompanyat durant el doctorat i no voldria deixar-me ningú. Primer de tot, vull agrair la dedicació dels directors de la meva tesi doctoral, el Jaume Pinyol i l'Enric Querol. Els seus coneixements, la seva direcció i les discussions de resultats amb ells han sigut claus per portar tanta feina a bon port. També valoro l'interès i l'ajuda de tots els companys de biologia molecular, els qui ja han marxat i els qui encara hi corren, com el Mario, la Raquel, el Miquel, la Maria Lluch, el Raül, el Sergi Bru, la Noemí, la Maria Camats, l'Alicia, el Xavi, el Luis, el Sergi Torres, l'Ana, l'Òscar i el Carlos. No sé si em deixo algú! De veritat, a tots, gràcies, perquè no m'imagino fent el doctorat envoltat d'altres científics. També he d'agrair la col·laboració dels membres del grup de l'Ignasi Fita, a l'IRB, i la de tota la gent del grup de biologia estructural de l'ESRF, en especial la del Daniele de Sanctis i la Bàrbara Calisto, per acollir-me durant tres mesos al seu grup i fer-me sentir, gairebé, com a casa.

També voldria agrair l'ajuda dels treballadors dels serveis de l'Autònoma. Al servei de cultius cel·lulars i citometria, en especial a la Manuela Costa, que va ser crucial per al tercer capítol; al servei de microscòpia, amb menció especial pel Pablo Castro, que va ser imprescindible per obtenir les imatges de criomicroscòpia i al servei de genòmica.

I, per suposat, vull agrair l'afecte de la família, segurament el més important. A la Mari, per aguantar-me, estimar-me i aconsellar-me, per donar-ho tot. Als meus pares, perquè sempre han sabut estar allà quan els he necessitat. També als meus sogres i al cunyat, als tiets i als cosins, com el què es baralla amb el meu ordinador de tant en tant. I també agraeixo la companyia dels amics de tota la vida, dels que ens vam trobar a la universitat i dels més nous, per les bones estones que hem passat junts durant aquests anys.

Per acabar, vull agrair el finançament de la beca FPU al Ministeri d'Educació, Cultura i Esports.